Physical-layer Network Coding in Multi-way Relay Channels

Hao Li

Department of Electrical & Computer Engineering

McGill University

Montreal, Canada

November 2021

A thesis submitted to McGill University in partial fulfillment of the requirements for the degree of Doctor of Philosophy.

Abstract

Physical-layer network coding (PNC) is an attractive approach to increasing the network throughput by exploiting the broadcast nature of wireless channels. This thesis focuses on the application of PNC in a class of wireless networks known as multi-way relay channels (MRWC), where multiple users share information through a single relay. The primary objective of the thesis is to develop new uplink and downlink schemes for PNC in MWRC, with the main focus on signal detection and power allocation.

First, we propose a novel signal detection scheme for PNC in MWRC from the perspective of sequential multi-user detection. The extraction of the network codes from the superimposed user signals at the relay node is formulated as an under-determined linear system. To solve this problem with low decoding complexity, the proposed method combines successive interference cancellation (SIC) with Babai estimation for regularized integer least squares (ILS). We develop a power allocation scheme to enhance the performance of both SIC and ILS steps, and discuss an optimal user pairing strategy based on the average decoding error probability. The performance of the proposed method improves the relay's capability of extracting network codes from multiple superimposed user signals, as demonstrated by the numerical results.

Next, we address the design of power allocation schemes for PNC in downlink MWRC. The power allocation is formulated as a constrained optimization problem, where the aim is to maximize the probability of successfully decoding a chain of network codes, so-called *success probability*, under a total power constraint when using Babai estimation for signal detection. Three aggregate measures of success probability are considered over the participating user terminals, i.e., arithmetic mean, geometric mean, and maximin, and the solutions are obtained based on the concavity of the related problems. Results demonstrate the effectiveness of the proposed schemes in improving the success probability in the reception of a chain of network codes.

Finally, we propose a new power allocation scheme based on the success probability of SIC detection for PNC in uplink MWRC. We develop a generalized expression for the closed-form success probability of the SIC detection at the relay in the case of pulse-amplitude modulation (PAM). A constraint optimization is formulated over this probability subject to the transmit power constraints at the user terminals. We develop an evolutionary particle swarm optimization (PSO) algorithm to solve the problem, whose cost function is relatively complex and not necessarily concave. Results show that the proposed method can improve the quality of network code extraction at the relay.

Abrégé

Le codage de réseau par couche physique (PNC) est une approche attrayante pour augmenter le débit du réseau en exploitant la nature de diffusion des canaux sans fil. Cette thèse se concentre sur l'application du PNC dans une classe de réseaux sans fil connue sous le nom de canaux de relais multi-voies (MRWC), où de multiples utilisateurs partagent des informations à travers un seul relais. L'objectif principal de la thèse est de développer de nouveaux schémas de liaison montante et descendante pour PNC dans les MRWC, avec un accent particulier sur la détection du signal et l'allocation de puissance.

Tout d'abord, nous proposons un nouveau schéma de détection de signal pour PNC en MWRC du point de vue de la détection multi-utilisateurs séquentielle. L'extraction des codes de réseau à partir des signaux superposés des utilisateurs au niveau du nœud de relais est formulée comme un système linéaire sous-déterminé. Pour résoudre ce problème avec une faible complexité de décodage, la méthode proposée combine l'annulation successive des interférences (SIC) avec l'estimation de Babai pour les moindres carrés entiers régularisés (ILS). Nous développons un schéma d'allocation de puissance pour améliorer les performances des étapes SIC et ILS, et discutons d'une stratégie optimale de couplage d'utilisateurs basée sur la probabilité moyenne d'erreur de décodage. La performance de la méthode proposée améliore la capacité du relais à extraire des codes de réseau à partir de multiples signaux d'utilisateurs superposés, comme le démontrent les résultats numériques.

Ensuite, nous abordons la conception des schémas d'allocation de puissance pour le PNC dans la liaison descendante MWRC. L'allocation de puissance est formulée comme un problème d'optimisation sous contrainte, où l'objectif est de maximiser la probabilité de décoder avec succès une chaîne de codes de réseau, appelée *probabilité de succès*, sous une contrainte de puissance totale lors de l'utilisation de l'estimation de Babai pour la détection du signal. Trois mesures agrégées de la probabilité de succès sont considérées sur les terminaux d'utilisateurs participants, c'est-à-dire la moyenne arithmétique, la moyenne

géométrique et la maximisation, et les solutions sont obtenues sur la base de la concavité des problèmes connexes. Les résultats démontrent l'efficacité des schémas proposés pour améliorer la probabilité de succès dans la réception d'une chaîne de codes de réseau.

Enfin, nous proposons un nouveau schéma d'allocation de puissance basé sur la probabilité de succès de la détection SIC pour PNC dans la liaison montante MWRC. Nous développons une expression généralisée de la forme fermée de la probabilité de succès de la détection SIC au niveau du relais dans le cas de la modulation d'amplitude d'impulsion (PAM). Une optimisation par contrainte est formulée sur cette probabilité sous réserve des contraintes de puissance d'émission aux terminaux des utilisateurs. Nous développons un algorithme évolutionnaire d'optimisation par essaims de particules (PSO) pour résoudre le problème, dont la fonction de coût est relativement complexe et pas nécessairement concave. Les résultats montrent que la méthode proposée peut améliorer la qualité de l'extraction du code du réseau au niveau du relais.

Acknowledgements

I would like to express my deepest gratitude to my supervisor, Prof. Benoit Champagne, for his inspiration and support throughout my Ph.D. studies. Without his guidance, none of my achievements could ever be made true. I would also like to address my sincere thankfulness to my co-supervisor, Prof. Xiao-Wen Chang, for his extensive help during my study. His dedication and in-depth views in mathematics have continuously inspired and helped me counter countless research problems. I would like to thank Prof. Ioannis Psaromiligkos, member of my Ph.D. supervisory committee, who regularly reviewed my progress and provided valuable feedback. I am also grateful to Prof. Yunlong Cai from Zhejiang University for his constructive advice related to the material in Chapter 3. I would also like to thank Dr. Benoit Pelletier for his support and guidance during my internship at InterDigital Inc Canada in Montreal.

I have greatly enjoyed the time with my fellow labmates at the Telecommunication and Signal Processing Laboratory on the seventh floor of the McConnell building. My particular thanks go to Dr. Jiaxin Yang, who is a beacon for me in research and a precious friend in life. It is also my honor to mention the names of my labmates here to engrave this unforgettable journey: Ali, Ryan, Djamel, Tianze, Alireza, Hanwook, Kangli, Lu, Seyyed, Jianfeng, Yuzhi, Wang, Zhi.

I am grateful to many friends who have brought help, joy, and happiness to me in Montreal. Mainly, I would like to thank Dr. Chu Wang and Kaiyuan Xie for their friendship throughout these years.

Last but not least, my eternal gratitude goes to my beloved parents. It is beyond my ability to properly recognize in this universe my appreciation of their unconditional love and support. None will be more convincing than the two plain but not simple words from the bottom of my heart: ”Thank you.” While on the other hemisphere, home is always by my side.

Contents

1 Introduction **1**

1.1 Motivations and Problem Area 1

1.2 Existing works and challenges 2

1.2.1 Extension of TWRC PNC 3

1.2.2 Robustness of Network Code Chain 4

1.2.3 Efficacy of Relay Detection 5

1.3 Thesis Contributions 6

1.4 Organizations 8

2 Background **9**

2.1 Network Coding 9

2.2 Physical-layer network coding 11

2.2.1 Challenges in Wireless Environments 11

2.2.2 Exploiting the Nature of Wireless Medium 13

2.2.3 Principles of Physical-layer Network Coding 13

2.2.4 Issues and Existing Studies of PNC in TWRC 16

2.3 Multi-way Relay Channels 18

2.3.1 Application Scenarios 19

2.3.2 General Channel Model 20

2.3.3 Relay Strategies 21

2.3.4 Existing Studies on MWRC 22
2.4 Chapter Summary 26

3 Efficient Detection Scheme for Physical-layer Network Coding in Multiway Relay Channels 27
3.1 System Model 28
3.1.1 MA Stage 28
3.1.2 BC Stage 30
3.2 The Proposed Method 32
3.2.1 Successive Interference Cancellation 32
3.2.2 Babai Estimation for Overdetermined ILS 34
3.2.3 Formulation of Regularized ILS 35
3.2.4 The Proposed Algorithm 37
3.3 Power Allocation and User Pairing 41
3.3.1 Power Allocation for Babai Estimation 41
3.3.2 Power Allocation for SIC 42
3.3.3 Power Allocation for Proposed Algorithm 44
3.3.4 User Pairing Strategy 46
3.4 Simulation Experiments and Discussions 48
3.4.1 Conventional SIC and Babai Estimation 49
3.4.2 Evaluations of Proposed Method 51
3.4.3 User Pairing Strategy 58
3.5 Chapter Summary 60

4 Optimal Power Allocation Based on Success Probability for Downlink PNC in Multi-way Relay Channels 62
4.1 System model 63
4.1.1 System Configuration 63
4.1.2 Downlink Transmission 64

4.2 Essential Background 65
4.2.1 Babai Estimation 66
4.2.2 Success Probability of Babai Estimator 67
4.2.3 Conventional Adaptive Power Allocation 67
4.2.4 Particle Swarm Optimization 68
4.3 Proposed methods 69
4.3.1 Average Success Probability (Arithmetic Mean) 70
4.3.2 Overall Success Probability (Geometric Mean) 76
4.3.3 Minimal Success Probability (Maximin) 77
4.4 Simulation Results 79
4.4.1 Methodology 79
4.4.2 PSO Solution Analysis 81
4.4.3 PSO and Alternative problem solutions 83
4.4.4 Comparison Among Different Design Goals 84
4.5 Chapter Summary 87

5 Optimal Power Allocation Based on Success Probability of SIC Detection in MWRC PNC 88

5.1 System model 89
5.2 The proposed method 90
5.2.1 Success Probability of the SIC Detection 90
5.2.2 Problem Formulation 95
5.2.3 PSO Solution 95
5.3 Simulation Results 97
5.4 Chapter Summary 99

6 Conclusion 101

6.1 Summary 101
6.2 Potential future works 103

References **105**

List of Figures

2.1 Example of network coding in a butterfly structure. 11
2.2 Time-division multiplexing and frequency-division multiplexing techniques. 12
2.3 Physical layer network coding in TWRC. 14
2.4 An illustration of the general model of MWRC. 20

3.1 Illustration of the MWRC system model. 28
3.2 Example of the iterative recovery process for $\mathcal{C}_{seq}$ at user 3. User 3 first uses its self-information to decode s_2 and s_4 and then detects s_1 and s_5. 31
3.3 Illustration of the tree structure of the sequential pairing strategy $\mathcal{C}_{seq}$ in a 6-way relay network. The graph demonstrates a process where user 3 decodes all other user signals by proceeding through the branches in two directions. 46
3.4 BER performance of conventional SIC and Babai estimation for different choices of N and K 49
3.5 Impact of λ on the BER performance for Babai estimation. 50
3.6 BER performance of the proposed algorithm, conventional SIC, Babai estimation, MMSE estimation and ML estimation for $N = 6$ and $K = 2$. 51
3.7 Throughput performance of the proposed algorithm and the Atom I building block approach 53
3.8 Decoding complexity for the proposed algorithm and the constellation design approach 54

3.9 CPU time for the proposed algorithm and the searching algorithm. 55
3.10 Comparison between the approximation approach 56
3.11 BER performance and decoding complexity of the proposed algorithm with QPSK modulation. 57
3.12 BER performance for different user pairing strategies. 58
3.13 Comparisons between the optimal strategy and the star-shape strategy . . . 59

4.1 Downlink model of PNC in MWRC. The relay broadcasts $N-1$ network codes to the users, which then use Babai estimation to decode messages from the other users. 64
4.2 Convergence speed of PSO algorithm regarding different swarm size. 80
4.3 Convergence speed of PSO algorithm regarding damping ratio μ. 80
4.4 Performance comparison between PSO approach and alternative problem approach to problem (4.15) regarding SNR. 82
4.5 Performance comparison between PSO approach and alternative problem approach to problem (4.15) regarding different number of users. 83
4.6 Complementary values $(1-\rho'_{ave})$ of the arithmetic mean of the success probabilities. 85
4.7 Complementary values $(1-\rho_{all})$ of the geometric mean of the success probabilities. 85
4.8 Complementary values $(1-\rho_{min})$ of the minimal success probability. 86

5.1 Illustration of the PNC in MWRC. 89
5.2 Comparison between theoretical analysis and simulation results. 99
5.3 Comparison between the effect of power allocation strategy on the rate of correctly generated network code chain. 100

List of Tables

2.1 PNC mapping at the relay. 15

Acronyms

1G	1st generation
5G	5th generation
AWGN	additive white Gaussian noise
AF	amplify-and-forward
BER	bit error rate
BPSK	binary phase modulated keying
BP	belief propagation
BC	broadcast
CF	compress-and-forward
DF	decode-and-forward
FDM	frequency-division multiplexing
FCC	Federal Communication Commission
ILS	integer least squares
LOS	line of sight
MA	multiple access
MIMO	multiple-input and multiple-output
MISO	multiple-input and single-output
MMSE	minimum mean square error
MWRC	multi-way relay channel
MUD	multi-user detection

NC	network coding
NOMA	non-orthogonal multiple access
PAM	pulse-amplitude modulation
PNC	physical-layer network coding
PSO	particle swarm optimization
QoS	quality of service
RCRM	rank-constrained rank-minimization
SER	symbol error rate
SINR	signal-to-interference-plus-noise ratio
SIC	successive interference cancellation
SLNR	signal-to-leakage-and-noise ratio
SNR	signal-to-noise ratio
TDM	time-division multiplexing
TWRC	two-way relay channel
UAV	unmmanned aerial vehicle
WER	word error rate

CHAPTER 1

Introduction

In this chapter, we introduce the problem area of the thesis, survey relevant literature and then summarize the main contributions.

1.1 Motivations and Problem Area

In this modern era, wireless communications have enabled the connection among billions of people around the globe and become an essential part of our daily lives. From transaction and entertaining to transportation and manufacturing, nearly every sector of today's society relies on wireless technologies in fundamental ways. The increasing need for faster connections and higher data throughput has become an iconic desire of the contemporary general public. Thanks to the efforts of countless researchers and engineers, evolving technologies from the 1st generation (1G) to the 5th generation (5G) and beyond are constantly pushing the limits of wireless communications to a whole new level [1].

Physical-layer network coding (PNC) [2, 3], which exploits the broadcast nature of wireless channels to improve the network throughput, has drawn considerable attention in recent years [4–6]. In a traditional half-duplex two-way relay channel (TWRC) scenario, two end users attempt to exchange information with the help of a relay. In contrast to the conventional network coding (NC) scheme [7, 8], which requires 2 time slots for uplink

and 1 time slot for downlink transmissions [9], PNC in TWRC only consumes 2 time slots in total. By exploiting the additive nature of electromagnetic waves at the physical layer, PNC allows users to send signals simultaneously to the relay using only 1 time slot. After extracting and decoding the superimposed user signals, the relay encodes this information into an NC signal and broadcasts it in a subsequent time slot. Upon reception of the broadcast NC signal, each user decodes the desired signal from the other user by employing its self-information. Compared with the conventional NC scheme, PNC leads to a 33% throughput improvement. Hence, it provides an appealing solution to meet the exacting demands of various applications envisaged for 5G wireless networks and beyond, such as streaming 4K video, machine-to-machine communications, online cloud sharing, etc. [10–13]. To explore the full advantage of PNC for these applications, several studies have been carried out with a focus on specific TWRC issues, such as the design of symbol mapping [14,15], the effect of time or phase synchronization [16–20], and channel estimation [21–23].

To extend the application scenarios beyond the conventional TWRC, this thesis focuses on the use of PNC in a class of wireless networks known as multi-way relay channels (MRWC), where multiple users share information through a single relay. The primary objective of the thesis is to develop new uplink and downlink schemes for PNC in MWRC, with the main focus on signal detection and power allocation.

1.2 Existing works and challenges

This section provides a literature review on existing works and challenges of the PNC in MWRC regarding the extension of TWRC, the robustness of the network code chain, and the efficacy of relay detection.

1.2.1 Extension of TWRC PNC

As a natural extension to TWRC, the use of PNC in MWRC [24] has been less studied. The superposition of multiple, say $N > 2$, user signals at the relay increases the difficulty of extracting network codes due to the mutual interference. The use of a relay equipped with multiple antennas, say K, provides a simple solution to the MWRC problem since the spatial diversity can be exploited to diminish interference. Most of the literature on PNC in MWRC [25–27] focuses on implementation scenarios where the number of relay antennas is greater than the number of users, i.e., $K \geq N$. To some degree, this assumption defeats the inherent idea behind PNC, i.e., that the boost in throughput should result from natural coding in the wireless medium rather than from the additional cost of space-time processing. From this perspective, it would seem worthwhile to consider the case $K < N$ for PNC in MWRC, where the throughput gain is not so much dependent on the spatial diversity.

To the best of our knowledge, only a limited number of studies have addressed the problem of PNC in MWRC in the case $K < N$. In [28], the multiway relay network is decomposed into smaller building blocks, or *atoms*, over which existing TWRC techniques can be applied. In [29], a similar concept is considered where an opportunistic transmission protocol selects pairs of users for sequential transmission. Nonetheless, these approaches require at least $N - 1$ time slots for uplink transmission in an N-way relay channel. In [30], constellation design for simultaneous transmission of user signals in MWRC is formulated as a constrained optimization, where the aim is to maximize the minimal distance among the set of network-coded symbols. However, this scheme is designed for AWGN channels where the multiple user signals barely suffer from channel distortions, and their constellations are correctly superimposed at the relay. Aside from the intricate design, the scheme's complexity also increases rapidly when the number of users or the modulation order becomes large. In general, we find that existing approaches to the multiway PNC problems tend to follow concepts advanced for TWRC PNC, and rely on directly obtaining network codes from the superimposed signals at the

relay. However, unlike the TWRC scenario, this task becomes exceptionally challenging when the number of colliding signals increases, requiring: the use of special scheduling via the decomposition of the network into smaller subnets, mitigation of the multiuser interference for each code extraction, or complicated signaling designs allowing the relay to resolve codewords from a large superimposed constellation unambiguously. Consequently, these approaches often turn out to either have limited efficiency or suffer from high complexity.

1.2.2 Robustness of Network Code Chain

In a multi-way PNC system between N users, the relay typically broadcasts a chain of $N-1$ network codes, or symbols, that are designed to be strongly correlated with each other. Due to the correlation, the decoding performance of the complete set of messages at the user terminals highly depends on the probability of successfully detecting each network code in such chains. Hence, it is critical to devise mechanisms that can improve the probability of symbol detection for downlink PNC transmissions in MWRC.

Existing techniques for multi-user communications, e.g., precoding and power allocation schemes, are often devised based on power domain metrics, such as the signal-to-noise ratio (SNR), signal-to-interference-plus-noise ratio (SINR), and related quantities, including achievable information rates. For instance, the design of a precoding matrix for a multi-user system with an arbitrary number of antennas at the user terminals is addressed in [31], to mitigate the multi-user interference in the downlink channel. A block diagonalization approach is considered for the design of downlink multi-user precoders in [32], [33] where the precoding matrix is generated from the QR decomposition of the relay-to-user channel matrix to improve the achievable sum rate of the system. In [34], as an alternative to the SINR and SNR criteria, the authors present a so-called signal-to-leakage-and-noise ratio (SLNR) precoding scheme that considers the leaked power from one user to other users in a multi-user multiple-input and multiple-output (MIMO) system; the precoder design is thus based on maximizing the SLNR for all users. Some recent

works focus on alternative metrics such as the energy efficiency for the downlink multi-user multiple-input and single-output (MISO) systems [35] and target rates for downlink non-orthogonal multiple access (NOMA) systems [36].

Few works explicitly focus on improving the detection performance of a chain of correlated symbols, as needed for PNC in MWRC. In this regard, the success probability of Babai estimation introduced in [37], can provide a valuable metric for determining and enhancing the integrity of a chain of network codes received at user terminals. Babai estimation is an efficient tool that can be applied to the solution of a variety of estimation problems in wireless communications. In particular, it provides a suboptimal solution with low complexity to integer least squares problems occurring in the estimation of certain linear models [38, 39]. In this context, the success probability of Babai estimation characterizes the detection performance of a group of symbols within a successive detection process. However, these works mainly focus on theoretical performance analysis and do not utilize the success probability as a metric for practical system design.

1.2.3 Efficacy of Relay Detection

Successive interference cancellation (SIC) [40], which mitigates the effects of interference by discriminating superimposed signals based on their relative power levels, is a widely adopted detection scheme for multi-user communications. Existing studies on the efficiency of SIC mainly emphasize improving the sum rate of the system, where the aim is to enhance the average detection accuracy of the signals. For instance, an opportunistic relay selection strategy for an NC scheme is proposed in [41], where the goal is to choose the best relay maximizing the SINR among a subset of relays that correctly decoded the source signals in a previous time slot. In [42], a new superposition code based on PNC concepts along with two beamforming optimization approaches are presented to achieve an acceptable symbol error rate (SER) in the SIC detection, as part of an energy harvesting system for massive MIMO communications at millimeter waves (mmWaves) frequencies.

Many works exploiting the SIC detection for NOMA systems, such as [43–46], also address their respective problems from the perspective of the sum-rate maximization.

Unfortunately, only a limited number of works explicitly focus on improving the accuracy of the entire chain of correlated signals during the SIC process, which is critical for PNC in MWRC. In this regard, the work in [47] analyzes the closed-form expression of the word error rate (WER) for the SIC decoders, which characterizes the success probability of detecting all signals in the successive process. Thus, the WER provides a valuable metric for evaluating the quality of the entire chain of detected signals. However, this work mainly emphasizes theoretical analysis and does not provide further consideration on how to utilize the metric for practical system design.

1.3 Thesis Contributions

As pointed out earlier, the primary objective of the thesis is to develop new uplink and downlink schemes for PNC in MWRC. Specifically, we mainly focus on signal detection and power allocation to address various challenges in the extension of PNC to MWRC, i.e.: the network code extraction, the code chain robustness, and the relay detection efficacy. The thesis makes several contributions toward this general goal, as further explained below.

In Chapter 3, we propose a novel scheme for PNC in MWRC from the perspective of sequential multiuser detection. We consider an uplink MWRC scenario where N users, each equipped with a single antenna, simultaneously transmit their signal to a relay equipped with K antennas, where $K < N$. The extraction of the network codes from the superimposed user signals at the relay node is formulated as an under-determined linear system. To solve this problem with low decoding complexity, the proposed method combines SIC with Babai estimation for regularized integer least squares (ILS). Specifically, SIC decoding is first employed to detect a selected subset of stronger user signals and remove their interfering effects. Babai estimation is then applied to extract the remaining

user signals, which is formulated as an ILS problem with reduced dimension. We develop a power allocation scheme to enhance the performance of both the SIC and ILS steps and discuss an optimal user pairing strategy based on the average decoding error probability. Numerical results demonstrate the performance improvement of the proposed method in extracting network codes from multiple superimposed user signals.

In Chapter 4, we propose a novel power allocation scheme for PNC in downlink MWRC. The power allocation is formulated as a constrained optimization problem, where the aim is to maximize the success probability under a total power constraint when using Babai estimation for signal detection. Optimizing over this metric allows us to maximize the probability of successfully decoding a chain of network codes. The main contributions in this part can be summarized as follows. To meet diverse requirements for transmission quality in applications, we consider different aggregate measures of success probability over the participating user terminals, i.e., the arithmetic mean, the geometric mean, and the maximin. We first use an evolutionary particle swarm optimization (PSO) algorithm to solve the problem for the arithmetic mean, which is non-concave. We then formulate an alternative concave problem for this measure and find the solution via iterative methods. We obtain the solutions of the other two problems for the geometric mean and maximin, which are shown to be concave, via efficient iterative search methods. The proposed power allocation schemes for downlink PNC in MWRC are evaluated using computer simulations over Rayleigh fading channels. The results demonstrate the effectiveness of the proposed schemes in improving the success probability in the reception of a chain of network codes.

In Chapter 5, which focuses on the uplink of PNC in MWRC, we propose a novel power allocation for the SIC detection of pulse amplitude modulation (PAM) signals at the relay. To be specific, we first extend the work in [47] and develop a generalized expression for the closed-form success probability for SIC detection of the PAM signals. We then formulate a constrained optimization problem, where the aim is to maximize the success probability of the SIC detection at the relay under transmitting power constraints

at the user terminals. Optimizing over this metric maximizes the probability of correctly detecting the superimposed signals from all the users, which improves the efficacy of the network code generation at the relay. We conceive a PSO algorithm to solve this optimization problem where the cost function is complex and not necessarily concave. The simulation results confirm the validity of the newly derived expression for the success probability and also demonstrate the effectiveness of the proposed power allocation scheme in improving the relay's ability to extract network codes from the superimposed signals.

1.4 Organizations

The rest of the thesis is organized as follows. Chapter 2 provides a comprehensive review of essential background knowledge regarding the conventional NC, PNC, and MWRC. Chapter 3 focuses on the design of an efficient detection scheme for PNC in MWRC combining the SIC and Babai estimation. Chapter 4 investigates the design of power allocation schemes for the downlink PNC in MWRC from the perspective of success probability. Chapter 5 develops a closed-form expression for the success probability of SIC detection at the relay and presents a power allocation scheme for uplink PNC in MWRC based on this formulation. Finally, Chapter 6 summarizes and concludes the thesis.

Notations: The following notations are used throughout the thesis, unless otherwise specified. We use bold lower-case and upper-case letters for vectors and matrices, respectively. $\mathbf{A} = [a_{ij}]_{M\times N}$ denotes an $M \times N$ matrix with a_{ij} as the $(i,j)^{th}$ entry, while $\mathbf{I}$ and $\mathbf{0}$ are identity and zero matrices of appropriate dimensions. $\mathbf{A}^T$ and $\mathbf{A}^H$ denote the transpose and Hermitian transpose of a matrix $\mathbf{A}$. $\text{diag}(d_1, \ldots, d_n)$ returns a square diagonal matrix with diagonal entries $d_1, \ldots, d_n$. $||\cdot||$ and $|\cdot|$ refer to the Euclidean norm of vectors and modulus of scalars, respectively.

CHAPTER 2

Background

This chapter provides a review of essential background knowledge on the conventional NC scheme, the PNC scheme, and the MWRC. It serves as a foundation to help the reader better understand the proposed methods in subsequent chapters. The presentation is organized as follows: In Section 2.1, we reviewed the basic concept of the NC scheme. In Section 2.2, we proceed to review the PNC scheme, including its principles and more recent developments. In Section 2.3, the review of the MWRC is provided, including its application scenarios, general channel model, relay strategies, and recent studies. In Section 2.4, some concluding remarks are given at last.

2.1 Network Coding

For a long period in the history of communications, the traditional store-and-forward switching technique has been broadly adopted for conveying information from a source to a destination through a series of intermediate nodes [48]. The simplicity of this approach, in which intermediate nodes merely forward the received data without further modifying the original data contents, has made it dominant in transferring data over a network. However, with the rapid evolution of modern technologies has come the need for much increased data throughput. Traditional switching techniques have gradually

and inevitably fallen behind the curve to meet such demanding needs, especially in today's crowded network environment environments resulting from the massive production of affordable consumer-level electronic devices.

Within this burgeoning context, network coding has emerged as a new paradigm for boosting the network capacity [7]. In contrast to store-and-forward techniques where the intermediate node is merely a passive switch, the central idea of network coding is to allow intermediate nodes to be actively involved in the data transfer by mixing and processing original information from multiple data links. By doing this, the amount of information transmitted through the network can be greatly reduced and hence, the available network throughput is improved given the same condition of crowdedness.

The basic concept of network coding in a butterfly structure is illustrated in Fig. 2.1. A source node S seeks to transfer two bits X_1 and X_2 to destinations D_1 and D_2 through a series of intermediate nodes, labeled as R_1,R_2, R_3, and R_4. For simplicity, the data links are assumed to be error-free with unit capacity. When traditional store-and-forward techniques are utilized, intermediate nodes only forward the received information to their neighbors. The network throughput will be mainly limited by the bottleneck node R_2. As the data link between R_2 and R_4 only has unit capacity but needs to convey both data bits X_1 and X_2, it requires 4 time slots to complete the transmission, i.e.: 2 time slots for receiving and 2 time slots for broadcasting. When network coding is enabled, R_2 can mix X_1 and X_2 through an exclusive or operation (XOR), denoted as $X_1 \oplus X_2$, and only broadcast the mixture. Since D_1 and D_2 respectively know X_1 and X_2 from other data links, they can reconstruct X_2 and X_1 respectively by applying a reverse operation on the mixed data. In this way, the bottleneck node R_2 only needs 3 time slots to convey the information, i.e., 2 for receiving and 1 for broadcasting.

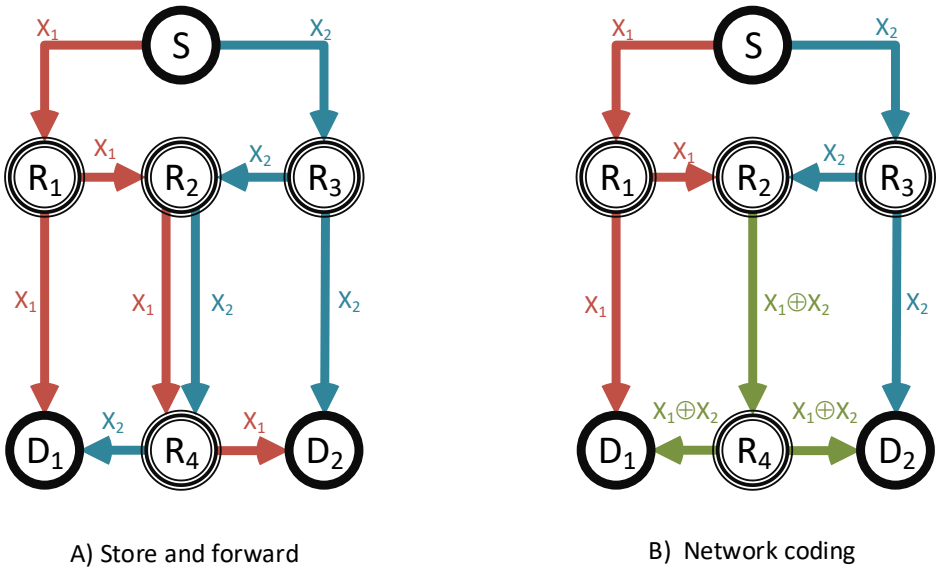

Fig. 2.1: Example of network coding in a butterfly structure.

2.2 Physical-layer network coding

Network coding was first introduced to boost the throughput of wired networks. However, with the rapid development of wireless technologies and widespread availability of low-cost mobile devices in the past decades, the need for larger network throughput has become a critical matter [49]. Below, we briefly discuss some of the challenges faced in boosting the efficiency of wireless communication networks, and how the application of PNC can help in addressing some of these challenges.

2.2.1 Challenges in Wireless Environments

One major factor that hinders transmission efficiency in wireless communications is signal interference in the open air. Indeed, in addition to the intended signal from a given transmitter, a receiver will capture other signals simultaneously emitted by different transmitters. In general, the superposition of the unwanted radio waves corrupts the intended signals and creates ambiguity when the receiver tries to reconstruct the original information. As an inevitable consequence of radio wave propagation in the open air, this

interference has has traditionally been treated as a destructive phenomenon in wireless communications.

For years, researchers have spent considerable efforts to find practical solutions to minimizing or eliminating such interference. Multiplexing techniques such as time-division multiplexing (TDM) and frequency-division multiplexing (FDM) [50] are probably the most well-known mechanisms to achieve such a goal. The basic idea behind them, as illustrated in Fig. 2.2, is to avoid interference by assigning radio signals from different sources into separated "cells" in either the time domain or the frequency domain. In this way, collisions among radio waves in the respective are ideally avoided due to the orthogonality among cells.

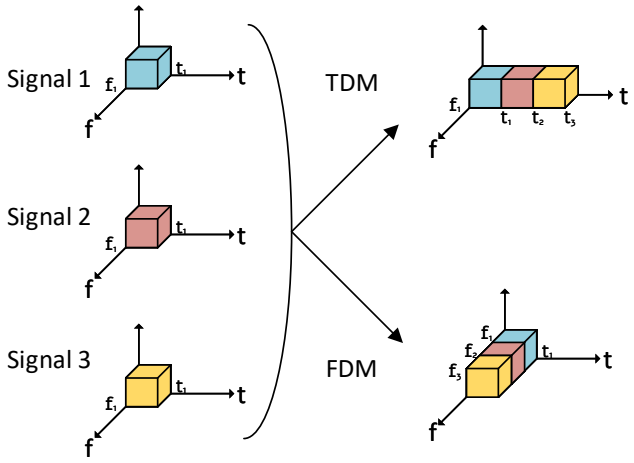

Fig. 2.2: Time-division multiplexing and frequency-division multiplexing techniques.

Although popular, the multiplexing techniques relying on the separation of signals in orthogonal domains have their disadvantages. The cost of avoiding interference in such manners is the need to occupy radio resources in the corresponding domain, i.e., time and frequency slots. With an excessively high demand for data transmission in today's wireless networks, radio resources are becoming incredibly expensive. For example, according to a report from the Federal Communication Commission (FCC) of the United States in 2021 [51], an auction of flexible-use overlay licenses in the 3.7-3.98 GHz band

alone raised a total of $ 81 billion in gross bid. In practice, the limited nature of available radio resources leads to network congestion or the reduced quality of service (QoS).

2.2.2 Exploiting the Nature of Wireless Medium

Besides continued efforts to eliminate interference, a new perspective has gradually emerged and gained popularity. Indeed, by exploiting the nature of the wireless medium, the unwanted radio waves that come from other transmitters need not be considered destructive: with a proper system design, the "interference" could be put to good use.

As explained in Fig. 2.1, the key to efficiency improvement with network coding lies in the use of the data mixture. As we have seen, if the intermediate node can directly receive such a mixture instead of receiving signals separately, the network efficiency will be improved. Still, achieving this in a wired network is usually challenging, as it requires modifications to the network structure, such as adding a node to mix the incoming data before the intermediate node receives them. This is because the data traveling in separated wires do not mix until they arrive at a common one.

In contrast, the wireless medium provides a natural way of mixing signals through the superposition principle (i.e., linearity of wave propagation). Since the introduction of *physical-layer network coding* (PNC) in [2], the broadcast nature of the wireless medium has been extensively exploited to further increase the efficiency. Instead of treating interference as an harmful factor in the transmission, the PNC scheme takes the mixture (or superposition) of radio waves in the open air as a natural input to the intermediate node. The intermediate node then can interpret this mixture and generate the desired network code from it. By doing so, the number of time slots required for the intermediate nodes to process the data is reduced.

2.2.3 Principles of Physical-layer Network Coding

The fundamental concept of PNC is illustrated in a two-way relay channel (TWRC) as shown in Fig. 2.3. TWRC refers to a three-node linear network structure, where source

nodes, S_1 and S_2, try to communicate via a relay R. The transmission process can be completed in 2 time slots by proceeding as follows: In the first time slot, S_1 and S_2 are allowed to transmit messages X_1 and X_2 simultaneously to the relay. For simplicity, we assume that these messages are binary, i.e., can only take two values represented by opposite polarities as in binary phase-shift keying (BPSK) modulation. The electromagnetic waves carrying the signals are mixed in the open air. The relay thus directly receives the superimposed signals Y_R containing superimposed information of X_1 and X_2. By properly selecting the permissible values of the messages X_1 and X_2, and under favorable conditions of transmissions, it is possible for the relay to generate a network code such as $X_R = X_1 \oplus X_2$ from the received signal Y_R Subsequently, the relay broadcasts X_R to S_1 and S_2 in the second time slot. Each node can then recover the desired information by respectively applying the mixing function on X_R and its self-information, e.g., obtaining $\hat{X}_2 = X_R \oplus X_1$ at node 1.

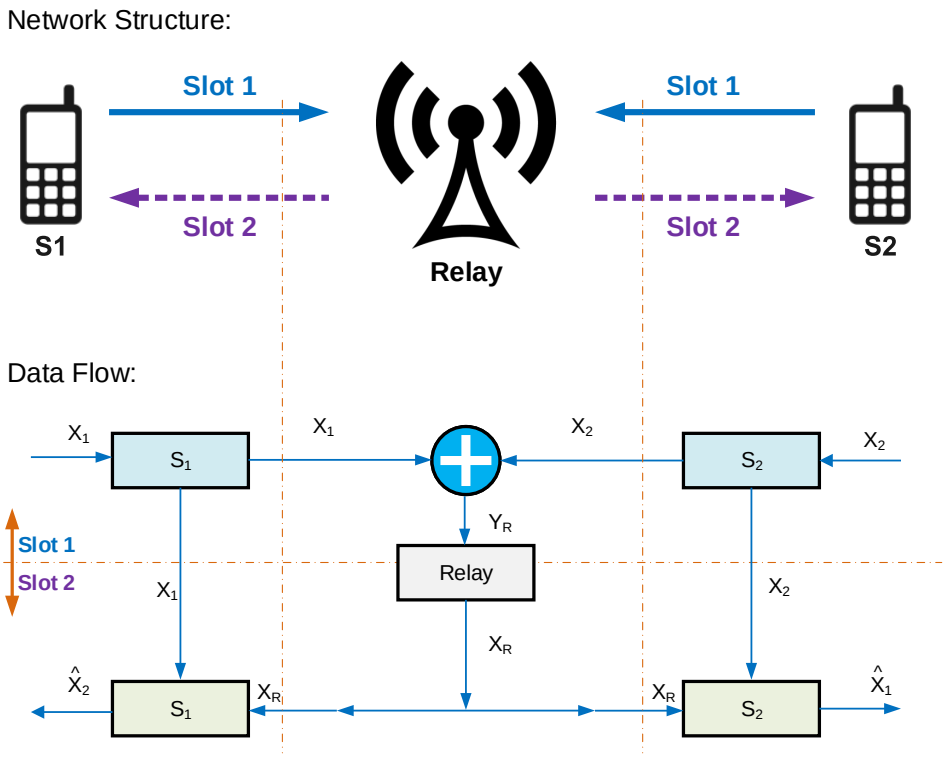

Fig. 2.3: Physical layer network coding in TWRC.

X_1 from node 1	X_2 from node 2	Received signal Y_R	Mapping to X_R
+1	+1	+2	+1
+1	-1	0	-1
-1	+1	0	-1
-1	-1	-2	+1

Table 2.1: PNC mapping at the relay.

The key to PNC lies with the relay's ability to deduce the network code X_R from the superposition Y_R of the transmitted signals. To provide a better understanding of this process, let us consider a particular example. Suppose that we adopt the exclusive-or operation as the mixing function, i.e., $X_R = X_1 \oplus X_2$, where values of $X_1, X_2 \in \{-1, +1\}$. We also assume a noise-free channel with unit gain and perfect synchronization at the relay. In such a case, the superimposed signals Y_R at the relay can take on three possible values depending on the input symbol X_1 and X_2 as shown in Table 2.1. That is,

- $Y_R = +2$ when $X_1 = +1, X_2 = +1$.
- $Y_R = 0$ when $X_1 = +1, X_2 = -1$ or $X_1 = -1, X_2 = +1$.
- $Y_R = -2$ when $X_1 = -1, X_2 = -1$.

It is clear that the relay does not necessarily need to know the exact value of X_1 and X_2 are to generate X_R. The proper mapping can be obtained directly from the observation of Y_R as follows:

$$X_R = \begin{cases} -1, & \text{if } Y_R = 0 \\ \\ +1, & \text{if } Y_R = -2 \text{ or } +2 \end{cases} \tag{2.1}$$

Based on the observation of X_R, S_1 and S_2 then use their self-information X_1 and X_2 to retrieve the desired information from the network code respectively.

It can be noticed that the difference between PNC and traditional NC is how the relay generates X_R. In the traditional NC, X_1 and X_2 are transmitted in different time slots, and the relay generates the network codes based on the explicit information of both signals. In

PNC, the network code can be directly generated from the superimposed signals, which requires one less time slot than the traditional method.

2.2.4 Issues and Existing Studies of PNC in TWRC

In this subsection, we provide an extensive literature review on the issues of PNC in TWRC regarding synchronization, error control, channel estimation.

Synchronization

One of the problems with PNC is that performance degrades when PNC does not run in perfect synchronization. There are different scales of synchronization problems. First, packets sent simultaneously by two user nodes do not necessarily arrive at the relay at the same time. Second, even if packets arrive at the same time, their symbol boundaries may not coincide, and the symbols of one node may overlap with two or more symbols of the other node. Third, even if the symbols of two nodes can be perfectly aligned, carrier frequency synchronization and relative phase shifts may cause problems.

Researchers' attention has been drawn to solving this key problem of the PNC. In [52], the authors first present the synchronization problem of PNC and investigate the impact of imperfect synchronization (i.e., finite synchronization error). In [53], the authors investigate a general framework for belief propagation (BP)-based receiver decoding that can efficiently handle the symbol and phase asynchrony problems and incorporate both channel coding. For non-channel coded PNCs, the BP approach reduces the asynchronous penalty compared to previous approaches. For channel-coded PNCs, the BP method improves the system performance with both symbol and phase asynchrony compared to the fully synchronous case. In [54], the authors propose a time synchronization scheme for broadband TWRC based on two-phase PNC. The synchronization scheme effectively separates the mixed signals and jointly estimates the time difference and channel parameters using the preamble in the frequency and time domains.

Error control

In general communication systems, noise and interference can be destructive to the signal in the open air. It is no exception for PNC systems, as the disturbance essentially reduces the ability of the relay to resolve the network code from the superimposed signal. Therefore, error control with channel coding is one of the most commonly used methods to cope with these problems.

The paper in [55] investigates link-by-link channel coding for PNC, where a key process of the relay station is to transform the superimposed channel coded packets received from both end nodes into a network coded combination of source packets. It designs a BP decoding algorithm for repeated accumulation codes of conventional point-to-point channels to accommodate PNC multiple access channels. In [56], a forward error correction is employed with a TWRC PNC system. Convolutional codes are considered to counteract the harmful effects of free-space turbulent channels to improve the reliability of the system. The authors in [57] design a practical modulation-coded PNC scheme to approach the capacity limit of Gaussian and fading TWRC. The method can be considered as a practical embodiment of the compute-and-forward scheme with well nested lattice codes that can be applied to a wide range of network configurations. The authors implemented a low-overhead channel precoding system in [58] that accurately aligns the channels of distributed nodes. The alignment are achieved by three methods, i.e., a channel precoding system implemented over field-programmable gate array (FPGA) to realize fast feedback of channel state information, a highly-accurate carrier frequency offset estimation method, and a partial-feedback channel estimation method reducing the amount of feedback information from the receiver to the transmitters for channel precoding at the transmitters.

Channel estimation

In a practical PNC system, the fading channel is also a key factor affecting the ability of the relay to resolve network codes. Therefore, the relay must effectively estimate both user-relay channels in TWRC to identify the superimposed signals. Otherwise, an incorrect estimation of the channel state can significantly mislead the network code generation at the relay station. Therefore, channel estimation in PNC systems has also received extensive attention.

The authors in [59] study the effect of incorrect channel estimation on the performance of PNC over fading channels. In this study, a statistical lower bound on the variance of the estimation error is shown, i.e., the relay terminal can tolerate it without introducing NC errors into the system. In [60], the authors address the joint channel estimation and channel decoding problem in TWRC PNC systems by combining an expectation-maximization algorithm and a BP algorithm on a unified factor graph framework. With this approach, the challenges posed by overlapped signals of multiple users, correlation between data symbols due to channel coding, and time-varying channels can be effectively addressed.

2.3 Multi-way Relay Channels

A multi-way relay channel (MWRC) is a basic structure of a relay network that generally involves all possible topological families of information flow between a relay node and its neighboring nodes. MWRC faces several challenges. For example, relay nodes usually operate in half-duplex mode, i.e., relay nodes receive and transmit signals in orthogonal blocks of time or frequency resources, which costs spectral efficiency. In addition, simultaneous signals from multiple user nodes usually cause multi-user interference. These challenges are usually more difficult to conquer than those in TWRC. In this section, we review the essential background of MWRC, including its application scenarios, general channel models, relaying strategies, and recent research.

2.3.1 Application Scenarios

MWRC is a generic channel model that can be used in a wide range of wireless application scenarios, such as cellular, satellite and aerial communications.

Cellular Communications As the millimeter wave band is used to meet the throughput demands of evolving wireless services [61–63], the high path attenuation and low penetration of electromagnetic waves at higher frequencies significantly reduces the coverage of conventional base stations. To solve this problem, the use of repeaters provides an efficient and economical solution. A typical scenario is when a user is in an enclosed area, such as an underground parking lot, and intends to connect to a base station on the ground. A relay can be deployed in the enclosed area to compensate for signal attenuation and connect to the base station via a wired line. The user, the repeater and the base station thus form a MWRC.

Statellite Communications Satellite communication is another key scenario for MWRC applications. The architecture of MWRC can be naturally applied to satellite communications, where satellites act as relay nodes in outer space, receiving signals from sources on Earth and forwarding them to their destinations [64, 65]. In addition, due to the advantages of broadband, large coverage and line-of-sight (LOS) transmission, satellites can effectively serve multiple users and support data exchange over long distances, such as intercontinental transmissions, which forms an MWRC on a large scale.

Unmanned Aerial Vehicle (UAV) Communications In recent years, UAVs have grown in popularity for a variety of uses. Due to the high altitude at which the vehicles fly, the communications established by UAVs are usually subject to less interference. Therefore, attention has been paid to the use of UAVs as flying wireless access points [66, 67]. In addition, the flexibility and convertibility of UAVs make it possible to act as an intermediate mobile node for challenging communication scenarios [68]. For example, in mountainous areas where base stations are not available or difficult to build, they can act as relay sta-

tions to easily connect rescue teams. In this case, UAVs and user terminals can form an MWRC.

2.3.2 General Channel Model

The general model of MWRC can be explained as follows. Without loss of generality, it is assumed that MWRC consists of N users exchanging information, and due to the deep fading channel environment, no direct links can be made between users. The data exchange between all users is through a common relay node. Each user has M antennas and the relay has K antennas, as shown in the Fig. 2.4.

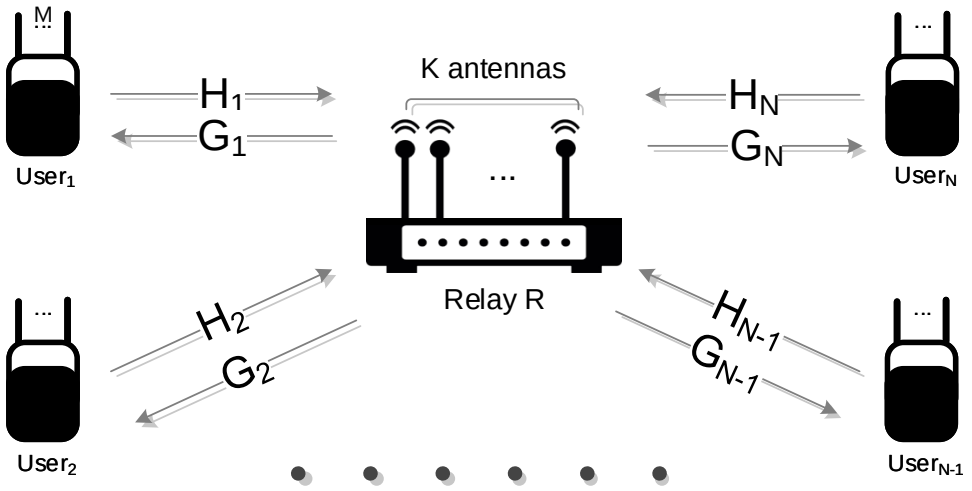

Fig. 2.4: An illustration of the general model of MWRC.

Each round of information exchange consists of two phases. The first phase is called the uplink phase, or the multiple access (MA) phase, in which users transmit signals to the relay station simultaneously. The signals received at the relay station are represented as follows:

$$\mathbf{y}_R = \sum_{i=1}^{N} \mathbf{H}_i \mathbf{x}_i + \mathbf{n}_R, \tag{2.2}$$

where $\mathbf{H}_i \in \mathbb{C}^{K\times M}$ denotes the channel matrix between user i and the relay in the uplink phase; $\mathbf{x}_i \in \mathbb{C}^M$ represents the transmit signal from user i; $\mathbf{y}_R \in \mathbb{C}^K$ is the superimposed signals received at the relay. $\mathbf{n}_R \in \mathbb{C}^K$ represents the additive white Gaussian noise (AWGN) at the relay.

The second stage refers to the downlink phase, or alternatively the broadcast (BC) phase, in which the relay broadcast signals to the user ends. The i^{th} user's received signal is thus represented as follows:

$$\mathbf{y}_i = \mathbf{G}_i\mathbf{x}_R + \mathbf{n}_i, \tag{2.3}$$

where $\mathbf{G}_i \in \mathbb{C}^{M\times K}$ represents the channel matrix between the relay and the i^{th} user during the BC phase; $\mathbf{x}_R \in \mathbb{C}^K$ denotes the signal from the relay; $\mathbf{n}_i \in \mathbb{C}^M$ denotes AWGN at user i.

2.3.3 Relay Strategies

As the central node of MWRC, the relay station plays an important role in data transmission. How it receives and forwards data has a direct impact on the performance of the entire transmission network. There are different strategies for the relay to process the received data. The most commonly used ones are described below.

Amplify-and-forward (AF) In AF relaying [69], the relay terminal amplifies its received signal subject to its power constraint and broadcasts to the receivers. The signal sent out from the relay is typically a linear transformed version of its received signal. That is:

$$\mathbf{x}_R = \mathbf{A}_R[\sum_{i=1}^{N}\mathbf{H}_i\mathbf{x}_i + \mathbf{n}_R], \tag{2.4}$$

where $\mathbf{A}_R = \text{Diag}(\sqrt{P_1},\ldots,\sqrt{P_K})$ for P_i, $i = 1,\ldots,K$ are the power allocated to each antenna of the relay. The AF relay is simple and cost-efficient to implement in practice. However, its downside is that the amplification operation by the relay also inevitably

increases the noise power. Consequently, performance degrades, especially in the low SNR region where noise is relatively large.

Decode-and-forward (DF) DF relay [70] decodes messages from all the users upon receiving and broadcasts them to all their receivers. Ideally, with perfect detection, the relay can recover the exact transmitted user signals and re-encode or pack them for the downlink transmission. A typical signal sent out from the relay thus can be given as:

$$\mathbf{x}_R = \mathbf{A}_R \sum_{i=1}^{N} \mathbf{x}_i, \tag{2.5}$$

The DF relay avoids noise amplification in theory. However, the decoding operation at the relay consumes more resources. Plus, the imperfect detection of user signals also imposes noises for the downlink transmission.

Compress-and-forward (CF) CF relay utilizes Wyner-Ziv coding [71] to compress the received signals before forwarding it to the destination. A scheme closely related to the CF strategy is quantize-map-and-forward (QMF) cooperation [72], in which the received signals at the relay are quantized before being forwarded to the destination. Like the DF scheme, the scenario is equivalent to broadcasting a common source to multiple receivers with correlated side information. However, unlike the DF scheme, the relay only needs to send a quantized version of the received signals rather than the lossless detected signals.

2.3.4 Existing Studies on MWRC

In this subsection, we review existing research on MWRC in channel estimation, power allocation, precoding, and beamforming.

Channel estimation

Channel state information is an important to a series of MWRC studies on MWRC, such as power allocation, precoding, beamforming and relay selection. Channel estimation in

point-to-point wireless communication systems typically requires two steps. The transmitter first sends a series of pilot signals that are known to both the transmitter and the receiver; then the receiver estimates the channel after receiving the known pilot signals. Similarly, in a MWRC system, all users send pilot signals to the relay simultaneously during the MA phase, and the relay estimates the state of the user-relay channel after receiving the pilot signals. In the BC phase, the user receives the pilot signal from the relay and estimates the state of the relay-user channel accordingly.

In [73], the authors develop a channel estimation framework for a multi-way quantized distributed relay network. Three sub-optimal channel estimators (including a linear channel estimator) are derived to provide lower complexity estimators. In [74], the authors investigate the asymptotic performance of MWRC with MIMO by modeling the channels to capture imperfect channel estimation, co-channel interference, pilot contamination, and channel aging. The authors in [75] analytically characterize the symbol-error rate (SER) performance of a functional decode and forward (FDF) MWRC in the presence of channel estimation errors. Asymptotic expressions for the average SER for a user in FDF MWRC are obtained based on the M-ary quadrature amplitude modulation with square constellations. The analysis shows that when a user decodes other users with better channel conditions than itself, the decoding user experiences better error performance.

Power allocation

The transmission power of nodes in MWRC needs to be appropriately allocated to improve the QoS of the system. QoS is usually measured by achievable total rate, SNR, bit error rate (BER) and other metrics. QoS-based power allocation is therefore also one of the important topics for MWRC research.

In [76], the authors propose a transmission protocol that combines massive MIMO technology with linear processing, self-interference cancellation, and successive cancellation decoding. Two power allocation schemes are proposed for this system. In the first scheme, transmit powers at the users and the relay are chosen to maximize the sum spec-

tral efficiency, subject to a given QoS requirement for each user. In the second scheme, the objective is energy efficiency, considering the hardware power consumption. The proposed transmission protocol based on both power allocation schemes effectively reduces the number of time-slots for data exchange among users. The authors in [77] propose a NOMA based massive MIMO MWRC transmit protocol to enable full-mutual data exchange. Closed-form results for the sum rate and the energy efficiency of the proposed scheme are obtained by using AWGN approximation. A relay power allocation matrix is designed to maximize the minimum among the user rates, thus maximizing user fairness. The authors in [78] propose an optimization design of beamforming vectors and power allocation for the MIMO asymmetric MWRC. An iterative algorithm based on orthogonal projection with signal subspace alignment is developed for the beamforming optimization to maximize the effective SNR. Based on the results of beamforming vectors, an optimal power allocation is designed to maximize the system sum rate.

Precoding and Beamforming

Precoding and beamforming have similar evaluation metrics to power allocation, i.e. they are also usually measured by the total achievable rate, SNR, BER, etc. Similarly, the performance of a communication system in MWRC can be greatly improved by proper precoding and beamforming. Therefore, this area of research has also attracted a large number of scholars' attention.

In [79], the paper studies the beamforming design for the MIMO MWRC with clustered full data exchange. A linear signal alignment in the model under a rank-constrained rank-minimization (RCRM) framework is considered. The RCRM problem is decomposed into independent rank-minimization subproblems, and an iterative algorithm for the beamforming design is thus proposed. The authors of [80] consider a network in MWRC with multiple users exchanging information. In this work, relay beamforming matrices and users' linear processing receivers are designed in the broadcast phases to maximize SINR under the relay power constraint. To further improve the performance,

the SIC at each user's receiver is implemented based on the SINR criterion to sequentially decode symbols from other users. The work of [81] introduces a non-regenerative MWRC, where a half-duplex multi-antenna relay station assists multiple nodes communicating with each other. Three low complexity linear transceiving beamformers based on zero-forcing, minimum mean square error, and maximization of SNR criteria are developed for N-phase multi-way relaying.

Relay Selection

In a larger scale MWRC communication network, the presence of multiple relay nodes provides higher adaptability and greater redundancy to the system. In such systems, effective optimization of communication links will allow the whole system to operate more efficiently. Therefore, relay selection or scheduling is also one of the many techniques investigated to improve the performance of MWRC systems.

In [82], the authors present a cloud-driven uplink framework for multi-way multiple-antenna relay systems, which aids joint symbol detection in the cloud. A multi-way relay selection protocol is proposed based on the selection of the best user link. A selection algorithm is devised based on the maximum-minimum-distance and channel-norm of user link to find the optimal link in the proposed system. In [83], the authors consider a network in MWRC in which all source nodes share their data with the help of multiple single-antenna relay nodes. A joint relay selection and power allocation scheme based on an approximation of the instantaneous symbol error probability incorporating error propagation is devised for the network. The authors in [84] develop a relay-selection strategy for multi-way cooperative multi-antenna systems that are aided by a central processor node. A multi-way relay selection strategy is proposed based on selecting the best link, exploiting the use of buffers and PNC, called multi-way buffer-aided max-link.

2.4 Chapter Summary

This chapter presented a review of the conventional NC schemes, the PNC scheme, and the MWRC architecture. Specifically, we first introduced the development of the conventional NC and its fundamental principle, which serves as a technical basis for this thesis. We then introduced PNC, which is an evolutionary scheme based on the conventional NC. Next, we discussed the most common issues of PNC in TWRC and reviewed existing solutions to them. Finally, we reviewed the background of MWRC, including its application scenarios, general channel model, relay strategies, and existing studies. This background review provides necessary information and serves as the basis for the research contributions presented in the subsequent chapters of this thesis.

CHAPTER 3

Efficient Detection Scheme for Physical-layer Network Coding in Multiway Relay Channels

In this chapter, we propose a novel scheme for PNC in MWRC from the perspective of sequential multiuser detection. We consider an uplink MWRC scenario where N users, each equipped with a single antenna, simultaneously transmit their signal to a relay equipped with K antennas ($K < N$). Extraction of the network codes from the superimposed user signals at the relay node is formulated as an under-determined linear system. The proposed method combines SIC with Babai estimation for regularized ILS to solve this problem with low decoding complexity. Specifically, SIC decoding is first employed to detect a selected subset of stronger user signals and remove their interfering effects. Babai estimation is then applied to extract the remaining user signals, which is formulated as an ILS problem with reduced dimension. We develop a power allocation scheme to enhance both SIC and ILS steps' performance and discuss an optimal user pairing strategy based on the average decoding error probability. Numerical results demonstrate the performance improvement of the proposed method in extracting network codes from multiple superimposed user signals.

3.1 System Model

As illustrated in Fig. 3.1, we consider a half-duplex multiway relay network where N users share information with each other through a common relay R. User terminals are equipped with single antenna while the relay is equipped with $K < N$ antennas[1]. We assume that there is no direct link among users, i.e., information exchange between two users needs to go through the relay. We consider radio transmission over narrow-band, i.e., frequency flat, slow fading channels. As a common assumption adopted in most existing works on PNC in TWRC [19, 85], perfect channel estimation and time synchronization are available for any node in the network. Data transmission proceeds in two stages, namely: multiple access (MA) or up-link and broadcast (BC) or downlink.

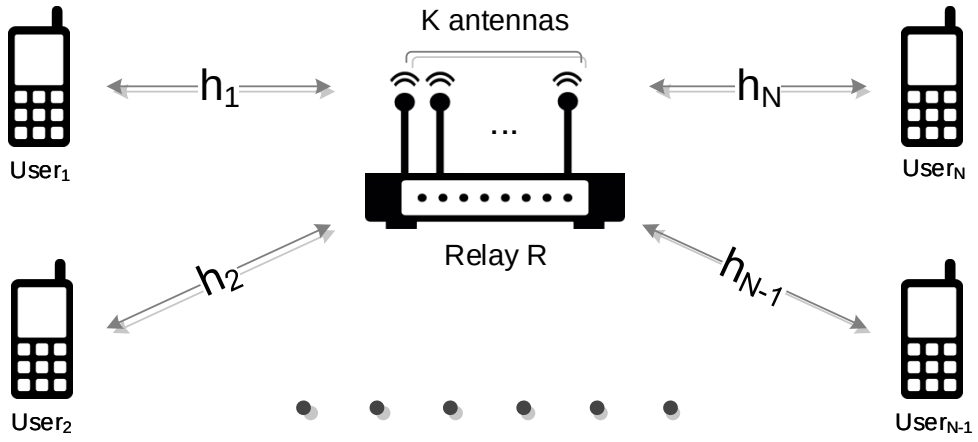

Fig. 3.1: Illustration of the MWRC system model.

3.1.1 MA Stage

Simultaneous Transmission

In the MA stage, all users simultaneously transmit signals to the relay so that only a single time slot is consumed. The signal transmitted by the i^{th} user is given by $\sqrt{P_i}s_i$, where s_i is a discrete random modulation symbol with zero mean and unit variance,

[1]The use of $K \geq 2$ makes it possible to exploit spatial diversity. While K can take on any integer value, the main focus in this work is on the case $K < N$.

while P_i is the allocated power to this user. To simplify the exposition, binary phase shift keying (BPSK) modulation is assumed, i.e., $s_i \in \{-1, +1\}$, although generalization to other symbol constellations are possible. The superimposed signals received at the relay are represented by:

$$\mathbf{y} = \mathbf{HAs} + \mathbf{n}_R, \tag{3.1}$$

where $\mathbf{y} = [y_1, \ldots, y_K]^T \in \mathbb{C}^{K\times 1}$ is the vector of received signals at the relay antennas, $\mathbf{s} = [s_1, \ldots, s_N]^T \in \{-1, +1\}^{N\times 1}$ is the vector of user symbols, $\mathbf{H} = [\mathbf{h}_1, \mathbf{h}_2, \ldots, \mathbf{h}_N] \in \mathbb{C}^{K\times N}$ is the channel matrix with column $\mathbf{h}_i \in \mathbb{C}^{K\times 1}$ representing the channel vector between the i^{th} user and the relay, $\mathbf{A} = \text{diag}(\sqrt{P_1}, \sqrt{P_2}, \ldots, \sqrt{P_N})$, and $\mathbf{n}_R \in \mathbb{C}^{K\times 1}$ is an additive noise vector with zero mean and covariance matrix $\sigma^2\mathbf{I}$.

Relay Detection and Network Coding

After the transmission, the relay generates $N-1$ valid codewords by selecting $N-1$ pairs of users and assigning to each pair a network code based on the received signal vector $\mathbf{y}$. Different strategies are possible for the selection of the $N-1$ user pairs [86], represented by (i, j) where $i, j \in \{1, 2, \ldots, N\}$, $i < j$. In the sequel, we denote by $\mathcal{C}$ the selected set of $N-1$ signal pairs. For instance, a straightforward approach consists in forming pairs by sequentially selecting neighboring user signals, i.e.:

$$\mathcal{C}_{seq} = \{(i, i+1) \mid i = 1, 2, \ldots, N-1\}. \tag{3.2}$$

Alternative strategies that lead to improved performance are considered in Section 3.3.4.

For each pair $(i, j) \in \mathcal{C}$, the next step consists in estimating the selected user signals s_i and s_j. To elucidate this step, let us expand (3.1) as follows:

$$\mathbf{y} = \underbrace{\left(\mathbf{h}_i\sqrt{P_i}s_i + \mathbf{h}_j\sqrt{P_j}s_j\right)}_{\text{desired signals}} + \underbrace{\left(\sum_{\substack{m=1\\ m\notin\{i,j\}}}^{N} \mathbf{h}_m\sqrt{P_m}s_m + \mathbf{n}_R\right)}_{\text{interference+noise}}, \tag{3.3}$$

where the first term contains the desired signal pair while the second term represents multi-user interference and noise. Based on (3.3), in the literature on PNC, estimation of the desired signal pair is typically formulated as a constrained least-squares problem, i.e.:

$$\{\hat{s}_i, \hat{s}_j\} = \arg \min_{s_i, s_j \in \{-1,+1\}} ||\mathbf{y} - \mathbf{h}_i \sqrt{P_i} s_i - \mathbf{h}_j \sqrt{P_j} s_j||^2. \tag{3.4}$$

Clearly, the multi-user interference may severely degrade the quality of these estimates when N increases.

At last, a valid network code is generated for each pair of estimated signals by applying a so-called mixing function, represented by $s_{ij} = \phi(\hat{s}_i, \hat{s}_j)$, where s_{ij} denotes the resulting network code. A common choice of mixing function $\phi(\cdot)$, which is used in this work for simplicity, is the bit-wise modulo-2 sum on the logical values of the estimated signals. Equivalently, this corresponds to multiplication in the finite field $\{-1, +1\}$, i.e.:

$$s_{ij} = \phi(\hat{s}_i, \hat{s}_j) = \hat{s}_i \hat{s}_j. \tag{3.5}$$

Consequently, by proceeding in this manner for every selected pair $(i, j) \in \mathcal{C}$, a finite sequence of $N - 1$ codewords is generated, i.e., $\{s_{ij}\}_{(i,j)\in\mathcal{C}}$.

3.1.2 BC Stage

During this stage, the relay broadcasts the network codes in $\{s_{ij}\}_{(i,j)\in\mathcal{C}}$ to the users. Since any uplink performance gain or loss will be accordingly passed on to the BC stage, the choice of the downlink transmission approach does not directly affect the performance evaluation of the detection schemes at the relay. For simplicity, we therefore consider a conventional scheme for the BC stage, namely, sequential broadcast using one time slot per code so that $N-1$ time slots are needed for a complete broadcast of the code sequence. Specifically, if s_{ij} is broadcast in a given time slot, the signal received at user m is given by:

$$r_m = g_m \sqrt{P_r} s_{ij} + n_m, \tag{3.6}$$

where P_r is the total transmit power of the relay, $g_m = h_m \in \mathbb{C}$ is the reciprocal downlink channel gain, and $n_m \in \mathbb{C}$ is the downlink noise. The channel gain g_m includes the combined effect of beamforming or pre-coding at the relay followed by parallel transmission from the K relay antennas to user m. Under the slow fading assumption, g_m remains constant during the BC stage.

Based on the observation of r_m in the corresponding time slot, user m obtains an estimate of s_{ij} (which we assume error-free for simplicity). Once the broadcast phase is completed after $N-1$ time slots, user m stores the detected code sequence $\{s_{ij}\}_{(i,j)\in\mathcal{C}}$ and then uses its self-information s_m to obtain the complete signal vector $\mathbf{s}$. For instance, if $\mathcal{C} = \mathcal{C}_{seq}$, user m obtains $\mathbf{s}$ by iteratively recovering each user signal from the detected sequence $\{s_{ij}\}_{(i,j)\in\mathcal{C}_{seq}}$, which is described as:

$$\begin{aligned} s_{k+1} &= \phi(s_{k,k+1}, s_k), \text{ for } k = m, m+1, \dots N-1 \\ s_{l-1} &= \phi(s_{l-1,l}, s_l), \text{ for } l = m, m-1, \dots 2 \end{aligned} \tag{3.7}$$

where the initial input s_m is the self-information of user m. An example of such process

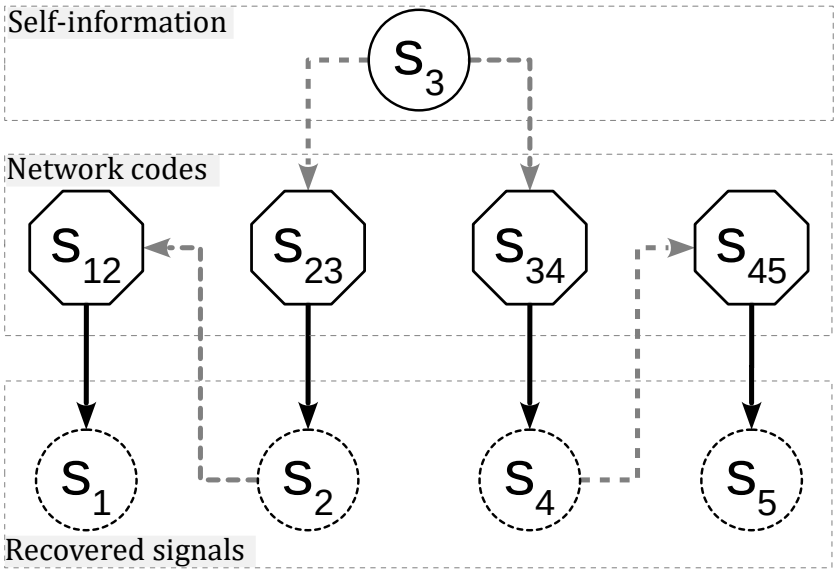

Fig. 3.2: Example of the iterative recovery process for $\mathcal{C}_{seq}$ at user 3. User 3 first uses its self-information to decode s_2 and s_4 and then detects s_1 and s_5.

is presented in Fig. 3.2. For the recovery to be effective, the selection strategy (i.e., set $\mathcal{C}$) must guarantee that all user signals are retrievable at an arbitrary user terminal. If $\mathcal{C}$ is not well designed, e.g., replacing $(3,4)$ by $(1,3)$ in $\mathcal{C}_{seq}$, the code sequence is invalid since the signal vector $\mathbf{s}$ can not be fully recovered in the BC stage.

3.2 The Proposed Method

According to (3.3)-(3.4), the presence of multi-user interference in the superimposed signals at the relay decreases the reliability of the estimated network codes $\{s_{ij}\}_{(i,j)\in\mathcal{C}}$, especially when N is large. In this section, we discuss methods to overcome this issue with the relay detection by first investigating the SIC process, Babai estimation for ILS, and the regularized ILS. We then develop the proposed method to resolve the user symbols from the superimposed signals in the MA stage.

3.2.1 Successive Interference Cancellation

SIC can be used at the relay to mitigate the interfering effect, by discriminating signals on the basis of their relative power levels. Specifically, the user signal with the largest received power is first detected and its interfering effect removed from the observation; the detection then proceeds sequentially to the next strongest signal. SIC will be used here as a preliminary step to remove part of the multi-user interference in (3.4), thereby facilitating the subsequent estimation of weaker signals by a more sophisticated ILS technique.

Under the assumption of known channel state information and power allocation scheme[2], let us arrange the user signals in ascending order of their received power at the relay. That is, define $\varrho_i = ||\mathbf{h}_i||^2 P_i$ and assume that $\varrho_i < \varrho_j$, $\forall i < j$. Also let γ_i denote the SINR under the assumption of perfect signal cancellation at each iteration of the SIC process, i.e.:

$$\gamma_i = \frac{\varrho_i}{\sum_{j<i} \varrho_j + \sigma^2}. \tag{3.8}$$

[2]Power allocation is discussed in detail in Section 3.3.

Using this notation, the SIC detection can be described by Algorithm 1, where γ_o is a threshold for detection. At the i^{th} iteration, when $\gamma_i > \gamma_0$ the algorithm detects the dominant user signal s_i as the solution of LS problem (3.9) and then cancels its effect from the current observation vector in (3.10). Ideally, this process repeats for each iteration until the weakest signal s_1 is detected. Hence, with a proper power allocation scheme, an estimated signal vector consisting of all user symbols can be detected, as given by $\hat{\mathbf{s}} = [\hat{s}_1, \ldots, \hat{s}_N]^T$.

Algorithm 1 SIC

1: $i = N$, $\mathbf{y}^{(i)} \leftarrow \mathbf{y}$
2: **while** $i \geq 1$ **do**
3: **if** $\gamma_i > \gamma_0$ **then**
4: Detecting s_i from $\mathbf{y}^{(i)}$:

$$\hat{s}_i \leftarrow \arg \min_{\xi \in \{-1,+1\}} ||\mathbf{y}^{(i)} - \mathbf{h}_i \sqrt{P_i}\xi||^2. \tag{3.9}$$

5: Removing influence of s_i:

$$\mathbf{y}^{(i-1)} \leftarrow \mathbf{y}^{(i)} - \mathbf{h}_i \sqrt{P_i}\hat{s}_i. \tag{3.10}$$

6: **else** Break **while**
7: **end if**
8: $i = i - 1$.
9: **end while**

Note that the SIC process does not depend on the number of relay antennas K. Algorithm 1 is thus always executable as long as the condition on γ_0 is satisfied. In theory, this process can recover the user signals at the relay for systems with arbitrary dimensions including underdetermined ones, i.e., $N > K$. In practice, however, the estimation accuracy of $\hat{s}_i$ highly depends on the relative strength of the term $\mathbf{h}_i\sqrt{P_i}s_i$ in $\mathbf{y}^{(i)}$ at each iteration. Specifically, the accuracy of $\hat{\mathbf{s}}$ depends on the power difference among the received user signals at the relay. With a given power limit P_T on the user terminals (i.e., $P_i \leq P_T$) and fixed channel gains, when the number N of the colliding user signals increases, the conditions for successful application of SIC cannot be maintained. Either the power difference between user signals is too small or the weaker signals are dominated by noise

and interference. To overcome this critical dilemma, we propose to use a complementary ILS-based solution for the detection of weaker signals.

3.2.2 Babai Estimation for Overdetermined ILS

MUD in linear systems can also be achieved by solving an ILS problem for the unknown user signals [37, 87–89]. Specifically, upon receiving the superimposed signal vector $\mathbf{y}$ in (3.1), the relay may attempt to solve the following problem:

$$\min_{\mathbf{s}\in\mathcal{B}} ||\mathbf{y} - \mathbf{HAs}||^2, \tag{3.11}$$

where $\mathcal{B}$ is the constraint set of the transmitted signal vector $\mathbf{s}$. Here, $\mathcal{B}$ is determined by the constellation of user signal symbols, i.e., $\mathcal{B} = \{-1, +1\}^N$. A solution to (3.11) can be obtained by the reduction and search processes. When the system is overdetermined[3], i.e., $K \geq N$, matrix $\mathbf{H}$ can be reduced by an QR decomposition with column pivoting, written as:

$$\mathbf{H\Pi} = [\mathbf{Q}_1, \mathbf{Q}_2] \begin{bmatrix} \mathbf{R} \\ \mathbf{0} \end{bmatrix} = \mathbf{Q}_1\mathbf{R} \tag{3.12}$$

where $\mathbf{\Pi}$ is a permutation matrix of order N decided by algorithms such as LLL-P, V-BLAST, or SQRD (see [37] and the references therein), $\mathbf{Q} = [\mathbf{Q}_1, \mathbf{Q}_2] \in \mathbb{C}^{K\times K}$ is unitary, and $\mathbf{R} \in \mathbb{C}^{N\times N}$ is upper triangular. The reduced ILS problem is expressed as:

$$\min_{\bar{\mathbf{s}}\in\mathcal{B}} ||\bar{\mathbf{y}} - \bar{\mathbf{R}}\bar{\mathbf{s}}||^2 \tag{3.13}$$

where $\bar{\mathbf{y}} = {\mathbf{Q_1}}^H\mathbf{y}$, $\bar{\mathbf{R}} = \mathbf{R\Pi^H A\Pi}$, and $\bar{\mathbf{s}} = \mathbf{\Pi}^H\mathbf{s}$. For later convenience, we define the permuted matrix $\bar{\mathbf{A}} = \mathbf{\Pi^H A\Pi} = \text{diag}(\sqrt{\bar{P}_1}, \ldots, \sqrt{\bar{P}_N})$, where $\bar{P}_i$ denotes the power allocated to $\bar{s}_i$. Note that the optimization problem (3.11) is NP-hard. To efficiently find

[3] An overdetermined system is often defined as one for which $K > N$; however, to simplify the presentation, we include the case $K = N$ as part of this condition.

a reasonable estimate of $\bar{\mathbf{s}}$, a sub-optimal solution called the Babai point $\bar{\mathbf{s}}^{\mathrm{B}}$ is of interest instead [37, 90]. The determination of $\bar{\mathbf{s}}^{\mathrm{B}}$ involves a sequence of element-wise (binary searches) where at each step, starting from the bottom row of $\bar{\mathbf{y}} - \bar{\mathbf{R}}\bar{\mathbf{s}}$ and moving up, previously detected signals are canceled followed by nulling of the residual. This process can be described as follows:

$$\bar{s}_i = \left\lfloor (\bar{y}_i - \sum_{j=i+1}^{N} \bar{r}_{ij}\bar{s}_j)/\bar{r}_{ii} \right\rceil, \tag{3.14}$$

for $i = N, \ldots, 1$, where $\lfloor \cdot \rceil$ denotes the nearest integer in $\{-1, +1\}$. The Babai point for estimating $\mathbf{s}$ is thus $\mathbf{s}^{\mathrm{B}} = \mathbf{\Pi}\bar{\mathbf{s}}^{\mathrm{B}}$.

We note that the Babai estimator is designed to trade accuracy for low detection complexity. A hard decision on each $\bar{s}_i$ is used in Babai estimation since the interfering effect of detected signals needs to be removed at each iteration. Therefore, this could lead to error propagation in the successive cancellation process and cause the performance degradation compared to a soft decision on the complete set of signals $\bar{s}_i$, $i = 1, \ldots, N$. However, since the detection at each iteration depends on the information from previous iterations, the soft decision has much higher complexity as it requires the cancellation process to repeat multiple times to obtain enough information, i.e., all possible Euclidean distances from the received signals to the constellation points, for decision making.

3.2.3 Formulation of Regularized ILS

According to (3.14), Babai estimation finds a solution to the problem (3.11) for the over-determined system, i.e., when $K \geq N$; however, it fails for the under-determined system, i.e., when $K < N$. In such a case, (3.12) generates a $K \times N$ upper-trapezoidal matrix $\mathbf{R}$ that has $N - K + 1$ nonzero entries in the K^{th} row. The additional non-zero terms create difficulties in the successive estimation of $\bar{s}_i$ for $i = N, \ldots, K$ in (3.14). Specifically,

following the QR decomposition of (3.1), we obtain:

$$\bar{y}_i = \bar{r}_{ii}\bar{s}_i + \sum_{j=i+1}^{N} \bar{r}_{ij}\bar{s}_j + \bar{n}_i, \tag{3.15}$$

where $\bar{n}_i$ is the i^{th} entry of $\bar{\mathbf{n}} = \mathbf{Q}_1^H \mathbf{n}_R$. The interfering term $\sum_{j=i+1}^{N} \bar{r}_{Kj}\bar{s}_j$ in (3.15) causes error propagation in the successive estimation process, undermining the reliability of the estimates $\bar{s}_i$.

To overcome this problem, we can regularize the cost function in (3.11) and formulate the regularized problem as an over-determined system with extended dimensions, to which (3.14) can be applied. Specifically, the ILS problem (3.11) is equivalent to:

$$\min_{\mathbf{s}\in\mathcal{B}} ||\mathbf{y} - \mathbf{HAs}||^2 + \lambda||\mathbf{As}||^2, \tag{3.16}$$

where $\lambda > 0$ is a regularization parameter. Since $||\mathbf{As}||^2$ is constant under the constraint $\mathbf{s} \in \mathcal{B}$, if $\mathbf{s}^*$ is the optimal solution to (3.11), it is also the solution to (3.16). Once λ is determined, problem (3.16) can be formulated as:

$$\min_{\mathbf{s}\in\mathcal{B}} ||\breve{\mathbf{y}} - \breve{\mathbf{H}}\mathbf{As}||^2, \tag{3.17}$$

where $\breve{\mathbf{y}} = [\mathbf{y}^T, \mathbf{0}_{N\times 1}^T]^T$ and $\breve{\mathbf{H}} = [\mathbf{H}^T, \sqrt{\lambda}\mathbf{I}_{N\times N}]^T$. Since the dimension of $\breve{\mathbf{H}}$ is extended to $(K+N)\times N$, Babai estimation can be applied directly to solve (3.17). We thus can obtain a reduced system similar to (3.13) , but with corresponding variables given by $\bar{\mathbf{y}} = \breve{\mathbf{Q}}_1^H\breve{\mathbf{y}}$, $\bar{\mathbf{R}} = \breve{\mathbf{R}}\breve{\mathbf{\Pi}}^H\mathbf{A}\breve{\mathbf{\Pi}}$, $\bar{\mathbf{s}} = \breve{\mathbf{\Pi}}^H\mathbf{s}$, where matrices $\breve{\mathbf{Q}} = [\breve{\mathbf{Q}}_1, \breve{\mathbf{Q}}_2]$, $\breve{\mathbf{R}}$ and $\breve{\mathbf{\Pi}}$ now refer to the QR decomposition of $\breve{\mathbf{H}}$ as in (3.12).

The regularization parameter λ, whose choice is usually related to the noise variance σ^2, affects the efficiency of general search algorithms such as sphere decoding [91, 92]. In the context of Babai estimation, the regularized system corresponding to (3.16) is written

as:

$$\begin{bmatrix} \mathbf{y} \\ \mathbf{0} \end{bmatrix} = \begin{bmatrix} \mathbf{H} \\ \sqrt{\lambda}\mathbf{I} \end{bmatrix} \mathbf{As} + \begin{bmatrix} \mathbf{n}_R \\ -\sqrt{\lambda}\mathbf{As} \end{bmatrix}. \tag{3.18}$$

Since the noise and the signal vectors $\mathbf{n}_R$ and $\mathbf{s}$ are independent, $\breve{\mathbf{n}}_R = [\mathbf{n}_R^T, (-\sqrt{\lambda}\mathbf{As})^T]^T$ has the covariance matrix $\breve{\mathbf{\Sigma}} = \text{diag}(\sigma^2, \ldots, \sigma^2, \lambda P_1, \ldots, \lambda P_N)$. After the QR reduction, the variance of the i^{th} entry of $\bar{\mathbf{n}} = \breve{\mathbf{Q}}_1^H \breve{\mathbf{n}}_R$ is a weighted arithmetic mean of the diagonal entries of $\breve{\mathbf{\Sigma}}$, given by:

$$\breve{\mathbf{q}}_i^H \breve{\mathbf{\Sigma}} \breve{\mathbf{q}}_i = \sum_{j=1}^{K} \breve{q}_{ij}^2 \sigma^2 + \sum_{l=1}^{N-K} \breve{q}_{i,K+l}^2 \lambda P_l, \tag{3.19}$$

where $\breve{\mathbf{q}}_i$ is the i^{th} column vector of $\breve{\mathbf{Q}}_1$. On the one hand, a small value of λ is desirable to reduce the noise variance and its harmful effects on the estimation accuracy. On the other hand, too small a value of λ can make the matrix $\breve{\mathbf{H}}$ ill-conditioned, which may create numerical instability in the estimation process. In practice, we find that λ should be chosen so that the noise variances for $\bar{\mathbf{n}}$ and $\mathbf{n}_R$ are on the same level. In light of the power constraint $P_i \leq P_T$ and considering the variance expression in (3.19), we adopt $\lambda = \sigma^2/P_T$ as the regularization parameter for the Babai estimation in this chapter.

3.2.4 The Proposed Algorithm

There still remain some issues regarding SIC and Babai estimation. As pointed out earlier, under power constraint on the user terminals, i.e. $P_i \leq P_T$, the performance of SIC will degrade as N increases. Besides, the ILS regularization in (3.16) is achieved via the introduction of a non-informative term $\lambda||\mathbf{As}||^2$, which is equivalent to the injection of extraneous noise in an augmented system as seen in (3.18)-(3.19). When $N \gg K$, this noise becomes a dominant factor in the solution of (3.17), which ultimately limits the ability of Babai estimation to resolve the user signals.

To overcome these problems, we propose a new algorithm that combines SIC and Babai estimation to efficiently solve problem (3.11) in the under-determined case $K < N$. The algorithm derivation relies on two main ideas. First, we note from (3.15) that after

the QR decomposition, there only remain $N - K + 1$ superimposed users signals in $\bar{y}_K$, instead of the N original signals. From the perspective of SIC, this operation is beneficial since it allows for larger power differences among the remaining signals. This suggests that we only apply SIC to extract $\{\bar{s}_i | i = K, \ldots, N\}$ from $\bar{\mathbf{y}}$, thereby taking advantage of the reduced number of colliding signals. Second, if a portion of the user signals, say $N - L > 0$, can be removed from the detection before the application of Babai estimation, this will reduce the regularized system dimension, i.e., lessen the gap between N and K from $N - K$ to $L - K$. Consequently, this will limit the harmful effects of the non-informative term $\lambda ||\mathbf{As}||^2$ on the solution of the regularized ILS problem, as discussed above.

To be specific, the proposed algorithm, which is presented as Algorithm 2, starts with a QR reduction of the original system (3.11). Under the assumption $K < N$, this yields:

$$\bar{\mathbf{y}} = \mathbf{Q}_1^H \mathbf{y}, \ \bar{\mathbf{A}} = \mathbf{\Pi}^H \mathbf{A} \mathbf{\Pi}, \ \bar{\mathbf{R}} = \mathbf{R} \bar{\mathbf{A}}, \tag{3.20}$$

where $\mathbf{Q} = [\mathbf{Q}_1] \in \mathbb{C}^{K \times K}$ is unitary and $\mathbf{\Pi}$ is a permutation matrix of order N so that $|\bar{r}_{K,i}| \leq |\bar{r}_{K,j}|, \forall i < j \in \{K, \ldots, N\}$. The original system is now reduced to (3.13) where $\bar{\mathbf{s}} = \mathbf{\Pi}^H \mathbf{s}$.

The SIC detection is then executed, aiming to resolve the last $N - K + 1$ signals $\{\bar{s}_i | i = K, \ldots, N\}$ of $\bar{\mathbf{s}}$ from $\bar{y}_K$. Let γ_i denote the SINR at iteration i, and let L denote the first value of i, as this index decreases from N to K, at which the condition on the required SINR for SIC detection is no longer met, i.e. $\gamma_L < \gamma_0$ for some threshold γ_0. At this point, the SIC process is interrupted and we set $\bar{\mathbf{s}}_L = [\mathbf{0}_{1 \times L}, \bar{\mathbf{s}}_{L+1}, \ldots, \bar{\mathbf{s}}_N]^T$. The algorithm then cancels the effect of the detected signals in $\bar{\mathbf{s}}_L$ from $\bar{\mathbf{y}}$ and generates related quantities as follows:

$$\begin{aligned} \mathbf{y}_T &= \bar{\mathbf{y}} - \bar{\mathbf{R}} \bar{\mathbf{s}}_L, \quad \mathbf{s}_T = \mathbf{T} \bar{\mathbf{s}} \\ \mathbf{H}_T &= \mathbf{R} \mathbf{T}^T, \qquad \mathbf{A}_T = \mathbf{T} \bar{\mathbf{A}} \mathbf{T}^T \end{aligned} \tag{3.21}$$

where $\mathbf{T} = [\mathbf{I}_L, \mathbf{0}_{L\times(N-L)}]$ is a truncation matrix.

The above steps lead us to the following truncated ILS problem with reduced dimension:

$$\min_{\mathbf{s_T}\in\{-1,+1\}^L} ||\mathbf{y}_T - \mathbf{H}_T\mathbf{A}_T\mathbf{s}_T||^2, \tag{3.22}$$

where the aim is to determine the remaining user signals in $\mathbf{s}_T$. If $L = K$, the problem is overdetermined (see footnote 3) and Babai estimation as described in (3.14) can be applied directly to (3.22). If $L > K$, however, the truncated problem is under-determined and ILS regularization of (3.22) is needed prior to Babai estimation.

Proceeding as in Section 3.2.3, we define:

$$\breve{\mathbf{y}}_T = [\mathbf{y}_T^T, \mathbf{0}_{L\times1}^T]^T,\ \breve{\mathbf{H}}_T = [\mathbf{H}_T^T, \sqrt{\lambda}\mathbf{I}_L]^T. \tag{3.23}$$

We next perform the QR decomposition of $\breve{\mathbf{H}}_T$, which gives the unitary matrix $\breve{\mathbf{Q}}_T = [\breve{\mathbf{Q}}_{T1}, \breve{\mathbf{Q}}_{T2}] \in \mathbb{C}^{(K+L)\times(K+L)}$, the permutation matrix $\breve{\mathbf{\Pi}}_T$ of order L based on the CH algorithm in [87], and the upper triangular matrix $\breve{\mathbf{R}}_T = \breve{\mathbf{Q}}_{T1}^H\breve{\mathbf{H}}_T\breve{\mathbf{\Pi}}_T$,. With the help of this decomposition, the regularized system is reduced to

$$\min_{\bar{\mathbf{s}}_T\in\{-1,+1\}^L} ||\bar{\mathbf{y}}_T - \bar{\mathbf{R}}_T\bar{\mathbf{s}}_T||^2, \tag{3.24}$$

where $\bar{\mathbf{s}}_T = \breve{\mathbf{\Pi}}_T^H\mathbf{s}_T$ and

$$\bar{\mathbf{y}}_T = \breve{\mathbf{Q}}_{T1}^H\breve{\mathbf{y}}_T,\ \bar{\mathbf{R}}_T = \breve{\mathbf{R}}_T\bar{\mathbf{A}}_T,\ \bar{\mathbf{A}}_T = \breve{\mathbf{\Pi}}_T\mathbf{A}_T\breve{\mathbf{\Pi}}_T^H \tag{3.25}$$

At this point, Babai estimation can be applied to solve (3.24).

Algorithm 2 The proposed algorithm

procedure QR-FACTORIZATION:
  Input: $\mathbf{H}$, $\mathbf{A}$, $\mathbf{y}$.
  QR decomposition: $[\mathbf{Q}, \mathbf{R}, \mathbf{\Pi}] = \text{qr}(\mathbf{H})$
  Return: $\bar{\mathbf{y}}$, $\bar{\mathbf{A}}$, $\bar{\mathbf{R}}$. ▷ Refer to (3.20)
end procedure
procedure PARTIAL DETECTION USING SIC
  Initialize: $i = N,\ \bar{y}^{(i)} \leftarrow \bar{y}_K$.
  while $i > K$ **do**
    if $\gamma_i \geq \gamma_0$ **then**
      Detect $\bar{s}_i$ from $y^{(i)}$:

$$\bar{s}_i \leftarrow \arg \min_{\xi \in \{-1,+1\}} |\bar{y}^{(i)} - \bar{r}_{K,i}\xi|^2.$$

      Cancel the effect of $\bar{s}_i$:

$$\bar{y}^{(i-1)} \leftarrow \bar{y}^{(i)} - \bar{r}_{K,i}\bar{s}_i.$$

    else Break **while**
    end if
    $i = i - 1$.
  end while
  Return $L = i,\ \bar{\mathbf{s}}_L = [\mathbf{0}, \bar{s}_{L+1}, \bar{s}_{L+2}, \ldots, \bar{s}_N]^T$.
  Removing the effect of $\bar{\mathbf{s}}_L$.
  Obtain: $\mathbf{y}_T$, $\mathbf{H}_T$, $\mathbf{A}_T$. ▷ Refer to (3.21)
end procedure
procedure REGULARIZED ILS
  Regularization of the truncated system.
  Obtain: $\breve{\mathbf{y}}_T$, $\breve{\mathbf{H}}_T$ ▷ Refer to (3.23)
  QR reduction of the regularized ILS system.
  Obtain: $\bar{\mathbf{y}}_T$, $\bar{\mathbf{R}}_T$, $\bar{\mathbf{A}}_T$ ▷ Refer to (3.25)
  Apply Babai estimation to solve:

$$\min_{\bar{\mathbf{s}}_T \in \{-1,+1\}^{L-1}} ||\bar{\mathbf{y}}_T - \bar{\mathbf{R}}_T\bar{\mathbf{s}}_T||^2$$

  ▷ Refer to (3.14)
  Return: $\bar{\mathbf{s}}_T$
end procedure

3.3 Power Allocation and User Pairing

In this section, a power allocation scheme for the proposed method that combines Babai estimation and SIC is developed. An optimal selection strategy for user pairs is also presented based on the decoding error probability.

3.3.1 Power Allocation for Babai Estimation

The comprehensive performance analysis of Babai estimation for overdetermined ordinary and box-constrained ILS problems can be found in [37, 87, 93]. Key results from these studies indicate that in the absence of a power allocation mechanism and when the noise level is small, the success probability, i.e., $\Pr(\mathbf{s}^{\mathrm{B}} = \mathbf{s})$ where $\mathbf{s}^{\mathrm{B}}$ is the Babai point, is upper bounded by a function of the determinant of the upper triangular factor from the QR decomposition (see (3.11)-(3.12)). Furthermore, the upper bound is reached if the diagonal entries of this matrix factor are identical.

In the context of Algorithm 2, Babai estimation is applied to (3.24) where the upper triangular matrix $\bar{\mathbf{R}}_T$ (following the QR decomposition of $\breve{\mathbf{H}}_T$) is given by:

$$\bar{\mathbf{R}}_T = \breve{\mathbf{R}}_T \bar{\mathbf{A}}_T = \begin{bmatrix} \sqrt{\bar{P}'_1}\breve{r}_{11} & \dots & \sqrt{\bar{P}'_L}\breve{r}_{1,L} \\ & \ddots & \vdots \\ & & \sqrt{\bar{P}'_L}\breve{r}_{L,L} \end{bmatrix}, \tag{3.26}$$

where $\bar{\mathbf{A}}_T = \mathrm{diag}(\sqrt{\bar{P}'_1}, \dots, \sqrt{\bar{P}'_L})$ is the corresponding power allocation matrix of $\bar{\mathbf{s}}_T$ after the permutation $\breve{\mathbf{\Pi}}_T$. According to the stated property of the success probability, it is desirable that the diagonal entries of $\bar{\mathbf{R}}_T$ be equal, i.e.:

$$\bar{P}'_i |\breve{r}_{ii}|^2 = \eta, \ \forall i \in \{1, \dots, L\}, \tag{3.27}$$

where η is a constant. However, when considering the power constraint on the user terminals, i.e. $\bar{P}'_i \leq P_T$, power allocation based on (3.27) is not always practical. Indeed, when

matrix $\breve{\mathbf{R}}_T$ is ill-conditioned, i.e. $\max\{|\breve{r}_{ii}|\}/\min\{|\breve{r}_{ii}|\} \gg 1$, the fulfillment of (3.27) for larger $|\breve{r}_{ii}|$ requires the transmitted power $\bar{P}_i'$ needs to be very small, causing the additive noise to become overwhelming during the detection.

Instead of equalizing the diagonal entries of $\bar{\mathbf{R}}_T$, we could try to maximize the SNR of each received user signal. Assuming perfect cancellation at each iteration of the Babai estimation, the SNR of the i^{th} user signal in $\bar{\mathbf{s}}_T$ is given by:

$$\tau_i = \bar{P}_i'|\breve{r}_{ii}|^2/\sigma_i^2,\ i = 1, \ldots, L, \tag{3.28}$$

where σ_i^2 is the noise variance after the regularization and the QR reduction, which is given by $\sigma_i^2 = \breve{\mathbf{q}}_{T1i}^H \breve{\mathbf{\Sigma}}_T \breve{\mathbf{q}}_{T1i}$, where $\breve{\mathbf{\Sigma}}_T = \text{diag}(\sigma^2, \ldots, \sigma^2, \lambda\bar{P}_1, \ldots, \lambda\bar{P}_L)$ and $\breve{\mathbf{q}}_{T1i}$ is the i^{th} column vector of $\breve{\mathbf{Q}}_{T1}$ in (3.25). While the SNR in (3.28) is maximized by allocating maximum power to each user, i.e. $P_i' = P_T$, this approach cannot be employed here. Indeed, we note from (3.15) that some of the user signals contained in $\mathbf{s}_T$, specifically $\bar{s}_i$ for $i = K, \ldots, L$, will interfere during the SIC process of Algorithm 2, which is aimed at removing the last $N - L$ signals in $\bar{\mathbf{s}}_L$ from $\bar{\mathbf{y}}$ prior to the Babai estimation. Hence, the elaboration of an adequate power allocation also requires consideration of the SIC process, which is discussed in next.

3.3.2 Power Allocation for SIC

Let's consider the power allocation for the user signals detected during the SIC process, i.e., $\{\bar{s}_i |\ i = L+1, \ldots, N\}$. Referring to (3.8), (3.20) and the SIC procedure in Algorithm 2, the SINR of $\bar{s}_i$ is given by:

$$\gamma_i = \frac{\bar{P}_i|r_{K,i}|^2}{\sum_{j=K}^{i-1} \bar{P}_j|r_{K,j}|^2 + \sigma^2}, \tag{3.29}$$

where the noise variance σ^2 is preserved by the unitary transformation $\mathbf{Q}_1$. Assuming perfect interference removal, a reliable estimate of $\bar{s}_i$ is achieved if it is sufficiently stronger than the remaining interference plus noise. This requires γ_i to exceed a given threshold, say $\gamma_i \geq \gamma_0,\ i = L+1, \ldots, N$. On the one hand, the greater the value of γ_i, the more

reliable is the estimate of $\bar{s}_i$ is. On the other hand, each $\bar{s}_i$ (except for $\bar{s}_N$) is seen as interference to its predecessors in the SIC process, suggesting that γ_i for $i = L+1, \ldots, N-1$ be also restrained. Considering this trade-off, a suitable approach for the selection of the powers $\bar{P}_i$ under the constraint $\bar{P}_i \leq P_T$, is to maximize the minimum value of γ_i [94]. The problem can be formulated as:

$$\max_{\{\bar{P}_i\}_{i=L+1}^{N}} \quad \min\left\{\gamma_i |\, i = L+1, \ldots, N\right\} \tag{3.30a}$$

$$\text{s.t. } \bar{P}_i \leq P_T,\ i = L+1, \ldots, N, \tag{3.30b}$$

where in this discussion, the values of $\bar{P}_K, \ldots, \bar{P}_L$ are assumed to be fixed. We find that the direct solution of such a maximin problem is quite challenging. Alternatively, we therefore replace problem (3.30) by the following more tractable form, where the goal is to maximize a lower bound on the SINRs γ_i:

$$\max_{\{\bar{P}_i\}_{i=L+1}^{N}, \gamma} \quad \gamma \tag{3.31a}$$

$$\text{s.t. } \frac{\bar{P}_i |r_{K,i}|^2}{\sum_{j=K}^{i-1} \bar{P}_j |r_{K,j}|^2 + \sigma^2} \geq \gamma, \tag{3.31b}$$

$$\bar{P}_i \leq P_T,\ \ i = L+1, \ldots, N. \tag{3.31c}$$

To solve problem (3.31), we first express constraint (3.31b) into the following form:

$$\bar{P}_i |r_{K,i}|^2 \geq \gamma \left(\sum_{j=K}^{i-2} \bar{P}_j |r_{K,j}|^2 + \sigma^2 + \bar{P}_{i-1} |r_{K,i-1}|^2\right) \tag{3.32}$$

where the last term is constrained as:

$$\bar{P}_{i-1} |r_{K,i-1}|^2 \geq \gamma \left(\sum_{j=K}^{i-2} \bar{P}_j |r_{K,j}|^2 + \sigma^2\right). \tag{3.33}$$

Substituting (3.33) into (3.32) and proceeding iteratively for $i = N, \ldots, L+2$, we obtain a relaxed set of conditions:

$$\bar{P}_i |r_{K,i}|^2 \geq \gamma(\gamma+1)^{i-L-1}\varsigma^2, \; i = L+1, \ldots, N, \tag{3.34}$$

where

$$\varsigma^2 = \sum_{j=K}^{L} \bar{P}_j |r_{K,j}|^2 + \sigma^2 \tag{3.35}$$

is the variance of the interfering terms from the perspective of $\bar{s}_{L+1}$. For the largest value of γ satisfying each inequality in (3.34), we have:

$$\bar{P}_i |r_{K,i}|^2 = \gamma(\gamma+1)^{i-L-1}\varsigma^2, \; i = L+1, \ldots, N. \tag{3.36}$$

Since $\bar{P}_i |r_{K,i}|^2 / \bar{P}_{i-1} |r_{K,i-1}|^2 = \gamma + 1 > 1$, we infer that $\bar{P}_i |r_{K,i}|^2$ is decreasing as index i runs from N to $L+1$. Note that signal $\bar{s}_N$ is the first one to be canceled and hence does not interfere with the detection of the remaining signals. For this reason, the maximum power can be assigned to this signal, i.e., $\bar{P}_N = P_T$, such that:

$$P_T |r_{K,N}|^2 = \gamma(\gamma+1)^{N-L-1}\varsigma^2, \tag{3.37}$$

from which γ can be obtained.

3.3.3 Power Allocation for Proposed Algorithm

Referring to (3.25)-(3.24), let us represent permutation matrix $\breve{\mathbf{\Pi}}_T$ of order L by a bijection π of $\{1, \ldots, L\}$ onto itself, mapping index i of $\mathbf{s}_T$ to index $j = \pi(i)$ of $\bar{\mathbf{s}}_T$, so that $\bar{s}_i = \bar{s}_{Tj}$ and accordingly, $\bar{P}_i = \bar{P}'_j$. Since the signals $\bar{s}_i$ for $i = K, \ldots, L$ are detected as part of the Babai estimation process, it is desirable for their SNRs to be as large as possible. This suggests that the value of ς^2 in (3.35), which involves $\bar{P}_i$ for $i = K, \ldots, L$, can not be too small.

However, considering (3.37), we see that under a power constraint, this requirement on ς^2 conflicts with that of maximizing γ.

To overcome this difficulty, we modify the single objective problem (3.31) into a multi-objective optimization problem over γ for the SIC process and τ_i, $i = 1, \ldots, L$, for the Babai estimation. The modified problem is formulated as:

$$\max_{\{\bar{P}_i\}_{i=1}^{L}, \gamma} [\gamma, \tau_1, \ldots, \tau_L], \tag{3.38a}$$

$$\text{s.t. } \bar{P}_T |r_{K,N}|^2 = \gamma(\gamma+1)^{N-L-1}\varsigma^2 \tag{3.38b}$$

$$\bar{P}_i \leq P_T, \text{ for } i = 1, \ldots, L, \tag{3.38c}$$

where ς^2 is given in (3.35) and $\bar{P}_i = \tau_j \sigma_j^2 / |\breve{r}_{jj}|^2$ with $j = \pi(i)$.

There exist several approaches [95] to solve the multi-objective problem (3.38). Here, we adopt the weighted-sum method, which aggregates the multiple objectives into a single objective via a linear combination with positive weight. Since all user signals are of equal importance in the network coding process, it is fair to consider that variables γ and τ_i are also equally important. In addition, γ has an influence on the detection performance of $N - L$ user signals. Hence, we assign the weight $N - L$ to γ and a unit weight to each τ_i for $i = 1, \ldots, L$. The problem (3.38) is then converted into:

$$\max_{\{\bar{P}_i\}_{i=1}^{L}, \gamma} (N-L)\gamma + \sum_{j=1}^{L} \tau_j \tag{3.39a}$$

$$\text{s.t. } \bar{P}_T |r_{K,N}|^2 = \gamma(\gamma+1)^{N-L-1}\varsigma^2, \tag{3.39b}$$

$$\bar{P}_i \leq P_T, \text{ for } i = 1, \ldots, L. \tag{3.39c}$$

Since problem (3.39) involves a single objective with non-linear constraint, a standard nonlinear programming solver can be applied to obtain the solution, denoted as $\{\bar{P}_i^*\}_{i=1}^{L}$

and γ^*. The power allocation in terms of $\bar{P}_i$ is thus given as:

$$\bar{P}_i = \begin{cases} \bar{P}_i^*, & i = 1, \ldots, L \\ \gamma^*(\gamma^*+1)^{i-L-1}\varsigma^{*2}/|r_{K,i}|^2, & i = L+1, \ldots, N \end{cases}, \tag{3.40}$$

where $\varsigma^{*2} = \sum_{i=K}^{L} \bar{P}_i^* |r_{K,i}|^2 + \sigma^2$, and $\gamma_0 = \gamma^*$ is set as the threshold for stopping the SIC process. Finally, the desired powers P_i of the transmitted signals in (3.1) can be obtained by applying an inverse permutation of $\mathbf{\Pi}$ in (3.20) to $\bar{P}_i$ for $i = 1, \ldots, N$.

3.3.4 User Pairing Strategy

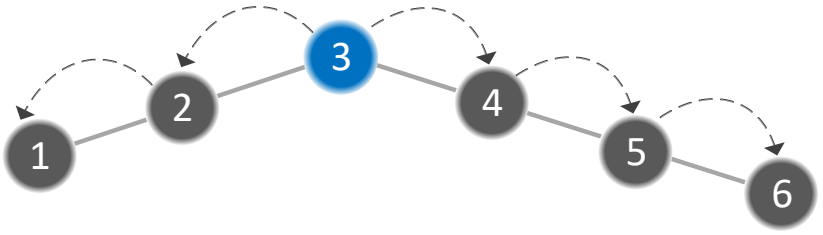

Fig. 3.3: Illustration of the tree structure of the sequential pairing strategy $\mathcal{C}_{seq}$ in a 6-way relay network. The graph demonstrates a process where user 3 decodes all other user signals by proceeding through the branches in two directions.

As explained in Section 3.1, the detected user signals at the relay need to be encoded into network codes. The pairing strategy, represented by the set $\mathcal{C}$ of pairs (i, j), will influence the decoding performance of user terminals in the BC stage. For this reason, it is worth considering an optimal selection strategy for the user pairs at the relay.

From the perspective of graph theory, a valid strategy $\mathcal{C}$ can be represented as a tree, where the N users and the $N-1$ user pairs form the vertices and edges respectively, and each pair of vertices in the tree is connected by a unique path. Taking a 6-way relay network as an example, the graph of a sequential pairing strategy $\mathcal{C}_{seq}$ (see (3.2)) takes the form of the tree depicted in Fig. 3.3. The iterative decoding process in a specific user terminal, as given by (3.7) for $\mathcal{C}_{seq}$, is equivalent to a walk in tree, starting from the vertex

of that user, and progressing towards the other users. In general, when a user terminal i decodes the signal of a user j, the corresponding path along the tree $\mathcal{C}$ is given by:

$$\mathcal{L}_{(i,j)} = \{(i,a),(a,b),\ldots,(d,j)\} \subset \mathcal{C}, \tag{3.41}$$

where $a, b, \ldots, d$ represent the intermediate vertices.

Let us denote by ψ_{ij} the decoding error probability of signal s_j in user terminal i. Essentially, ψ_{ij} depends on the network codes $s_{\alpha\beta}$, where $(\alpha,\beta) \in \mathcal{L}_{(i,j)}$. The reliability of $s_{\alpha\beta}$ is related to both up-link and down-link transmissions, which can be characterized by error probabilities $\psi^{ul}_{(\alpha,\beta)}$ and $\psi^{dl,i}_{(\alpha,\beta)}$ respectively. For binary signaling, a correct code $s_{\alpha\beta}$ is generated in the MA stage when two correct or two wrong decisions are made on s_α and s_β. Hence, $\psi^{ul}_{(\alpha,\beta)}$ can be expressed as:

$$\psi^{ul}_{(\alpha,\beta)} = \psi_{e\alpha}(1-\psi_{e\beta}) + \psi_{e\beta}(1-\psi_{e\alpha}), \tag{3.42}$$

where $\psi_{e\alpha}$ and $\psi_{e\beta}$ represent the error probabilities for the estimation of signals s_α and s_β at the relay. The probability $\psi^{dl,i}_{(\alpha,\beta)}$ is determined by the quality of the link from the relay to user i during the BC stage, as represented by (3.6). Under the slow fading assumption for the downlink channels, the error probabilities $\psi^{dl,i}_{(\alpha,\beta)}$ can be regarded as identical for different edges $(\alpha,\beta) \in \mathcal{L}_{(i,j)}$.

We note that an odd number of incorrect codes along $\mathcal{L}_{(i,j)}$ leads to a wrong decision on s_j, while an even number leads to a right decision. Hence, obtaining the exact value of ψ_{ij} requires a careful consideration of the error propagation effects which entails high computational costs. For simplicity, we approximate these effects by adopting a high SNR assumption as proposed in [96], i.e., ignoring even numbers of propagated errors whose small probabilities have negligible influence on ψ_{ij}. Numerical results later demonstrate that our approximation approach has a comparable effect to that observed in [96]. Assuming independence of the uplink and the downlink transmissions, ψ_{ij} is hence given

by:

$$\psi_{ij} = 1 - \prod_{(\alpha,\beta)\in\mathcal{L}_{(i,j)}} (1 - \psi^{ul}_{(\alpha,\beta)})(1 - \psi^{dl,i}_{(\alpha,\beta)}). \tag{3.43}$$

For a given pairing strategy C, the average decoding error probability can be expressed as:

$$\psi_e^{avg} = \frac{1}{N^2 - N} \sum_{i=1}^{N} \sum_{j=1, j\neq i}^{N} \psi_{ij}, \tag{3.44}$$

where ψ_{ij} is given by (3.43).Finally, an optimal strategy $\mathcal{C}^*$ can be found by an extensive search over all valid pairing strategies $\mathcal{C}$ so that the minimum ψ_e^{avg} is achieved:

$$\mathcal{C}^* = \arg\min_{\mathcal{C}} \psi_e^{avg}. \tag{3.45}$$

In (3.45), the search space consists of all the spanning trees of a simple undirected connected graph on N vertices [97], the size of which is determined by Cayley's Formula [98]. In this work, the various error probabilities entering the calculation of the objective (3.44) are obtained through a simulation approach.

3.4 Simulation Experiments and Discussions

This section presents numerical evaluation results of the proposed scheme for PNC in MWRC. To this end, we use Monte Carlo experiments based on the following system configuration. BPSK signaling is adopted at both the relay and the user terminals, whose maximum transmitting power is normalized to $P_T = 1$. We assume the various radio links to be Rayleigh fading, i.e., the entries of the channel matrix $\mathbf{H}$ in (3.1) are modeled as independent complex circular Gaussian random variables with zero mean and unit variance. The noise variance at each receiving antenna is adjusted to obtain the desired SNR level. To simplify the discussion and minimize the effects of indirect factors in the

performance comparison among the different estimation schemes , we consider uncoded systems as in, e.g., [99]. [4]

3.4.1 Conventional SIC and Babai Estimation

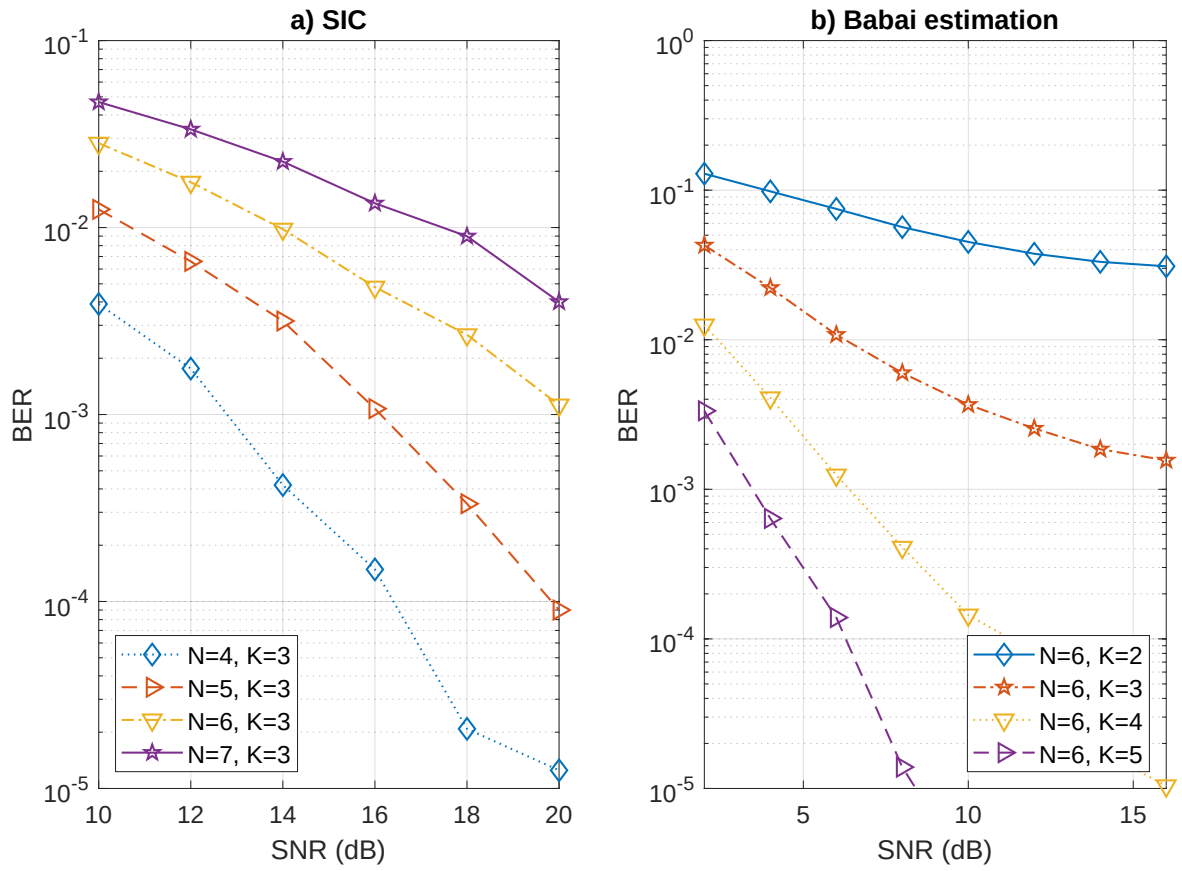

Fig. 3.4: BER performance of conventional SIC and Babai estimation for different choices of N and K

[4]Indirect factors, such as channel coding which adds redundant bits to the transmitted data stream for error corrections, can improve the BER performance regardless of what estimation scheme is employed. However, the use of such techniques can push down the BER values to an extremely low level where it can be more difficult to observe meaningful gains brought by the use of different estimation schemes. For this reason, we demonstrate the system performance in our simulations by only considering uncoded systems to avoid any ambiguity caused by these indirect factors. Nevertheless, the integration of channel coding within the proposed schemes remains worthy of investigation for real-world applications.

We begin by investigating the BER performance of the conventional SIC and the Babai estimation in solving underdetermined systems. Fig. 3.4(a) shows the BER performance of SIC for $K = 3$ relay antennas and different numbers of user N. We can observe that as N increases from 4 to 7 in this case the BER increases rapidly at any given SNR level. This effect, which is caused by the reduction of the power difference between the user signals as N increases, illustrates the fundamental limitation of SIC discussed in Section 3.2.4. Fig. 3.4(b) shows the BER performance of Babai estimation for $N = 6$ users and different numbers of antennas K. It is seen that as K increases from 2 to 5, the BER decreases rapidly at any given SNR level. This result illustrates the harmful effects of the non-informative term in (3.16) when the system becomes severely rank deficient.

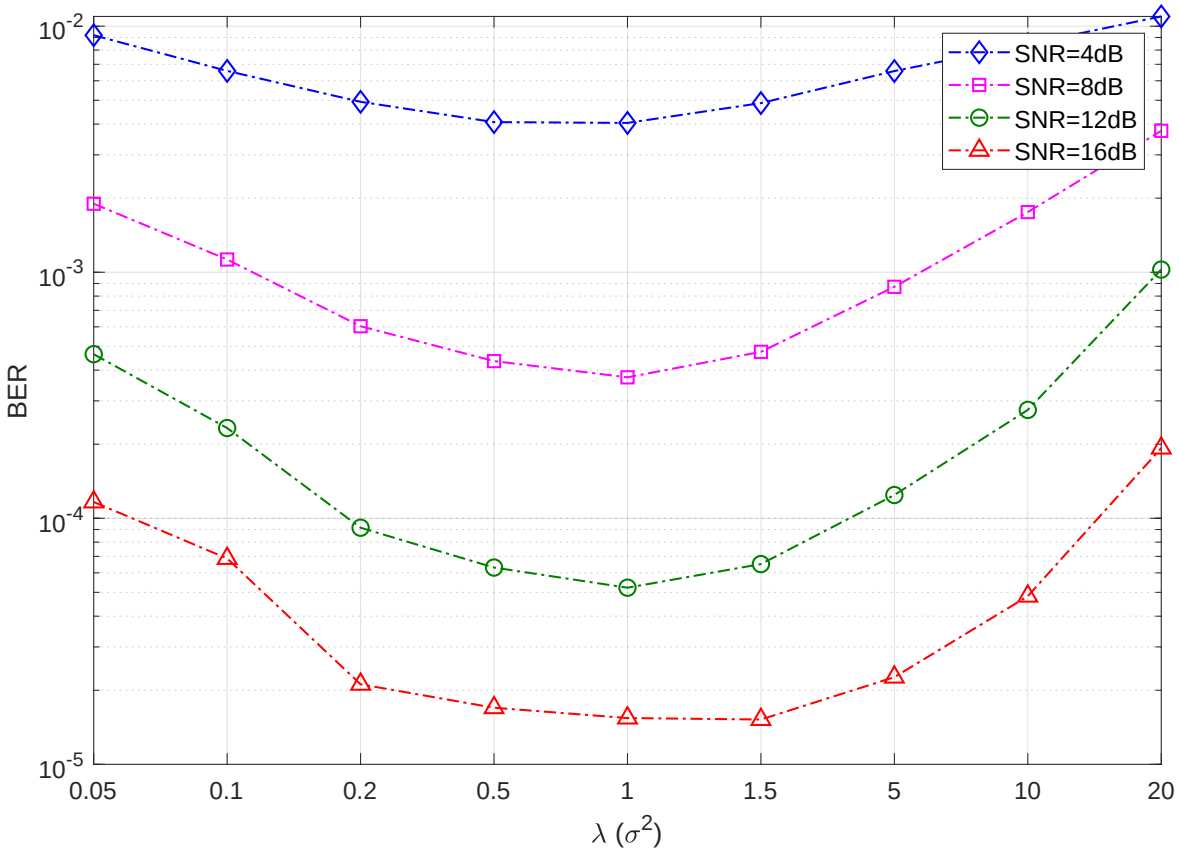

Fig. 3.5: Impact of λ on the BER performance for Babai estimation.

Next, we investigate the effect of the regularization parameter λ in (3.16) on the performance for Babai estimation. Fig. 3.5 illustrates the BER versus $\lambda = \ell\sigma^2$ with $\ell \in \{0.05, 0.1, 0.2, 0.5, 1, 1.5, 5, 10, 20\}$ for different SNR levels under configuration $N = 6, K = 4$. It can be seen that the best performance[5] is obtained when $\lambda \approx \sigma^2/P_T = \sigma^2$, which supports our proposed choice for this parameter in Section 3.2.3.

3.4.2 Evaluations of Proposed Method

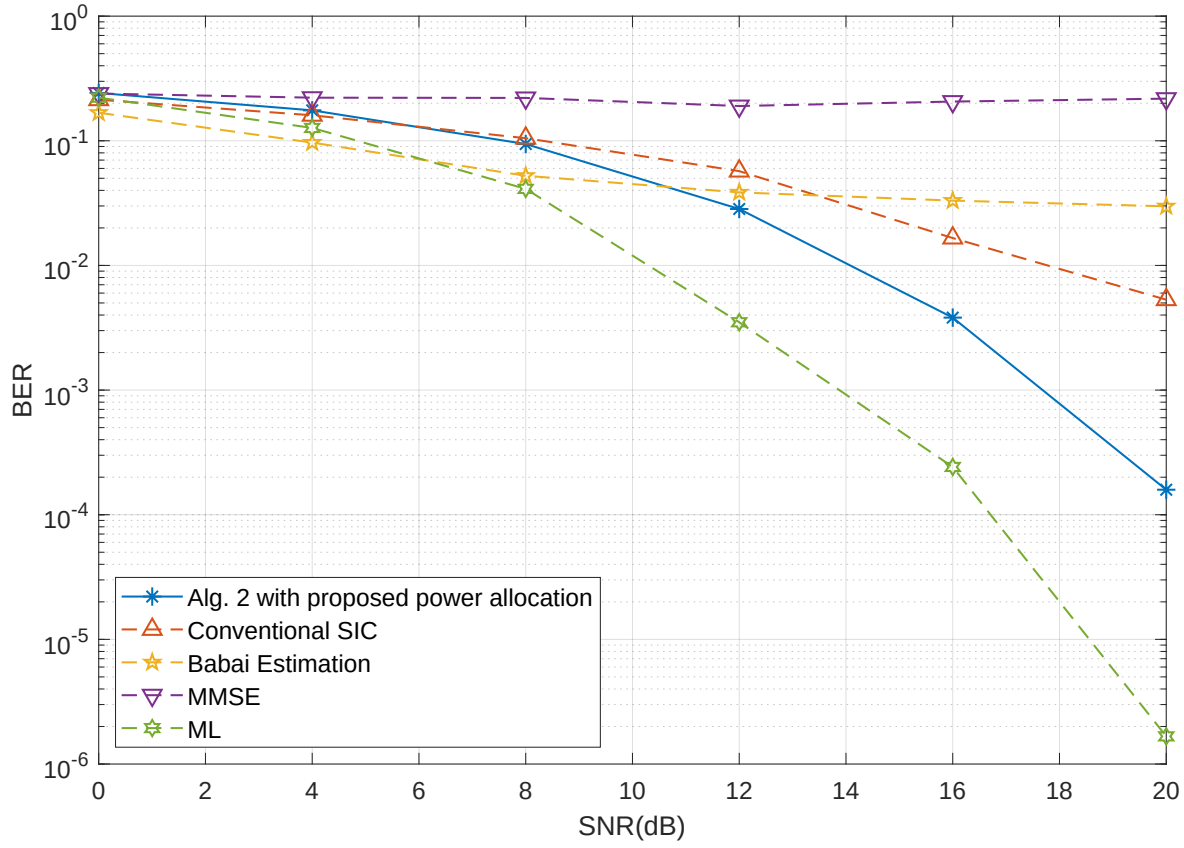

Fig. 3.6: BER performance of the proposed algorithm, conventional SIC, Babai estimation, MMSE estimation and ML estimation for $N = 6$ and $K = 2$.

[5]We note that different combinations of N and K will result in different BER vs λ curve. However, the trend of these various curves is similar to that exhibited in Fig. 3.5: in particular, the best performance is achieved when $\lambda \approx \sigma^2$. For this reason, we only consider a system with $N = 6$ and $K = 4$ for demonstration.

Fig. 3.6 compares the BER performance of the proposed Algorithm 2 to the conventional SIC and Babai estimation in the case $N = 6$ and $K = 2$. Results of minimum mean square error (MMSE) and ML estimations are also presented as benchmarks for comparison. A specific power allocation scheme is used for each one of these methods as exposed in Section 3.3, in order to optimize performance. From the result, we note that the Babai estimation slightly outperforms the other two methods in the low SNR range from 0dB to 12dB, but its advantage quickly disappears afterward. Beyond this point, our proposed Algorithm 2 with power allocation (3.40) exhibits the best performance, with a rapid falloff in BER as the SNR increases. Although the performance of SIC is superior to Babai estimation at high SNR, the gains are limited compared to the proposed algorithm. From the result, we also note that conventional MMSE estimation is not effective in solving under-determined problem while the ML estimation achieves the best performance at a cost of exhaustive search for the optimal solution.

In Fig. 3.7, we investigate the throughput performance of the proposed algorithm, which is defined as the rate of correct signal detection at the relay. For the sake of comparison, we also consider the Atom I building block structure in [28], which decomposes the network into $N - 1$ subnets to allow simultaneous transmission from only 2 users at a time (TWRC). This is in contrast to the proposed algorithm which allows simultaneous transmission from all N users (MWRC) during the MA stage. Specifically, Fig. 3.7 shows the throughput versus SNR for $K = 4$ and $N \in \{6, 8\}$, as obtained by transmitting 50×10^3 symbols from each user within a common time interval for both schemes. The results clearly illustrate the advantages of the proposed MWRC detection algorithm, which leads to a nearly 4dB SNR gain over the Atom I TWRC scheme. Indeed, under the constraint of a fixed transmission time, Atom I must reduce the amount of time allocated to each subnet, which tends to increase the error rate for the individual user signals.

Next, we compare the decoding complexity of Algorithm 2 to a constellation design approach, i.e., the minimal constellation distance maximization in [30]. The decoding complexity here refers to the number of constellation points that need to be searched at the

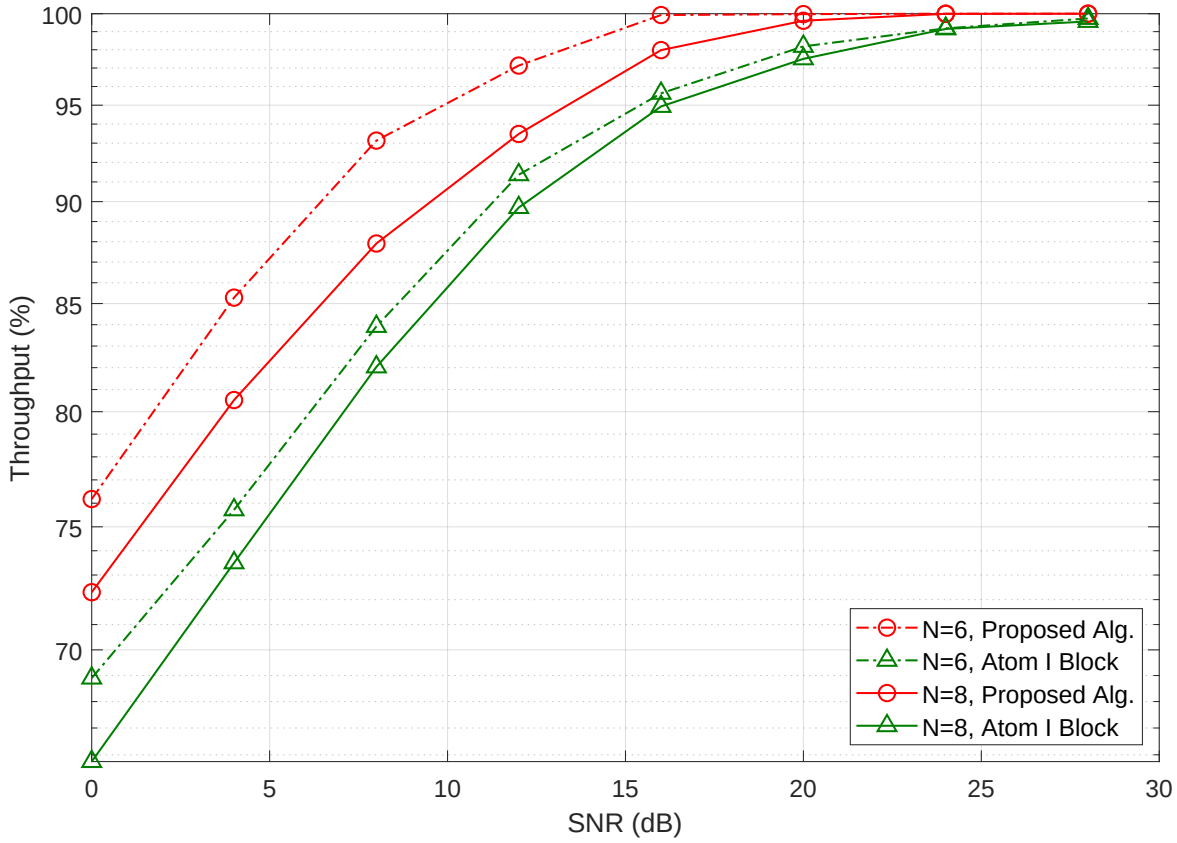

Fig. 3.7: Throughput performance of the proposed algorithm and the Atom I building block approach [28].

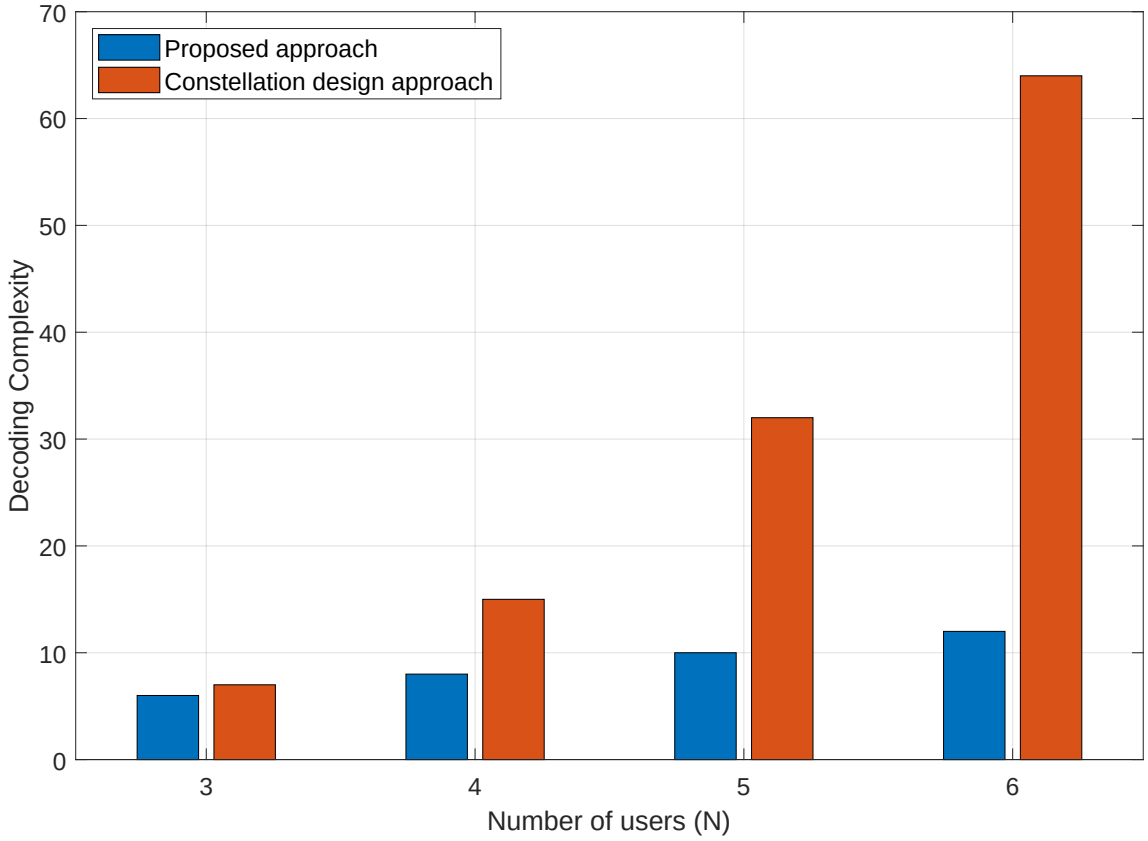

Fig. 3.8: Decoding complexity for the proposed algorithm and the constellation design approach [30].

relay for signal detection, assuming BPSK signaling. In our algorithm, due to its sequential nature, this number is simply $2N$; for the algorithm in [30], the complexity is obtained by simulations[6]. Fig. 3.8 illustrates the decoding complexities versus the number of users N for the two approaches. We note that our approach has a linear growth in complexity with N, which is a prominent advantage over the constellation design method. The latter needs to generate a large size constellation to avoid the codeword ambiguity as N increases, e.g., it is 64 when $N = 6$ in this experiment. Due to this nature, its decoding complexity grows exponentially with N.

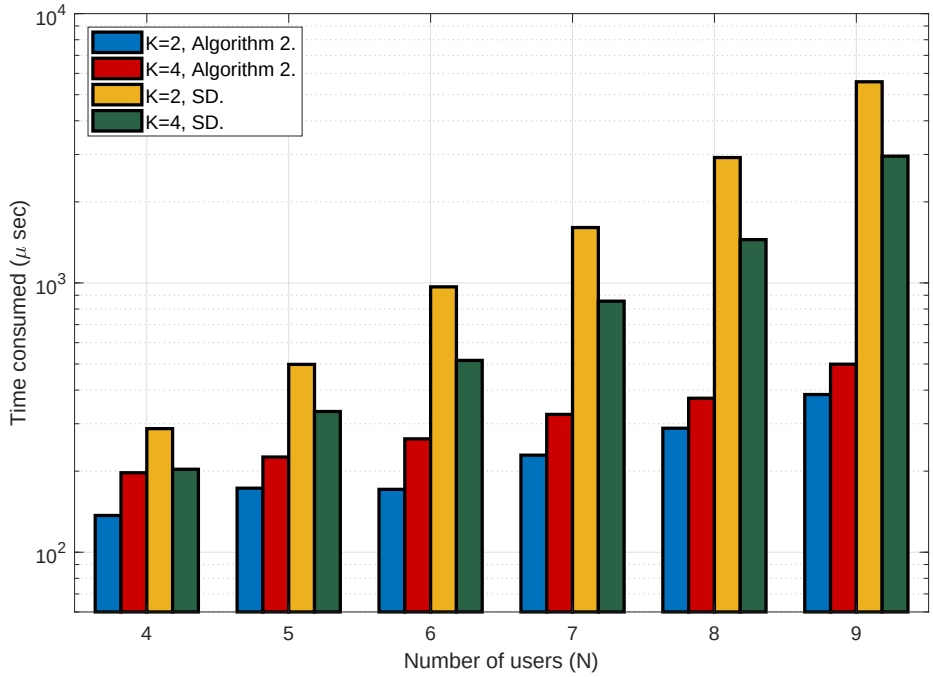

Fig. 3.9: CPU time for the proposed algorithm and the searching algorithm.

The effectiveness of Algorithm 2 in reducing the computational complexity of the estimation process is further demonstrated by comparing it to the sphere decoding (SD) approach [100], which is a widely used iterative search algorithm for solving ILS problems. Fig. 3.9 shows the consumed CPU time per user symbol versus the number of users

[6]We note that the method in [30] assumes an additive white Gaussian noise (AWGN) channel and does not perform well over Rayleigh channels. For this reason, AWGN is used in order to evaluate its decoding complexity. We also note that the case of BPSK corresponds to the choice $M = 2$ in [30].

N for both algorithms under $K \in \{2, 4\}$. We note that the CPU time of Algorithm 2 is significantly less than that consumed by SD. Indeed, due to the system's rank deficiency, the latter algorithm needs to search back and forth repeatedly to detect a given user signal, which is often costly. Meanwhile, the proposed algorithm can better cope with the rank deficiency by combining two different sequential process, namely SIC and Babai estimation, which simplifies the search process and allows for a significant reduction in complexity.

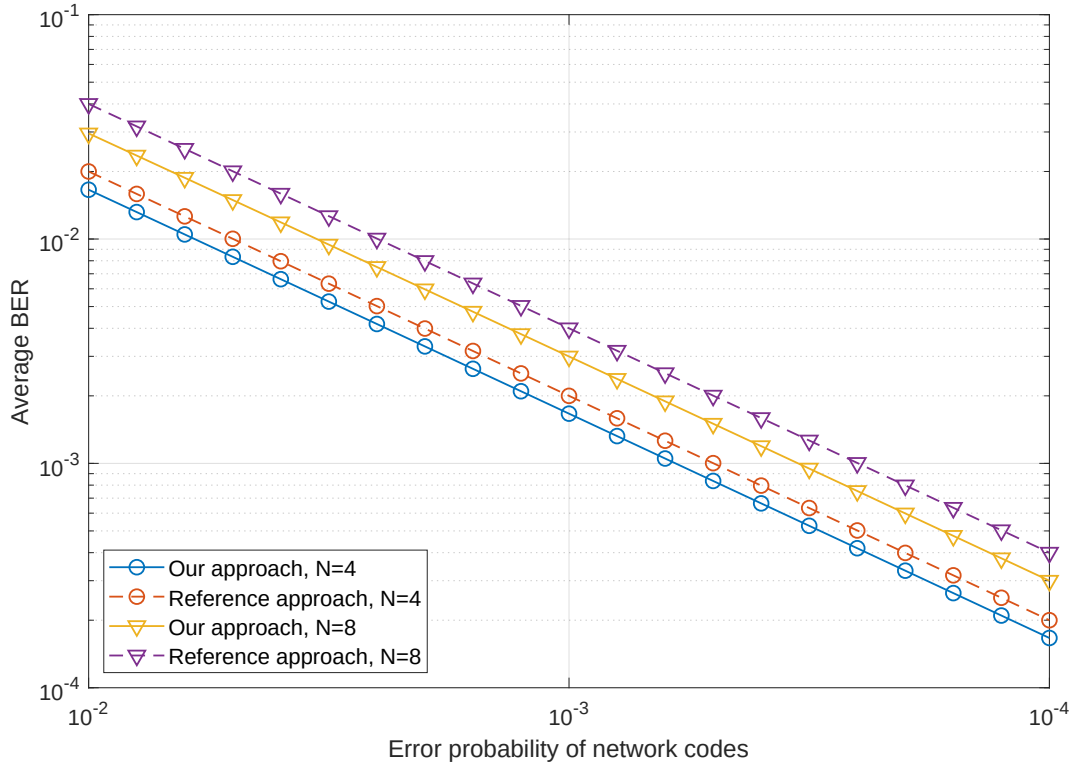

Fig. 3.10: Comparison between the approximation approach used in ψ_{ij} in (3.43) and the one adopted in [96].

In order to demonstrate the applicability of the proposed algorithm with higher modulation schemes, we also conduct an experiment using the QPSK modulation. Fig. 3.11(a) shows the BER performance of BPSK and QPSK modulations when $N = 6$ and $K = 2$. From the result, a 3 to 4 dB performance loss for the QPSK modulation is observed. We

note that the results are obtained from an uncodThe observed performance degradation in fgoing from BPSK to higher order modulation QPSK is reasonable for a system operating in the presence of multi-user interference. Fig. 3.11(b) shows the decoding complexity versus the number of users for the two modulation schemes. Although higher than that of the BPSK modulation, the complexity of the QPSK modulation remains linear with respect to N which is still efficient.

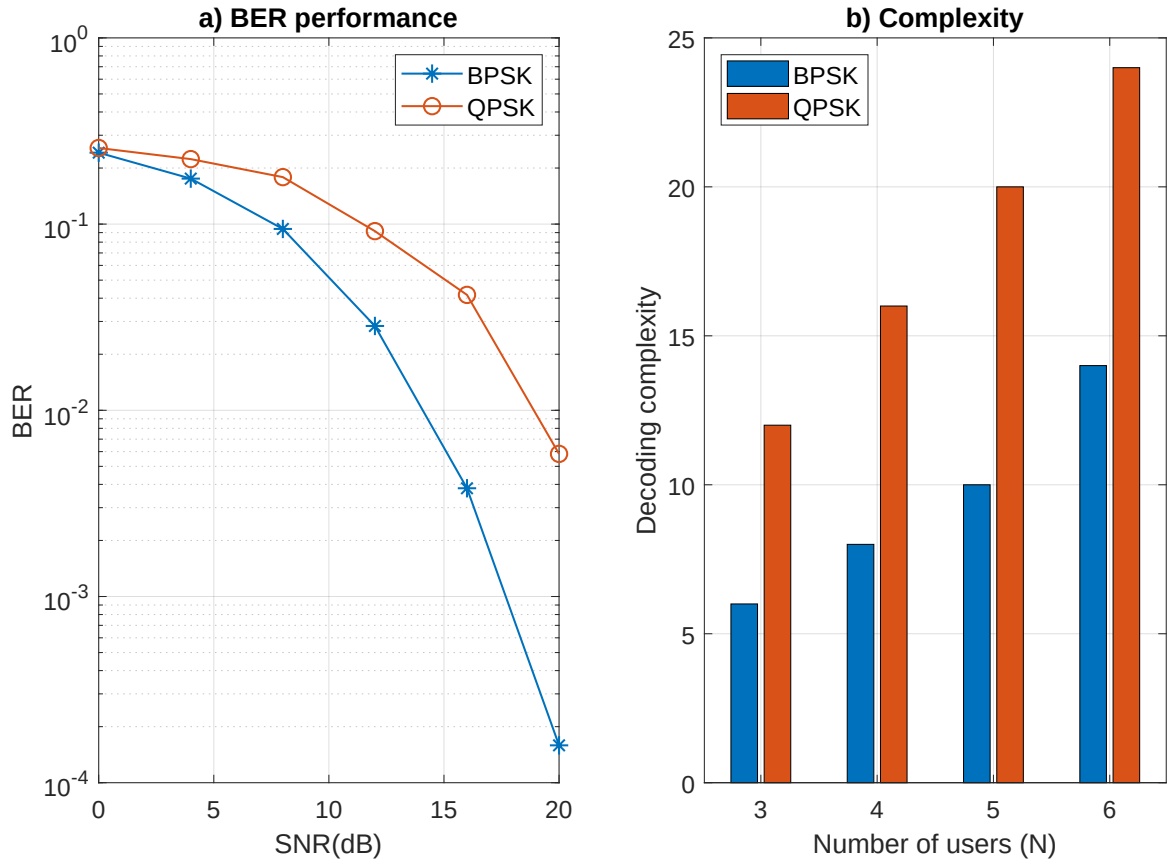

Fig. 3.11: BER performance and decoding complexity of the proposed algorithm with QPSK modulation.

3.4.3 User Pairing Strategy

In this part, we investigate the effect of the selected pairing strategy $\mathcal{C}$ on the performance of network coding in MWRC. To begin, we validate the approximation used in the derivation of the error probability (3.43) by comparing the results with the approach from [96], which also relies on the SNR assumption. Fig. 3.10 shows the average downlink BER versus the error probability of sequentially paired network codes at the relay, when evaluated according to the two approximation approaches for $N \in \{4, 8\}$. From this figure, we find that the BER curves for the two approaches exhibit a similar linear trend and remain reasonably close to each other.This shows that our approach has a similar effect to that of [96] when approximating the error propagation.

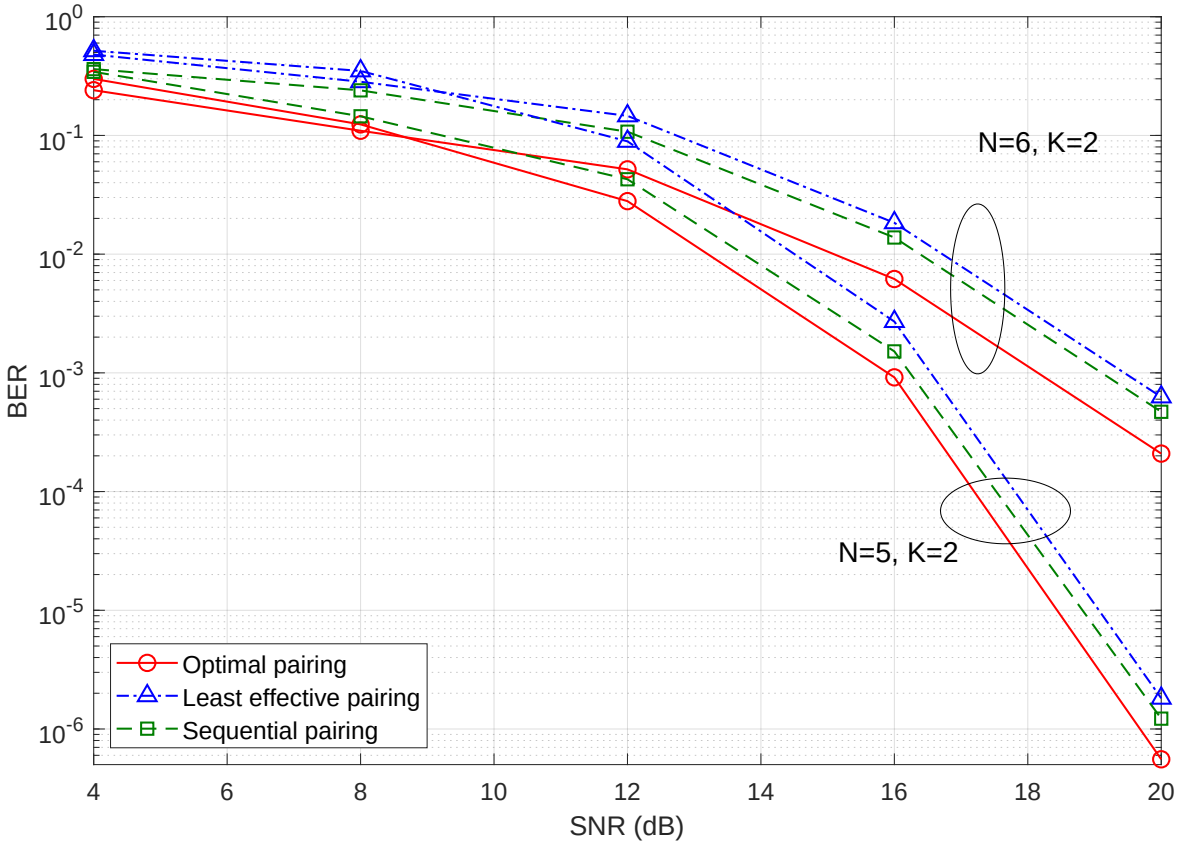

Fig. 3.12: BER performance for different user pairing strategies.

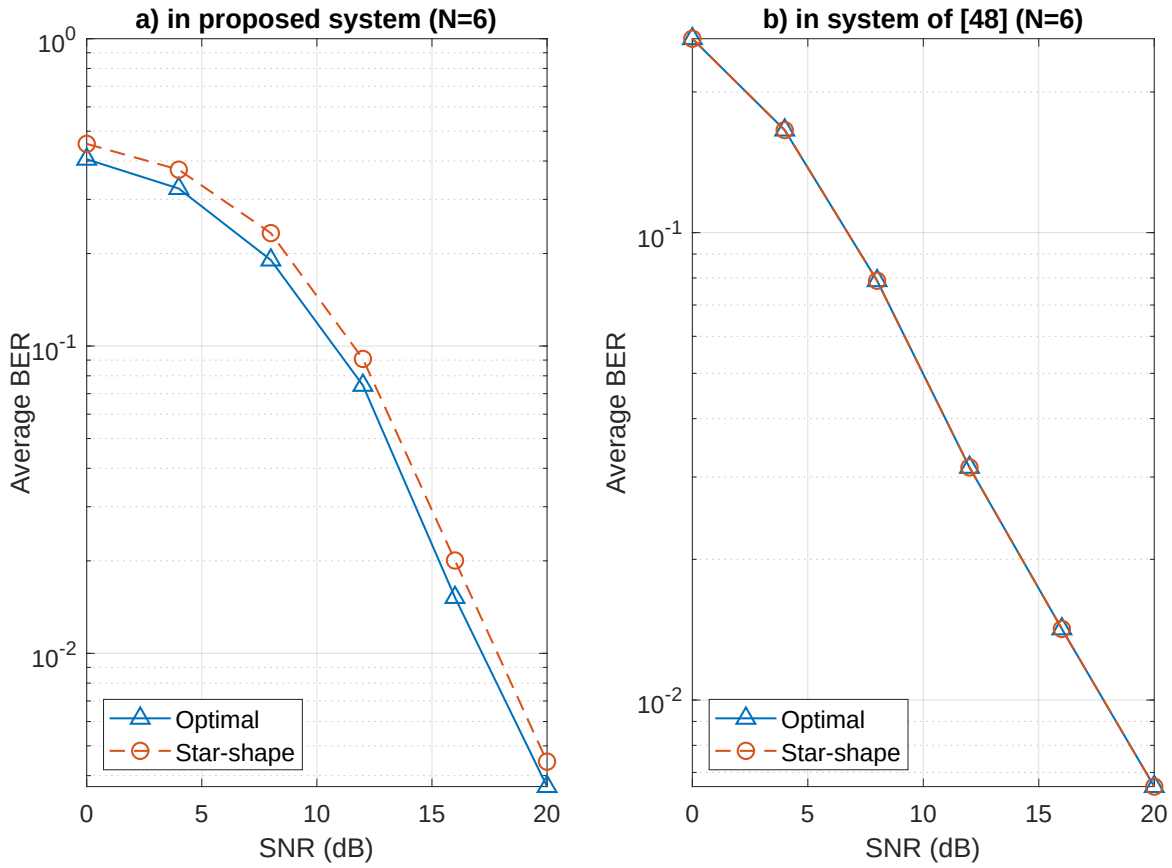

Fig. 3.13: Comparisons between the optimal strategy and the star-shape strategy of [101]. The corresponding BER performances of the two strategies are evaluated in both the proposed system and the non-simultaneous decode-and-forward system of [101].

Next, we consider three different strategies: the sequential strategy $\mathcal{C}_{seq}$ defined in (3.2) and commonly adopted in the literature [30]; the proposed optimal strategy $\mathcal{C}^*$ defined as the optimal spanning tree minimizing the average decoding error probability in (3.45); and a so-called least effective strategy $\mathcal{C}_w$, defined as the spanning tree that yields the worst performance in (3.45). Fig. 3.12 shows the BER versus SNR obtained with these three strategies for two different system configurations, corresponding to $K = 2$ and $N \in \{5, 6\}$. It is observed that the proposed optimal strategy $\mathcal{C}^*$ leads to a notable reduction in the BER when compared to the other two strategies, especially in the case $N = 6$, where the conventional strategy $\mathcal{C}_{seq}$ provides only a marginal improvement over the least efficient strategy $\mathcal{C}_w$.

Finally, we compare our optimal pairing strategy with the star-shape pairing strategy in [101], which pairs the signal from the user having the maximum channel gain with each one of the remaining signals. We incorporate each strategy in both the proposed system and the non-simultaneous system of [101], and then evaluate the corresponding average BER versus SNR. Fig. 3.13(a) and Fig. 3.13(b) respectively show the performance comparison between the two pairing strategies in each system. Due to the existence of multiuser interference in our system, the use of the signal with the maximum channel gain in the star-shape strategy does not yield the optimal performance, as shown in Fig. 3.13(a). In contrast, in a system with non-simultaneous transmission where multiuser interference does not exist, the performance of both strategies is identical, as seen in Fig. 3.13(b).

3.5 Chapter Summary

In this chapter, we considered an uplink MWRC scenario for PNC, where N users, each with single antenna, simultaneously transmit their signals to a relay equipped with K antennas ($K < N$). A novel detection scheme was proposed at the relay to iteratively resolve user signals and remove their interfering effects from the signal set. The proposed

scheme combines a conventional SIC and a regularized ILS solution using Babai estimation to solve an underdetermined ILS problem. We developed a power allocation scheme for the proposed method, and also investigated an optimal user pairing strategy to reduce the decoding error rate at the user terminals. Simulation results revealed the achievable performance improvement of the proposed method in the detection of network codes for PNC in MWRC. While this chapter focused on the signal processing aspects of PNC in MWRC, the further consideration of related information theoretic aspects (e.g., achievable rate region), remains an interesting avenue for future work.

CHAPTER 4

Optimal Power Allocation Based on Success Probability for Downlink PNC in Multi-way Relay Channels

In this chapter, we propose novel power allocation schemes for PNC in downlink MWRC. The power allocation is formulated as a constrained optimization problem, where the aim is to maximize the probability of successfully decoding a chain of network code, termed *success probability*, under a total power constraint when using Babai estimation for signal detection. Specifically, to meet the different requirements for quality of service in applications, we consider different aggregate measures of success probability over the participating user terminals, i.e.: arithmetic mean, geometric mean, and maximin. For each measure, we formulate a constrained optimization and solve the problem accordingly based on its concavity. We first use an evolutionary PSO algorithm to solve the problem for the arithmetic mean, which is non-concave. We then formulate and iteratively solve an alternative concave problem for this measure. We also obtain the solutions of the other two problems for the geometric mean and maximin, which are concave via iterative search methods. The proposed power allocation schemes for downlink PNC in MWRC are evaluated using computer simulations over Rayleigh fading channels. The results demonstrate the effectiveness of the proposed schemes in improving the success probability in the reception of a chain of network codes.

4.1 System model

In this section, we introduce the system configuration and the downlink transmission model for PNC in MWRC.

4.1.1 System Configuration

The general setup for download PNC in MWRC is illustrated in Fig.4.1. The relay, say R, is equipped with K antennas, while each user terminal, say U_i, $i = 1, \ldots, N$, is equipped with M antennas. In this work, we focus on the so-called overdetermined problem where $M \geq K$. In practice, this corresponds to a situation where R and U_i are of similar scale, such as in collaborations among multiple base stations [102] or among mobile devices in vehicle-to-vehicle (V2V) communications [103] [1]. The radio channel between R and U_i is assumed to be flat fading, and therefore represented by a matrix $\mathbf{H}_i \in \mathbb{C}^{M \times K}$. It is assumed that R has full knowledge of all the channels while each U_i has knowledge of its respective channel $\mathbf{H}_i$. Each U_i has a message to share with all other users, which is denoted as $m_i \in \mathbb{F}_q$, where $\mathbb{F}_q$ is a finite integer field of q elements. It is assumed that these messages are available at R, following uplink transmission as in [104, 105].

In the downlink stage, R uses the messages in the set $\{m_1, m_2, ..., m_N\}$ to generate a code vector $\mathbf{c} = [c_1, c_2 \ldots, c_{N-1}]^T \in \mathbb{F}_q^{N-1}$, consisting of $N-1$ codewords c_i to be broadcast to the N users over multiple time slots. To be specific, each entry c_i is generated through the application of a network coding function ϕ on a pair of user messages, i.e., $(m_i, m_j),\ i \neq j$. In this work, the function $\phi : \mathbb{F}_q^2 \to \mathbb{F}_q$ is chosen as the modulo-q addition of its operands. That is, for any two integers $a, b \in \mathbb{F}_q$, we define:

$$\phi(a, b) = a \oplus b = (a + b) \mod q \tag{4.1}$$

[1] For clarification, in Chapter 3, we considered an underdetermined problem for the uplink relay reception where the number of users is greater than the number of receiving antennas at the relay ($N > K$). In this chapter, we focus instead on an overdetermined problem for the downlink user reception where the number of receiving antennas at users can realistically be greater than the number of transmitting antennas at the relay ($M \geq K$).

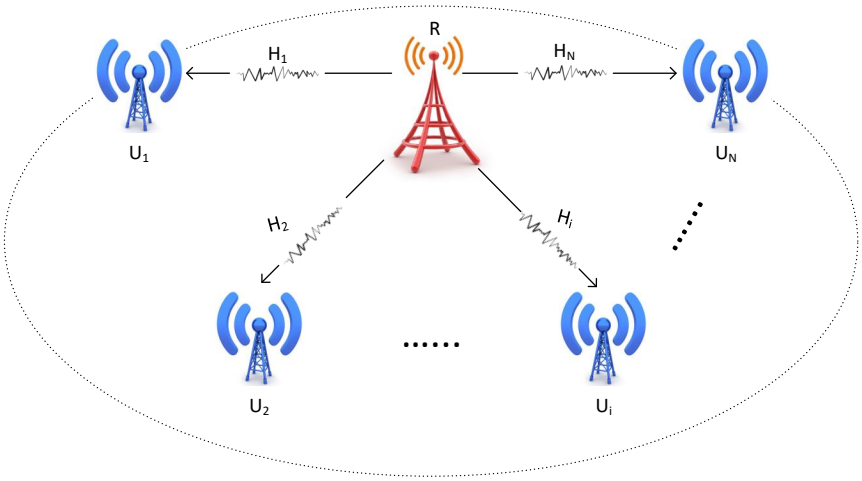

Fig. 4.1: Downlink model of PNC in MWRC. The relay broadcasts $N-1$ network codes to the users, which then use Babai estimation to decode messages from the other users.

For MWRC, there exist several ways to generate $\mathbf{c}$ [101]. Since our focus is on the downlink transmission, we select the sequential pairing strategy for simplicity, which is given as:

$$c_i = \phi(m_i, m_{i+1}),\ i = 1, \ldots, N-1 \tag{4.2}$$

4.1.2 Downlink Transmission

The transmission scheme of downlink PNC in MWRC is described as follows. The relay R breaks up $\mathbf{c}$ into $T = \lceil (N-1)/K \rceil$ packets, where $\lceil \cdot \rceil$ denotes the ceiling function. Each packet can be expressed as a length-K vector[2] $\mathbf{c}_t \in \mathbb{F}_q^K$ where the index $t \in \{0, 1, \ldots, T-1\}$. The relay R then broadcasts the packet $\mathbf{c}_t$ to all users over T consecutive time slots.

To this end, the relay maps each $\mathbf{c}_t$ to a baseband signal vector $\mathbf{s}(t) \in \mathbb{C}^K$ for the transmission. The mapping is implemented element-wise through a bijective function $\varphi : \mathbb{F}_q \to \mathcal{B}$, where $\mathcal{B}$ with cardinality q represents the transmitted signal constellation.

[2]To simplify the analysis, we ensure that every packet is of length K by appending a vector $\bar{\mathbf{c}} \in \mathbb{F}_q^l$, consisting of $l = KT - (N-1)$ pseudo codewords, to $\mathbf{c}$. We assume that $\bar{\mathbf{c}}$ is known to all terminals prior to the communication, so that it can be correctly removed by any receiving terminal.

Specifically, denoting by $s_i(t)$ and $c_{t,i}$ the i-th entries of $\mathbf{s}(t)$ and $\mathbf{c}_t$, respectively, we have:

$$s_i(t) = \varphi(c_{t,i}), \text{ for } i = 1, 2, ..., K. \tag{4.3}$$

The set $\mathcal{B}$ depends on the particular modulation scheme employed for digital transmission. To simplify our discussion, we hereby set $q = 2$ and define $\mathcal{B} = \{-1, +1\}$.

The signal $\mathbf{x}(t)$ sent from R is written as:

$$\mathbf{x}(t) = \mathbf{A}\mathbf{s}(t) \tag{4.4}$$

where the diagonal matrix $\mathbf{A} = \text{diag}(\sqrt{P_1}, \sqrt{P_2}, ..., \sqrt{P_K}) \in \mathbb{R}_+^{K\times K}$ is the power allocation matrix, with P_i being the power allocated to the i^{th} antenna. The signal received at U_i is thus given by:

$$\mathbf{y}_i(t) = \mathbf{H}_i\mathbf{x}(t) + \mathbf{n}_i(t) = \mathbf{H}_i\mathbf{A}\mathbf{s}(t) + \mathbf{n}_i(t) \tag{4.5}$$

where $\mathbf{n}_i(t) \in \mathbb{C}^{M\times 1}$ is the additive noise at U_i, which is modeled as a complex circular Gaussian vector with zero mean and covariance matrix $\sigma^2\mathbf{I}$.

Each U_i estimates $\mathbf{s}(t)$ for $t = 0, 1, ..., T-1$, obtains the corresponding codewords $c_{t,i}$ through (4.3), and collects them into the code vector $\mathbf{c}$. User U_i then utilizes its own message m_i and $\mathbf{c}$ to decode the messages m_j of U_j for all $j \neq i$. This concludes the general process of the downlink broadcast phase. From now on, we will focus on the transmission of a single packet in a specific time slot, hence the time index t will be dropped for convenience.

4.2 Essential Background

In this section, we review the underlying principles of Babai estimation and summarize key results for its success probability in terms of the signal power. A conventional power allocation method serving as a benchmark and a PSO serving as a numerical tool for non-convex optimization problems are also discussed.

4.2.1 Babai Estimation

After dropping time index t, the model in (4.5) becomes:

$$\mathbf{y}_i = \mathbf{H}_i\mathbf{x} + \mathbf{n}_i = \mathbf{H}_i\mathbf{A}\mathbf{s} + \mathbf{n}_i \tag{4.6}$$

for $i = 1, \ldots, N$. The maximum likelihood estimate of the transmitted signal $\mathbf{s}$ is the solution of the integer least squares (ILS) problem:

$$\min_{\mathbf{s}\in\{-1,+1\}^K} ||\mathbf{y}_i - \mathbf{H}_i\mathbf{A}\mathbf{s}|| \tag{4.7}$$

Since the ILS problem is NP-Hard, an optimal solution to the detection problem generally requires high time complexity. To reduce the computation load for user terminals with limited capability, we adopt a suboptimal solution approach, called the Babai estimation [37], which allows each U_i to estimate $\mathbf{s}$ by successively canceling interference.

Specifically, the so-called Babai point $\mathbf{s}^B$ for overdetermined problem (4.7) where $M \geq K$ and $s_i^B \in \{-1, +1\}$ is defined below:

$$s_K^B = \lfloor \Re(b_K) \rceil_{\mathcal{B}},\ b_K = \frac{\tilde{y}_K}{\sqrt{P_K} r_{KK}^{(i)}} \tag{4.8a}$$

$$s_j^B = \lfloor \Re(b_j) \rceil_{\mathcal{B}},\ \ b_j = \frac{\tilde{y}_j - \sum_{k=j+1}^{K} \sqrt{P_k} r_{jk}^{(i)} s_k^B}{\sqrt{P_j} r_{jj}^{(i)}} \tag{4.8b}$$

for $j = K-1, \ldots, 1$, where $\Re(\cdot)$ denotes the real part and the operator $\lfloor \cdot \rceil$ rounds to the nearest value in $\mathcal{B}$. In these equations, vector $\tilde{\mathbf{y}} = [\tilde{y}_1, \ldots, \tilde{y}_K]^T$ and upper triangular matrix $\mathbf{R}_i = [r_{jk}^{(i)}]_{K\times K}$ are obtained from the QR factorization of $\mathbf{H}_i$, i.e.:

$$\mathbf{H}_i = [\mathbf{Q}_1, \mathbf{Q}_2] \begin{bmatrix} \mathbf{R}_i \\ \mathbf{0} \end{bmatrix},\ \ \tilde{\mathbf{y}} = \mathbf{Q}_1^H \mathbf{y}_i. \tag{4.9}$$

Without loss of generality, according to [37], the diagonal entries of $\mathbf{R}_i$ can always be set to non-negative values through simple transformations of the QR decomposition in (4.9).

4.2.2 Success Probability of Babai Estimator

In the context of Babai estimation, the probability of successfully detecting a series of successive signals provides a convenient metric for characterizing the integrity of the detected chain of signals. Specifically, the so-called *success probability* of $\mathbf{s}^B$ at U_i is defined as [37]:

$$\begin{aligned}\rho_i = \Pr(\mathbf{s}^B = \mathbf{s}) = \Pr(s_1^B = s_1 | s_2^B = s_2, \cdots, s_K^B = s_K) \times \\ \cdots \times \Pr(s_{K-1}^B = s_{K-1} | s_K^B = s_K) \Pr(s_K^B = s_K)\end{aligned} \tag{4.10}$$

From the definition of $\mathbf{s}^B$, we can conclude that when $s_j = -1,\ s_j^B = s_j$ if and only if (iff) $\Re(b_j) \in (-\infty, 0]$, and when $s_j = 1,\ s_i^B = s_j$ iff $\Re(b_j) \in (0, +\infty)$. Thus, based on [37], the probability of $s_j^B = s_j$, given previous signals have been correctly detected, is given as:

$$\begin{aligned}&\Pr(s_j^B = s_j | s_{j+1}^B = s_{j+1}, \cdots, s_K^B = s_K) \\ &= \Pr(s_j = -1) \Pr(\Re(b_j) \le 0 | s_{j+1}^B = s_{j+1}, \cdots, s_K^B = s_K) \\ &\quad + \Pr(s_j = 1) \Pr(\Re(b_j) > 0 | s_{j+1}^B = s_{j+1}, \cdots, s_K^B = s_K) \\ &= \frac{1}{2} \frac{1}{\sqrt{\pi}\sigma} \left[\int_{-\infty}^{0} e^{-\frac{(t-(-1))^2}{\sigma^2/(P_j (r_{jj}^{(i)})^2)}} dt + \int_{0}^{+\infty} e^{-\frac{(t-(+1))^2}{\sigma^2/(P_j (r_{jj}^{(i)})^2)}} dt \right] \\ &= \frac{1}{2} \left(1 + \text{erf}(\sqrt{P_j} r_{jj}^{(i)} / \sigma) \right)\end{aligned} \tag{4.11}$$

where $\text{erf}(x) = \frac{2}{\sqrt{\pi}} \int_0^x e^{-t^2} dt$. Then we have:

$$\rho_i = \prod_{j=1}^{K} \frac{1}{2} \left(1 + \text{erf}(\sqrt{P_j} r_{jj}^{(i)} / \sigma) \right). \tag{4.12}$$

4.2.3 Conventional Adaptive Power Allocation

As power allocation is generally considered essential for multi-user systems, conventional strategies mainly focus on boosting the spectral efficiency. A typical example of such a strategy, as being discussed in [106], is to maximize the channel capacity. Specifically, the capacity of the channel between R and U_i is expressed as: $C_i = W \sum_{j=1}^{K} \log_2 \left(1 + \frac{\lambda_{i,j} P_j}{\sigma^2} \right)$, where W is the channel bandwidth which can be regarded as a constant value and $\lambda_{i,j}$ for

$j = 1, \cdots, K$ are the eigenvalues of $\mathbf{H}_i \mathbf{H}_i^H$. The optimal power allocation is obtained by maximizing the average channel capacity of all R-U channels, i.e.,

$$\max_{P_1,\cdots,P_K} \frac{1}{N} \sum_{i=1}^{N} \left[W \sum_{j=1}^{K} \log_2 \left(1 + \frac{\lambda_{i,j} P_j}{\sigma^2} \right) \right] \tag{4.13a}$$

$$\text{s.t.} : \sum_{j=1}^{K} P_j \leq P_T, P_j \geq 0. \tag{4.13b}$$

where P_T is the total transmit power at the relay. However, this metric is not practical for a PNC system whose performance highly depends on the success probability of the chain of network codes, i.e., the signal vector s in (4.6) being correctly received by user terminals. Hence, it is beneficial to find an alternative power allocation approach for the PNC system in MWRC.

4.2.4 Particle Swarm Optimization

When the objective function of an optimization problem is neither convex nor concave, it can take tremendous time for standard methods, such as the interior point and ellipsoid methods to identify every local optima and find out the global optimal solution [107,108]. PSO was introduced in [109] as an advanced, evolutionary computation technique for solving such complex optimization problems. Due to its many advantages, PSO has since been used widely in recent years to solve a variety of constrained optimization problems in science and engineering [110–115].

The PSO method, summarized as Algorithm 3, starts with random initialization of a swarm of individuals points or *particles*, within the problem feasible region. Each particle then iteratively approaches a gradually better approximation to the optimal solution by taking steps (i.e., directions and step sizes) that are coordinated by the movement of the entire swarm. This coordination is impacted by three factors of particle behaviors, namely: inertia, cognition and sociality. To be specific, in each step, a particle intends to move to its personal best position, called $\mathcal{O}_{best}$, while being attracted by the current best

position in the swarm found by other members, called $\mathcal{G}_{best}$. Hence, a particle will move forward to a new position reaching a compromise between these two best positions. The trajectory of such motion is determined by a weighted sum of three distinct components, i.e.: ΔCD along current direction of motion (inertia); $\Delta\mathcal{O}_{best}$ in the direction of $\mathcal{O}_{best}$, as obtained through exploitation of local search space (cognition); and $\Delta\mathcal{G}_{best}$ in the direction of $\mathcal{G}_{best}$, as obtained from swarm exploration (sociality) [116]. All particles follow such a common rule for compromising their personal $\mathcal{O}_{best}$ with the global $\mathcal{G}_{best}$, which is updated along with the entire swarm movement. Under appropriate conditions, the swarm iteratively converges to the same position which is a solution to the problem [117].

Algorithm 3 PSO algorithm

Randomly spread particles over the feasible region
Set starting locations of particles as their $\mathcal{O}_{best}$
Initialize $\mathcal{G}_{best}$ based on $\mathcal{O}_{best}$
while particles have not converge yet **do**
    for each particle **do**
        Update position:

$$\text{new direction} = \Delta CD + \Delta\mathcal{O}_{best} + \Delta\mathcal{G}_{best}$$
$$\text{new position} = \text{current position} + \text{new direction}$$

        Evaluate new position with objective function
        Update best positions:
        if new position is better than $\mathcal{O}_{best}$ **then**
            $\mathcal{O}_{best} \leftarrow$ new position
            if $\mathcal{O}_{best}$ is better than $\mathcal{G}_{best}$ **then**
                $\mathcal{G}_{best} \leftarrow \mathcal{O}_{best}$
            end if
        end if
    end for
end while
return $\mathcal{G}_{best}$

4.3 Proposed methods

The success probability of Babai estimation is a critical performance measure for the network codes. Hence, allocating power at relay R to improve this probability is a meaning-

ful way of enhancing the reliability of downlink PNC transmissions. In this section, the power allocation is formulated as constrained optimization problems, where the aim is to maximize the success probability under power constraints. Specifically, we consider three different aggregate measures of success probability over the participating user terminals, i.e.: arithmetic mean, geometric mean, and maximin.

4.3.1 Average Success Probability (Arithmetic Mean)

We focus on optimizing the average success probability at the user terminals, which benefits the reception reliability of the multi-way system over an ensemble of channel realizations. In our approach, the average success probability is estimated as the arithmetic mean of the success probability over all users terminals. Considering (4.12) for $i = 1, \cdots, N$, the average success probability is given as:

$$\rho_{ave} = \frac{1}{N}\sum_{i=1}^{N}\rho_i = \frac{1}{N}\sum_{i=1}^{N}\left[\prod_{j=1}^{K}\frac{1}{2}\left(1+\text{erf}(\sqrt{P_j}r_{jj}^{(i)}/\sigma)\right)\right]. \tag{4.14}$$

An optimization problem can be formulated to maximize (4.14) subject to a total power constraint P_T, i.e.:

$$\max_{P_1,\cdots,P_K}\frac{1}{N}\sum_{i=1}^{N}\left[\prod_{j=1}^{K}\frac{1}{2}\left(1+\text{erf}(\sqrt{P_j}r_{jj}^{(i)}/\sigma)\right)\right] \tag{4.15a}$$

$$\text{s.t.}: \sum_{j=1}^{K}P_j \leq P_T, P_j \geq 0. \tag{4.15b}$$

However, the cost function in (4.15a) is not necessarily concave in its feasible region. Popular numerical methods such as the interior point method thus may not necessarily converge to the global optima. In order to ease this difficulty and obtain a good result for the average success probability at user terminals, two approaches are proposed below.

PSO Approach

We solve non-concave optimization problem in (4.15), we conceive a PSO-based algorithm which stochastically searches for the global optima of the problem. The resulting procedure, which is summarized as Algorithm 4, is explained in further details below.

At iteration time $t \in \mathbb{N}$, each particle in a swarm of size S is characterized by its position vector $\mathbf{X}_m^t = [P_{m1}^t, \ldots, P_{mK}^t]^T \in \mathbb{R}_+^K$ and a velocity vector $\mathbf{V}_m^t = [v_{m1}^t, \ldots, v_{mK}^t]^T$, where $m \in \{1, \ldots, S\}$ is the particle index, P_{mj}^t is the particle m's current solution to power P_j, and v_{mj}^t is the jth velocity component, $j \in \{1, \ldots, K\}$. During the iteration, each particle adjusts its trajectory towards its own previous best position $\mathcal{O}_{best}$, and towards a global best position attained by any member within the swarm $\mathcal{G}_{best}$. $\mathcal{O}_{best}$ and $\mathcal{G}_{best}$ are determined by evaluation of the cost function $f(\mathbf{X}_m^t) \equiv \rho_{avg}$ in (4.14) during the particle's motion. In order to confine the motion within the feasible region of the problem, we incorporate a penalty to the cost function $f(\mathbf{X}_m^t)$, and use instead:

$$F(\mathbf{X}_m^t) = f(\mathbf{X}_m^t) - \Omega \max\{0, \Delta P_m, -P_{m1}, \ldots, -P_{mK}\}, \tag{4.16}$$

where $\Delta P_m = \sum_{j=1}^K P_{mj}^t - P_T$, and Ω is a penalty factor. Considering that $f(\mathbf{X}_m^t)$ ranges from 0 to 1, we set a relatively large value for Ω. Thus, once a particle motion violates the constraints, $F(\mathbf{X}_m^t)$ deteriorates dramatically to a small value so that this position will not be considered as any form of best positions in the swarm.

The velocity $\mathbf{V}_m^{t+1}$ directing the particle to its next position $\mathbf{X}_m^{t+1}$ is generated according to the three aforementioned factors characterizing the swarm movement, i.e., inertia, cognition, and sociality. Specifically, the component of $\mathbf{V}_m^{t+1}$ along dimension j is updated as:

$$v_{mj}^{t+1} = \omega^t v_{mj}^t + c_1 r_1^t (\mathcal{O}_{best,mj} - P_{mj}^t) + c_2 r_2^t (\mathcal{G}_{best,mj} - P_{mj}^t), \tag{4.17}$$

where ω^t is the inertia weight, c_1 and c_2 are the constant cognitive and social parameters respectively, and r_1^t and r_2^t are random scaling factors uniformly distributed in $[0, 1]$, as

represented by the function $Rand()$ in Algorithm 4. Then the new position on dimension j is accordingly given as:

$$P_{mj}^{t+1} = P_{mj}^{t} + v_{mj}^{t+1}. \tag{4.18}$$

The inertia weight ω^t and parameters c_1, c_2 control the impact of the previous motion onto the current one. The determination of these parameters largely depends on empirical results [117]. A large inertia weight is preferred to enhance the global exploration efficiency in the early stage of the search while its value is reduced for better local exploitation accuracy in the late stage. Hence, we damp ω^t at each iteration by a constant factor $0 < \mu < 1$ throughout the evolutionary process, i.e.:

$$\omega^{t+1} = \mu\omega^{t}. \tag{4.19}$$

The algorithm eventually comes to a stop when the movement of the swarm stalls. This is considered to occur when the largest change in the objective value for the swarm, i.e.: $\max\{\Delta_m = |F(\mathbf{X}_m^t) - F(\mathbf{X}_m^{t-1})|, m = 1, \ldots, S\}$, is less than a chosen small threshold value ϵ. Based on our experience, with the damping of the inertia weights in (4.19), the algorithm always converges within a certain number of iterations for a specific swarm size for our problem. The reason behind this observation is that the $\mathcal{G}_{best}$ always tends to attract all particles together. With each particle gradually approaching $\mathcal{G}_{best}$, the decreasing damping ratio on the inertia weight reduces the particle velocity which gradually prevents them escaping from $\mathcal{G}_{best}$. Thus, under a sufficiently large number of iterations, all particles will eventually converge to the same location. For this reason, to improve the efficiency and consistency of the algorithm, we set empirically a maximum number of iterations T_{max} as the ultimate stopping criterion. The eventual global best position of the swarm $\mathcal{G}_{best}$ is thus considered as the solution to the power allocation problem in (4.15).

Algorithm 4 PSO solution to average success probability based power allocation

Input: S = swarm size; T_{max} = number of max iterations; $F(\cdot)$ = penalized cost function for power allocation; ϵ = stopping criteria
Initialization:
Initialize parameters ω^0, c_1, c_2, r_1^0, r_2^0
for each particle $m = 1$ to S **do**
    Initialize positions $\mathbf{X}_m^0$ randomly in the feasible region
    Initialize velocity $\mathbf{V}_m^0 = \mathbf{0}$
    Initialize best known position $\mathcal{O}_{best,m} = \mathbf{X}_m^0$
    Evaluate cost $F(\mathbf{X}_m^0)$
end for
Initialize swarm's best known position $\mathcal{G}_{best}$, where $F(\mathcal{G}_{best}) = \max\{F(\mathbf{X}_m^0)|m = 1, \ldots, S\}$
Main iterations:
for $t = 1$ to T_{max} **do**
    for particle $m = 1$ to S **do**
        for dimension $j = 1$ to K **do**
            Update velocity:

$$\begin{aligned} v_{mj}^t =& \omega^{t-1} v_{mj}^{t-1} + c_1 r_1^{t-1}(\mathcal{O}_{best,mj} - P_{mj}^{t-1}) \\ &+ c_2 r_2^{t-1}(\mathcal{G}_{best,j} - P_{mj}^{t-1}) \end{aligned}$$

            Update position:

$$P_{mj}^t = P_{mj}^{t-1} + v_{mj}^t$$

        end for
        Update $\mathcal{O}_{best,m}$:
        if $F(\mathbf{X}_m^t) > F(\mathcal{O}_{best,m})$ **then**

$$\mathcal{O}_{best,m} \leftarrow \mathbf{X}_m^t$$

            Update $\mathcal{G}_{best}$:
            if $F(\mathcal{O}_{best,m}) > F(\mathcal{G}_{best})$ **then**

$$\mathcal{G}_{best} \leftarrow \mathcal{O}_{best,m}$$

            end if
        end if
        (Note: Continued on the next page.)

(Note: Continued from the previous page.)
Update parameters:

$$\omega^t = \mu\omega^{t-1}, \;\; r_1^t = Rand(), \;\; r_2^t = Rand()$$

$\Delta_m = |F(\mathbf{X}_m^t) - F(\mathbf{X}_m^{t-1})|$
end for
if $\max\{\Delta_m | m = 1, \ldots, S\} < \epsilon$ **then Break**
end if
end for
Assign global best position $\mathcal{G}_{best}$ as the final output for the power allocation:

$$\mathbf{X}^* = \mathcal{G}_{best}$$

return $\mathbf{X}^*$

Alternative Problem Approach

To ease the difficulty posed by non-concavity in (4.15), we can formulate an alternative objective which also represents, in some sense, the average success probability at the user terminals. Instead of directly averaging over ρ_i, we can average over $\rho_i^{1/K}$, i.e.:

$$\rho'_{ave} = \frac{1}{N}\sum_{i=1}^{N} \rho_i^{\frac{1}{K}} \tag{4.20}$$

Since each number $\rho_i^{1/K}$ still provides an indication of the success probability at U_i, ρ'_{ave} can also be used to characterize the the average reception reliability of the system. That is, we can alternatively formulate the problem as:

$$\max_{P_1,\cdots,P_K} \frac{1}{N}\sum_{i=1}^{N}\left[\prod_{j=1}^{K}\frac{1}{2}\left(1+\text{erf}(\sqrt{P_j}r_{jj}^{(i)}/\sigma)\right)\right]^{\frac{1}{K}} \tag{4.21a}$$

$$\text{s.t.}: \sum_{j=1}^{K} P_j \leq P_T, P_j \geq 0. \tag{4.21b}$$

Proposition 1. *The cost function in* (4.21a) *is concave in the closed and convex feasible region in* (4.21b).

Proof. Define the function

$$g_j^{(i)}(P_j) = 1 + \text{erf}(\sqrt{P_j} r_{jj}^{(i)}/\sigma) \tag{4.22}$$

The second order partial derivative of (4.22) with respect to (w.r.t.) P_j is non-positive, i.e.:

$$\frac{\partial^2 g_j^{(i)}(P_j)}{\partial^2 P_j} = -\frac{r_{jj}^{(i)}}{\sqrt{\pi}\sigma}\left[\frac{(r_{jj}^{(i)})^2}{\sigma^2\sqrt{P_j}} + \frac{1}{2}P_j^{-\frac{3}{2}}\right] e^{-\frac{P_j (r_{jj}^{(i)})^2}{\sigma^2}} \leq 0 \tag{4.23}$$

since $e^{-P_j (r_{jj}^{(i)})^2} \geq 0$ and $P_j \geq 0$. The Hessian of the function:

$$w_i(P_1, \ldots, P_K) = \rho_i^{\frac{1}{K}} = \frac{1}{2}\left[\prod_{j=1}^{K} g_j^{(i)}(P_j)\right]^{\frac{1}{K}} \tag{4.24}$$

is accordingly given by

$$\nabla^2 w_i = -\frac{1}{2K^2}\left(\prod_{j=1}^{K} g_j^{(i)}(P_j)\right)^{\frac{1}{K}} \left[K\,\text{diag}\,(\mathbf{d}) - \mathbf{q}\mathbf{q}^T\right], \tag{4.25}$$

where $\mathbf{d},\ \mathbf{q} \in \mathbb{R}^{K\times 1}$ with respective entries:

$$q_l = \frac{1}{g_l^{(i)}(P_l)}\frac{\partial g_l^{(i)}(P_l)}{\partial P_l}, d_l = q_l^2 - \frac{1}{g_l^{(i)}(P_l)}\frac{\partial^2 g_l^{(i)}(P_l)}{\partial^2 P_l} \tag{4.26}$$

For any vector $\mathbf{v} \in \mathbb{R}^{K\times 1}$, we have:

$$\begin{aligned}\mathbf{v}^T\nabla^2 w_i \mathbf{v} = -\frac{1}{2K^2}\left(\prod_{j=1}^{K} g_j^{(i)}(P_j)\right)^{\frac{1}{K}} \Bigg[K\sum_{j=1}^{K}\left(\frac{1}{g_j^{(i)}(P_j)}\frac{\partial g_j^{(i)}(P_j)}{\partial P_j}\right)^2 v_j^2 \\ - K\sum_{j=1}^{K}\frac{1}{g_j^{(i)}(P_j)}\frac{\partial^2 g_j^{(i)}(P_j)}{\partial^2 P_j}v_j^2 - \left(\sum_{j=1}^{K}\frac{1}{g_j^{(i)}(P_j)}\frac{\partial g_j^{(i)}(P_j)}{\partial P_j}v_j\right)^2\Bigg].\end{aligned} \tag{4.27}$$

Considering (4.23) and Cauchy-Schwarz inequality [118] $(\boldsymbol{a}^T\boldsymbol{a})(\boldsymbol{b}^T\boldsymbol{b}) - (\boldsymbol{a}^T\boldsymbol{b})^2 \geq 0$, where we set

$$\boldsymbol{a} = \mathbf{1}^{K\times 1},\ b_j = \frac{1}{g_j^{(i)}(P_j)} \frac{\partial g_j^{(i)}(P_j)}{\partial P_j} v_j, \tag{4.28}$$

we can show that $\mathbf{v}^T \nabla^2 w_i \mathbf{v} \leq 0$ for all $\mathbf{v} \in \mathbb{R}^{K\times 1}$, i.e.,$\nabla^2 w_i \preceq 0$. The function in (4.24) is thus concave. Since the concavity is preserved by non-negative weighted sum operations, the cost function in (4.21) is also concave. □

4.3.2 Overall Success Probability (Geometric Mean)

Another possible design goal of the design is to enhance the system's overall reception capability, especially, when the integrity of all the network chains received by all user terminals is critical. To achieve this, an optimization problem can be formulated to maximize the geometric mean of the success probabilities at all user terminals, i.e.:

$$\rho_{all} = \left(\prod_{i=1}^{N} \rho_i\right)^{\frac{1}{N}} = \left(\prod_{i=1}^{N} \left[\prod_{j=1}^{K} \frac{1}{2}\left(1 + \text{erf}(\sqrt{P_j} r_{jj}^{(i)}/\sigma)\right)\right]\right)^{\frac{1}{N}}. \tag{4.29}$$

To maximize ρ_{all} is equivalent to maximizing its logarithmic form, which is:

$$\log \rho_{all} = \frac{1}{N} \sum_{i=1}^{N} \left[\sum_{j=1}^{K} \log \frac{1}{2}\left(1 + \text{erf}(\sqrt{P_j} r_{jj}^{(i)}/\sigma)\right)\right]. \tag{4.30}$$

We can then formulate an optimization problem to maximize (4.30), i.e.:

$$\max_{P_1,\cdots,P_K} \frac{1}{N} \sum_{i=1}^{N} \left[\sum_{j=1}^{K} \log \frac{1}{2}\left(1 + \text{erf}(\sqrt{P_j} r_{jj}^{(i)}/\sigma)\right)\right] \tag{4.31a}$$

$$\text{s.t.}: \sum_{j=1}^{K} P_j \leq P_T,\ P_j \geq 0. \tag{4.31b}$$

Proposition 2. *The cost function*

$$f(P_1,\ldots,P_K)=\frac{1}{N}\sum_{i=1}^{N}\left[\sum_{j=1}^{K}\log\frac{1}{2}\left(1+erf(\sqrt{P_j}r_{jj}^{(i)}/\sigma)\right)\right] \tag{4.32}$$

is concave in the closed and convex feasible region in (4.31b).

Proof. The first order partial derivative of f w.r.t. P_j is:

$$\frac{\partial f(P_1,\ldots,P_K)}{\partial P_j}=\frac{1}{N}\sum_{i=1}^{N}\frac{r_{jj}^{(i)}e^{-P_j(r_{jj}^{(i)})^2/\sigma^2}}{\ln 2\sqrt{\pi}\sigma(1+\text{erf}(\sqrt{P_j}(r_{jj}^{(i)})/\sigma))\sqrt{P_j}}. \tag{4.33}$$

The second order partial derivative w.r.t. P_j is:

$$\begin{aligned}\frac{\partial^2 f(P_1,\ldots,P_K)}{\partial^2 P_j}&=\frac{r_{jj}^{(i)}}{N\ln 2\sqrt{\pi}\sigma(1+\text{erf}(\sqrt{P_j}(r_{jj}^{(i)})/\sigma))^2}\\ &\left[-\frac{r_{jj}^{(i)}e^{-P_j(r_{jj}^{(i)})^2/0.5\sigma^2}}{\sqrt{\pi}\sigma P_j}-\frac{P_j^{-1.5}e^{-P_j(r_{jj}^{(i)})^2/\sigma^2}}{2}-\frac{(r_{jj}^{(i)})^2e^{-P_j(r_{jj}^{(i)})^2/\sigma^2}}{\sigma^2\sqrt{P_j}}\right]\leq 0.\end{aligned} \tag{4.34}$$

The second order partial derivative w.r.t. P_j and P_k, where $k\neq j$, is:

$$\frac{\partial^2 f(P_1,\ldots,P_K)}{\partial P_j\partial P_k}=0. \tag{4.35}$$

Hence, the Hessian matrix $\nabla^2 f(P_1,\ldots,P_K)$ is negative semi-definite. The concavity of the cost function is proved. □

4.3.3 Minimal Success Probability (Maximin)

The goal of the optimization problem can be set on maximizing the minimal success probability of all users. By doing this, the worst case scenario of the reception capability in the

user groups will be improved. That is to say, the problem can be formulated as:

$$\max_{P_1,\cdots,P_K} \min_i \sum_{j=1}^{K} \log \frac{1}{2}\left(1+\text{erf}(\sqrt{P_j}r_{jj}^{(i)}/\sigma)\right) \tag{4.36a}$$

$$\text{s.t.}: \sum_{j=1}^{K} P_j \leq P_T,\ P_j \geq 0,\ i=1\ldots,N. \tag{4.36b}$$

Proposition 3. *The cost function*

$$f(P_1,\ldots,P_K) = \min_{i=1,\cdots,N} \sum_{j=1}^{K} \log \frac{1}{2}\left(1+erf(\sqrt{P_j}r_{jj}^{(i)}/\sigma)\right) \tag{4.37}$$

is concave in the closed and convex feasible region in (4.36b).

Proof. Similarly to the proof in 4.3.2, it is easy to find that for each user i, the function

$$u^{(i)}(P_1,\ldots,P_K) = \sum_{j=1}^{K} \log \frac{1}{2}\left(1+\text{erf}(\sqrt{P_j}r_{jj}^{(i)}/\sigma)\right) \tag{4.38}$$

is concave. Pick any $\mathbf{x}_1, \mathbf{x}_2 \in \text{dom}(f)$, $\lambda \in [0,1]$, and for some $m \in \{1,\ldots,N\}$, we have

$$\begin{aligned} f(\lambda\mathbf{x}_1+(1-\lambda)\mathbf{x}_2) &= u^{(m)}(\lambda\mathbf{x}_1+(1-\lambda)\mathbf{x}_2) \\ &\geq \lambda u^{(m)}(\mathbf{x}_1)+(1-\lambda)u^{(m)}(\mathbf{x}_2) \\ &\geq \lambda \min_{i=1,\ldots,N} u^{(i)}(\mathbf{x}_1)+(1-\lambda)\min_{i=1,\ldots,N} u^{(i)}(\mathbf{x}_2) \\ &= \lambda f(\mathbf{x}_1)+(1-\lambda)f(\mathbf{x}_2). \end{aligned} \tag{4.39}$$

The concavity of the cost function is thus proved. □

Based on the concavities of the cost functions, the global optima to problem (4.21), (4.31), and (4.36) hence can be found by using numerical programming tools respectively.

4.4 Simulation Results

This section presents simulation results of the proposed power allocation schemes for PNC in MWRC.

4.4.1 Methodology

Unless otherwise specified, the experiment environment is configured as follows. BPSK signaling is adopted at both the relay and the user terminals, whose maximum transmitting power is normalized to $P_T = 1$. The network has 1 relay and 4 user terminals, both equipped with 6 antennas, i.e., $M = K = 6$. We assume the various radio links to be Rayleigh fading, i.e., the entries of the channel matrix $\mathbf{H}$ are modeled as independent complex circular Gaussian random variables with zero mean and unit variance. The noise variance at receiving antennas is adjusted to obtain the desired SNR level. To simplify the discussion and minimize the effects of indirect factors in the performance comparison among the different estimation schemes, we consider uncoded systems as in, e.g., [99].

Six power allocation schemes are implemented for comparison in the following experiments, i.e.:

- Arithmetic mean with PSO solution as in (4.15);
- Arithmetic mean with alternative solution as in (4.21);
- Geometric mean as in (4.31);
- Maximin as in (4.36);
- Conventional channel capacity as in (4.13);
- Equal power allocation where the total transmitting power is equally distributed to all signals.

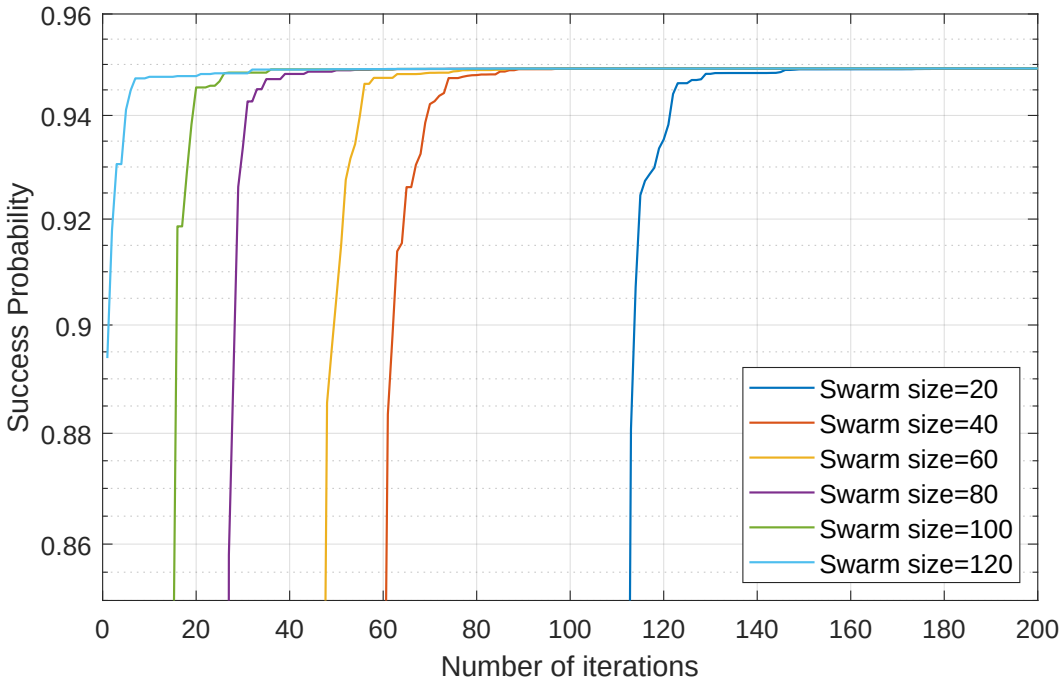

Fig. 4.2: Convergence speed of PSO algorithm regarding different swarm size.

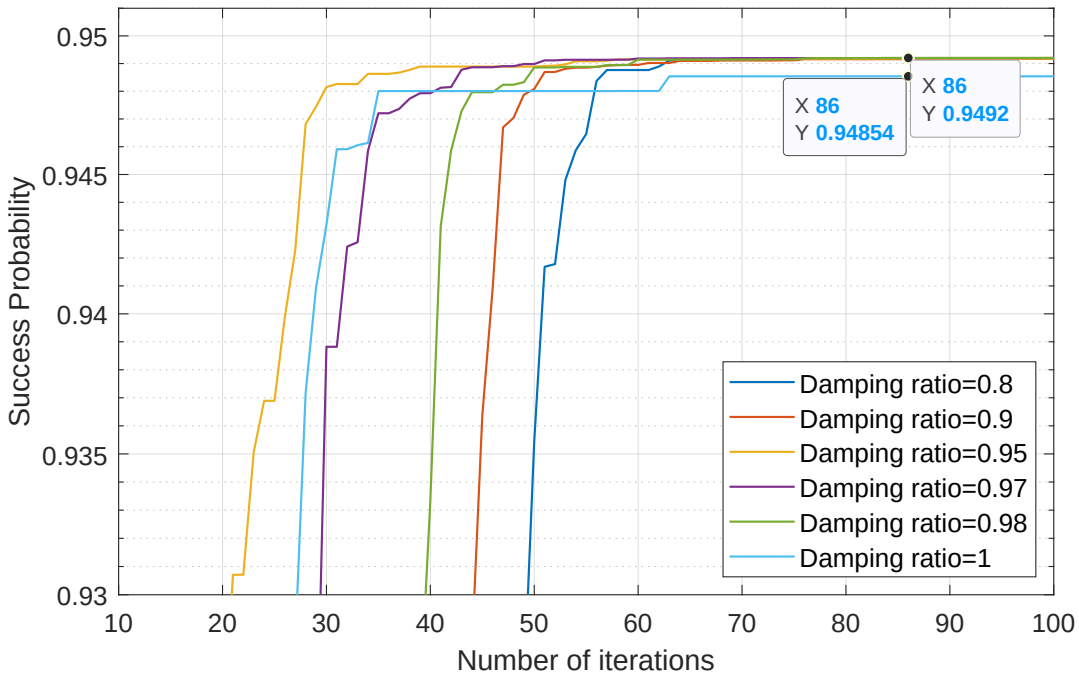

Fig. 4.3: Convergence speed of PSO algorithm regarding damping ratio μ.

4.4.2 PSO Solution Analysis

We first present a series of experiment results to validate our choices over the PSO parameters for Alg. 4 and discuss the corresponding effects on the solution to problem (4.15).

Swarm size

Fig. 4.2 shows the effect of swarm size S on the convergence speed of Alg. 2. We examine the number of iterations needed for the swarm to converge to the maximum average success probability in (4.14) with different swarm size, i.e., $S = \{20, 40, 60, 80, 100, 120\}$. From the results, it is obvious that the convergence speed increases. However, when the swarm size increases to a certain level, e.g., $S = 100$, the improvement on the convergence speed (i.e., number of iterations to get within say 0.1) becomes relatively insignificant. In addition, a larger swarm size usually requires larger memory space and computational complexity. In the sequel, in light of this observation, we set a swarm size $S = 100$.

Damping ratio

Fig. 4.3 shows the effect of damping ratio μ in (4.19). We evaluate the number of iterations needed for the algorithm to converge to the best value of the average success probability for several different damping ratio $\mu = \{0.8, 0.9, 0.95, 0.97, 0.98, 1\}$. With $\mu = 1$, i.e.: no damping, the swarm converges to a slightly smaller value than the best achievable value (0.94854 as compared to 0.9492). This observation indicates that the damped inertia weight improves the local exploitation of the swarm. However, we also notice that with $\mu = 0.8$, i.e.: more damping, the algorithm converges more slowly than those with less damping. The result indicates that the global exploration of the swarm will be hampered if excessive damping is imposed on ω. Based on the result in Fig. 4.3, we find that when damping ratio is around $\mu = 0.95$, the algorithm reaches a balanced point for the exploitation and exploration that leads to a relatively fast speed of convergence.

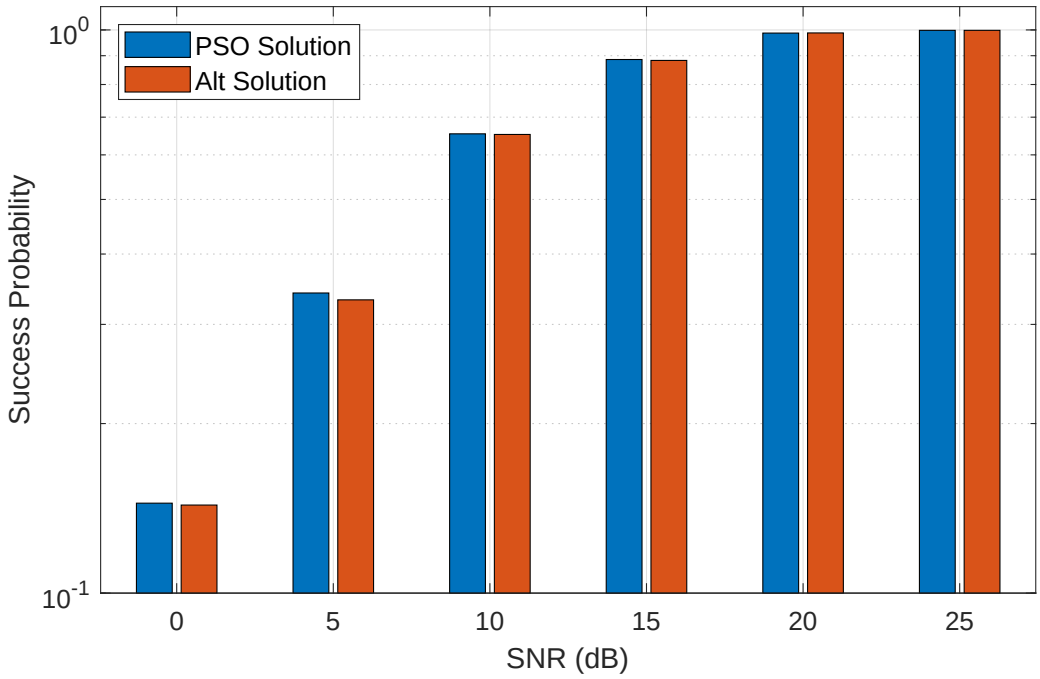

Fig. 4.4: Performance comparison between PSO approach and alternative problem approach to problem (4.15) regarding SNR.

4.4.3 PSO and Alternative problem solutions

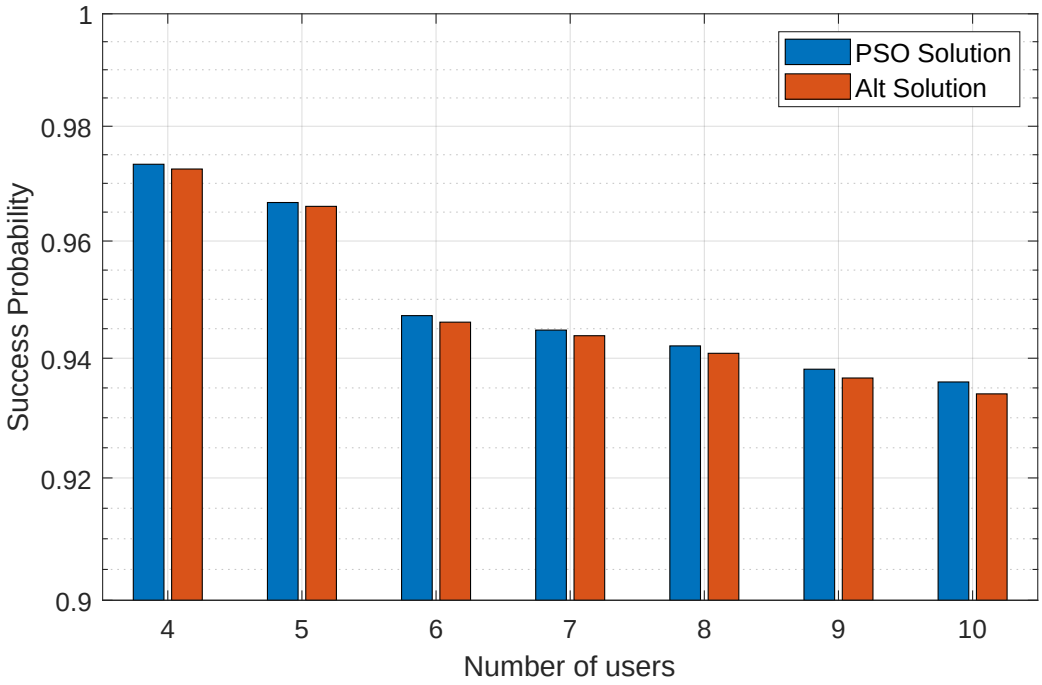

Fig. 4.5: Performance comparison between PSO approach and alternative problem approach to problem (4.15) regarding different number of users.

Fig. 4.4 and Fig. 4.5 compare the results of the PSO approach and the alternative problem approach regarding the SNR and the number of users respectively. Since the alternative problem approach does not directly solve problem (4.15), to maintain a fair comparison, we allocate the power according to the results from both approaches to our systems and compute the average success probability using Monte Carlo method. Fig. 4.4 demonstrates the effectiveness of both approaches in a varying channel environment. With SNR rising from $0\ dB$ to $25\ dB$ the results of both approaches remain relatively close. The alternative problem approach has a slight disadvantage over the PSO approach but the disadvantage is vanishing with the channel condition improves. Fig. 4.5 accordingly demonstrates the effectiveness of both approaches for different number of users with SNR being fixed at $20\ dB$. In this experiment, both approaches also maintain a close result but

there exhibits a slight and constant disadvantage of the alternative problem approach over the PSO approach.

4.4.4 Comparison Among Different Design Goals

We also present a series of experiments to compare the performance of power allocation schemes based on different design goals.

Average Success Probabilities

In Fig. 4.6, we present the test result of the proposed power allocation scheme of (4.21). The experiment evaluates the average probability ρ'_{ave} among all user terminals, indicating the system's average reliability of successfully receiving the network codes in the downlink phase. Fig. 4.6 compares the complementary values of the arithmetic mean of the success probability at all terminals under six power allocation schemes. Based on the result, we see that the proposed arithmetic mean scheme has the best performance among all in this case. The geometric mean scheme has a slight disadvantage to the arithmetic mean scheme. The maximin, the equal power allocation, and conventional channel capacity schemes have obvious disadvantages in such a scenario. The result herein shows the effectiveness of the proposed arithmetic mean scheme in improving the average reception capability of the system.

Overall Success Probabilities

In Fig. 4.7, we present the test result of the proposed power allocation scheme of (4.31). This experiment evaluates the overall success probability of all user terminals, indicating the system's capability of correctly receiving every network code at every user terminal in the downlink phase. Fig. 4.7 compares the complementary values of the geometric mean of the success probability when all six power allocation schemes are implemented. From the result, we observe that the proposed geometric mean scheme has a slight advantage over the arithmetic mean scheme while both schemes have obvious advantage over the

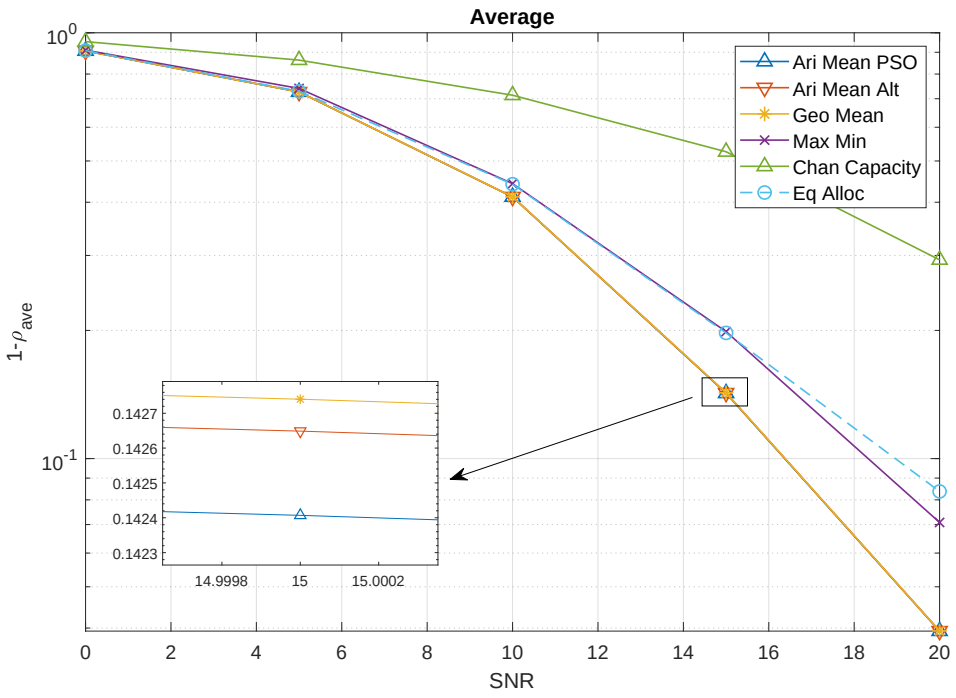

Fig. 4.6: Complementary values $(1 - \rho'_{ave})$ of the arithmetic mean of the success probabilities.

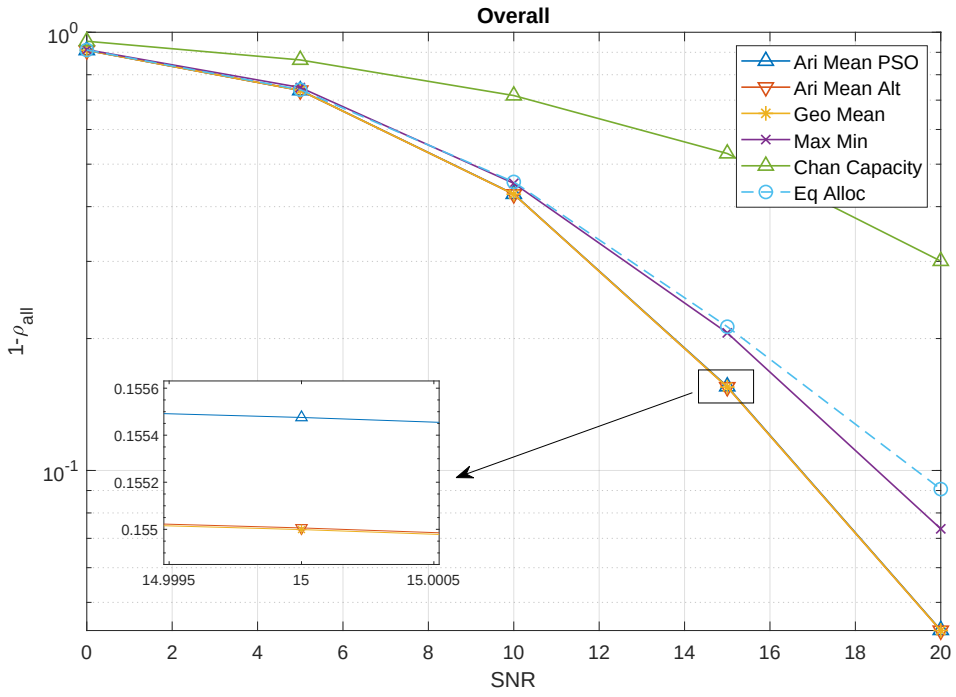

Fig. 4.7: Complementary values $(1 - \rho_{all})$ of the geometric mean of the success probabilities.

rest schemes. The proposed geometric mean scheme hence improves the overall reception capability.

Minimal Success Probabilities

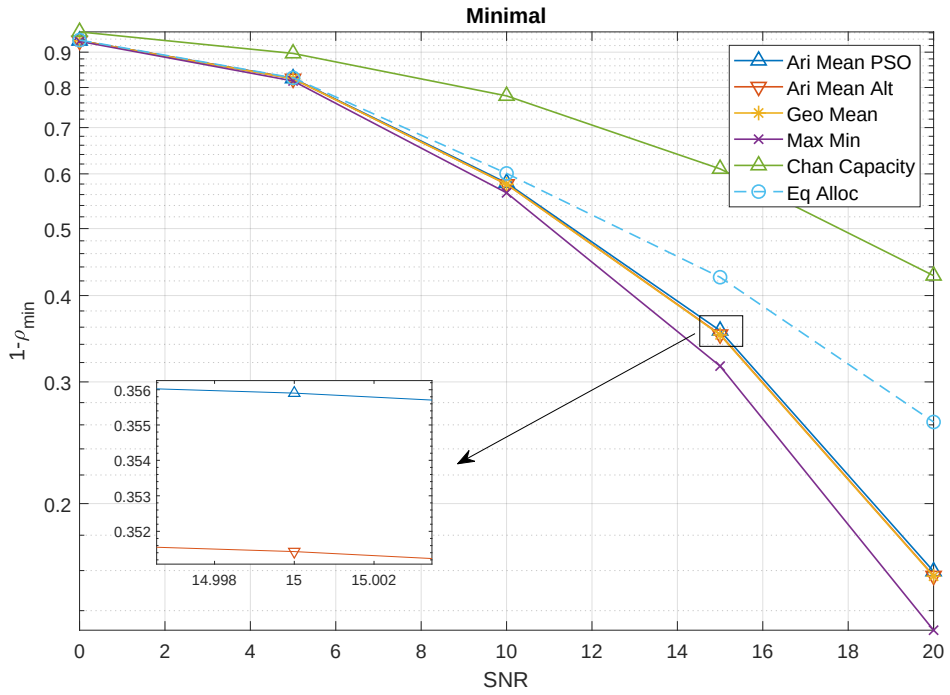

Fig. 4.8: Complementary values $(1 - \rho_{min})$ of the minimal success probability.

In Fig. 4.8, we present the test result of the proposed power allocation scheme of (4.36). In this experiment, the scenario is considered for a system where the worst user reception capability is critical, e.g., a collaborative file sharing process where the worst node in the network slows down the overall progress. Fig. 4.8 shows the complementary values of the lowest success probability of the terminal in the user group under six power allocation schemes. Comparing to all other schemes, we observe that the maximin scheme provides the best success probability for the worst user terminal in this case. This demonstrates the effectiveness of the proposed maximin scheme in helping enhancing the worst reception capability of the user terminals in the system.

4.5 Chapter Summary

In this chapter, we proposed a novel power allocation scheme for PNC in downlink MWRC. The power allocation is formulated as a constrained optimization problem, where the aim is to maximize the success probability under a total power constraint when using Babai estimation for signal detection. Optimizing over this metric allows us to maximize the probability of successfully decoding a chain of network codes, which is of crucial importance in downlink multi-way PNC. To meet the different requirements for transmission quality in applications, we consider different aggregate measures of success probability over the participating user terminals, i.e., the arithmetic mean, the geometric mean, and the maximin. For each measure, we formulate a constrained optimization and solve the problem accordingly based on their concavity. We use an evolutionary PSO algorithm to solve the problem with a non-concave objective while we obtain a solution to the concave problems via efficient iterative means by demonstrating the concavity of the corresponding objective. The proposed power allocation schemes for downlink PNC in MWRC are evaluated using computer simulations over Rayleigh fading channels. The results demonstrate the effectiveness of the proposed schemes in improving the success probability in the reception of a chain of network codes.

CHAPTER 5

Optimal Power Allocation Based on Success Probability of SIC Detection in MWRC PNC

In this chapter, we propose a novel power allocation scheme for PNC in uplink MWRC. The power allocation is formulated as a constrained optimization problem under the transmitting power constraint of user terminals, aiming at maximizing the success probability of the SIC detection at the relay. Optimizing over such a metric maximizes the probability of correctly detecting all user signals, which is critical to the network code generation at the relay. Specifically, we first develop a generalized expression for the closed-form success probability for the SIC detection of PAM signals at the relay. We then formulate a constraint optimization to maximize this probability subject to the power constraints at the user terminals. We conceive an evolutionary PSO algorithm to solve the problem whose cost function is complex and not necessarily concave. The simulation results confirm the validity of the newly derived expression for the success probability and also demonstrate the effectiveness of the proposed power allocation scheme in improving the relay's ability to extract network codes from the superimposed signals.

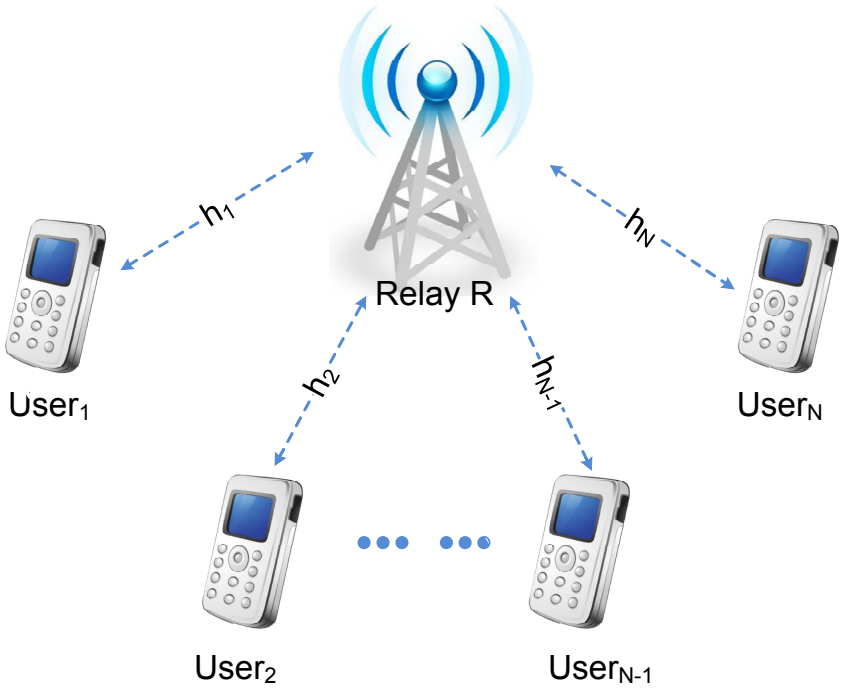

Fig. 5.1: Illustration of the PNC in MWRC.

5.1 System model

As illustrated in Fig. 5.1, we consider a half-duplex multiway relay network where N users share information with each other through a common relay R. User terminals are equipped with a single antenna while the relay is equipped with $K < N$ antennas. We assume that there is no direct link among users, i.e., information exchange between two users needs to go through the relay. We consider radio transmission over narrow-band, i.e., frequency flat, slow fading channels. We assume perfect channel estimation and time synchronization are available for any node in the network.

The superimposed signals received at the relay can be given as:

$$\tilde{\mathbf{y}} = \tilde{\mathbf{H}}\mathbf{A}\mathbf{s} + \tilde{\mathbf{n}}, \tag{5.1}$$

where $\mathbf{s} \in \mathbb{R}^{N\times 1}$ is the user signal vector whose i-th entry s_i is an M_i-PAM signal that is independently and uniformly distributed over a real set $\mathcal{B}_i = \{b_i^{(1)}, \ldots, b_i^{(M_i)}\}$ with $b_i^{(1)} < \cdots < b_i^{(M_i)} \in \mathbb{R}$, $\mathbf{y} \in \mathbb{C}^{K\times 1}$ is a received signal vector, $\tilde{\mathbf{H}} = [\tilde{\mathbf{h}}_1, \ldots, \tilde{\mathbf{h}}_N] \in \mathbb{C}^{K\times N}$ is the channel matrix, $\mathbf{A} = \text{diag}(\sqrt{P_1}, \ldots, \sqrt{P_N})$ with P_i being the power allocated to s_i, and $\tilde{\mathbf{n}} \in \mathbb{C}^K$ is the noise vector with each $\tilde{n}_i$ being independently distributed following $\mathcal{CN}(0, \tilde{\sigma}^2)$. For simplicity, we assume the distance between any two consecutive elements in each $\mathcal{B}_i$ is constant and denote it by $2d_i$, where

$$d_i = \frac{b_i^{(M_i)} - b_i^{(1)}}{2(M_i - 1)},$$

Since $\mathbf{s}$ has real-valued constellations, the estimation solely depends on the real domain. We can transform the system in to a real-valued system model, i.e.:

$$\mathbf{y} = \mathbf{HAs} + \mathbf{n}, \tag{5.2}$$

where $\mathbf{y} = \Re(\tilde{\mathbf{y}})$, $\mathbf{H} = \Re(\tilde{\mathbf{H}})$, and $\mathbf{n} = \Re(\tilde{\mathbf{n}})$.

5.2 The proposed method

In this section, we first present the derivation of a generalized closed-form success probability of the SIC detection on the PAM signaling. We then formulate a constrained optimization over this metric subject to the transmitting power constraint of user terminals and implement a particle swarm optimization algorithm to solve the problem.

5.2.1 Success Probability of the SIC Detection

Assuming that the successive process goes from column N to column 1 and for the i^{th} iteration, an estimator s_i^{sd} of s_i can be obtained after the removal of the previously detected signals s_j^{sd}, $j = i+1, \ldots, N$, from $\mathbf{y}$. Suppose that s_j^{sd} has been obtained for

$j = N, N-1, \ldots, i+1$ and we define:

$$\mathbf{y}^{(i)} = \mathbf{y} - \sum_{j=i+1}^{N} \mathbf{w}_j s_j^{sd}. \tag{5.3}$$

where $\mathbf{W} = \mathbf{HA} = [\mathbf{w}_1, \ldots, \mathbf{w}_N] \in \mathbb{R}^{K \times N}$, $\mathbf{w}_i = \sqrt{P}_i \mathbf{h}_i$. Then we solve:

$$\min_{s_i \in \mathcal{B}_i} \|\mathbf{y}^{(i)} - \mathbf{w}_i s_i\|_2. \tag{5.4}$$

The solution s_i^{sd} can then be obtained by:

$$c_i = \frac{\mathbf{w}_i^H \mathbf{y}^{(i)}}{\|\mathbf{w}_i\|_2^2}, \quad s_i^{sd} = \lfloor c_i \rceil_{\mathcal{B}_i}. \tag{5.5}$$

where $\lfloor c_i \rceil_{\mathcal{B}_i}$ denotes the nearest element to c_i in $\mathcal{B}_i$. From (5.5), (5.3) and (5.2), we obtain:

$$c_i = \frac{\mathbf{w}_i^H \mathbf{y}^{(i)}}{\|\mathbf{w}_i\|_2^2} = \sum_{j=1}^{i-1} \frac{\mathbf{w}_i^H \mathbf{w}_j s_j}{\|\mathbf{w}_i\|_2^2} + s_i + \sum_{j=i+1}^{N} \frac{\mathbf{w}_i^H \mathbf{w}_j (s_j - s_j^{sd})}{\|\mathbf{w}_i\|_2^2} + \frac{\mathbf{w}_i^H \mathbf{n}}{\|\mathbf{w}_i\|_2^2}. \tag{5.6}$$

When $\mathbf{s}_{i+1:N}^{sd} = \mathbf{s}_{i+1:N}$, from (5.6) we obtain:

$$c_i = \frac{\mathbf{w}_i^H \mathbf{y}^{(i)}}{\|\mathbf{w}_i\|_2^2} = \sum_{j=1}^{i-1} \frac{\mathbf{w}_i^H \mathbf{w}_j}{\|\mathbf{w}_i\|_2^2} s_j + s_i + \frac{\mathbf{w}_i^H \mathbf{n}}{\|\mathbf{w}_i\|_2^2}, \tag{5.7}$$

where $\mathbf{w}_i^H \mathbf{n}$ follows a normal distribution with

$$\begin{aligned} \mathrm{E}[\mathbf{w}_i^H \mathbf{n}] &= \mathbf{w}^H \mathrm{E}[\mathbf{n}] = 0, \\ \mathrm{Var}[\mathbf{w}_i^H \mathbf{n}] &= \mathbf{w}_i^H \mathrm{Cov}[\mathbf{n}] \mathbf{w}_i = \sigma^2 \|\mathbf{w}_i\|_2^2, \end{aligned}$$

where $\sigma = \frac{\sqrt{2}}{2}\tilde{\sigma}$. Thus, when $\mathbf{s}_{i+1:N}^{sd} = \mathbf{s}_{i+1:N}$, from (5.7) it follows that:

$$\frac{1}{\sigma}\left(\|\mathbf{w}_i\|_2 (c_i - s_i) - \sum_{j=1}^{i-1} \frac{\mathbf{w}_i^H \mathbf{w}_j}{\|\mathbf{w}_i\|_2} s_j \right) \sim \mathcal{N}(0, 1), \tag{5.8}$$

Our goal is to derive a formula for $\Pr(\mathbf{s}^{sd} = \mathbf{s})$. Note that by the chain rule,

$$\Pr(\mathbf{s}^{sd} = \mathbf{s}) = \prod_{i=1}^{N} \Pr(s_i^{sd} = s_i | \mathbf{s}_{i+1:N}^{sd} = \mathbf{s}_{i+1:N}). \tag{5.9}$$

Since events $(s_i = b_i^{(1)})$, $(b_i^{(1)} < s_i < b_i^{(M_i)})$, and $(s_i = b_i^{(M_i)})$ are mutually exclusive,

$$\begin{aligned}
&\Pr(s_i^{sd} = s_i \,|\, \mathbf{s}_{i+1:N}^{sd} = \mathbf{s}_{i+1:N}) \\
&= \underbrace{\Pr(s_i = b_i^{(1)}, c_i \le b_i^{(1)} + d_i \,|\, \mathbf{s}_{i+1:N}^{sd} = \mathbf{s}_{i+1:N})}_{P_{i,l}} \\
&+ \underbrace{\Pr(b_i^{(1)} < s_i < b_i^{(M_i)}, s_i - d_i < c_i < s_i + d_i \,|\, \mathbf{s}_{i+1:N}^{sd} = \mathbf{s}_{i+1:N})}_{P_{i,m}} \\
&+ \underbrace{\Pr(s_i = b_i^{(M_i)}, c_i \ge b_i^{(M_i)} - d_i \,|\, \mathbf{s}_{i+1:N}^{sd} = \mathbf{s}_{i+1:N})}_{P_{i,u}}.
\end{aligned} \tag{5.10}$$

In the derivation, we need to use the error function:

$$\mathrm{erf}(\zeta) = \frac{2}{\sqrt{\pi}} \int_0^{\zeta} \exp(-t^2) dt. \tag{5.11}$$

Given l and u with $l \le u$, if $x \sim \mathcal{N}(0,1)$, then

$$\Pr(x \le l) = \frac{1}{\sqrt{2\pi}} \int_{-\infty}^{l} e^{-\frac{t^2}{2}} dt = \frac{1}{2} \left(1 + \mathrm{erf}\left(\frac{l}{\sqrt{2}}\right)\right), \tag{5.12}$$

$$\Pr(x \ge u) = \frac{1}{\sqrt{2\pi}} \int_{u}^{\infty} e^{-\frac{t^2}{2}} dt = \frac{1}{2} \left(1 - \mathrm{erf}\left(\frac{u}{\sqrt{2}}\right)\right), \tag{5.13}$$

$$\Pr(l \le x \le u) = \frac{1}{2} \left(\mathrm{erf}\left(\frac{u}{\sqrt{2}}\right) - \mathrm{erf}\left(\frac{l}{\sqrt{2}}\right)\right). \tag{5.14}$$

In addition, for notational convenience, we label $b_t^{(1)}, \ldots, b_t^{(M_t)}$ in $\mathcal{B}_t$ by $0, 1, \ldots, M_t - 1$, respectively. Specifically, we define the bijection $\beta_t : \{b_t^{(1)}, \ldots, b_t^{(M_t)}\} \to \{0, \ldots, M_t - 1\}$. Let $\mathbf{s}_{1:i}^{(k_i)} = [s_1^{(k_i)}, \ldots, s_i^{(k_i)}]^T$ be the k_i-th possible instance of $\mathbf{s}_{1:i}$, where the index k_i is defined

by

$$k_i = 1 + \sum_{t=1}^{i} \Big(\beta_t(s_t) \prod_{j=t+1}^{i} M_j \Big). \tag{5.15}$$

For example, given $\mathcal{B}_1 = \{-1, 1\}, \mathcal{B}_2 = \{-3, -2, 0\}, \mathcal{B}_3 = \{2, 3, 4, 6, 7\}, \mathcal{B}_4 = \{-1, 0, 1, 2\}$, $\mathbf{s}_{1:4}^{(99)} = [-1, -2, 7, 1]^T$ represents the 99^{th} instance of $\mathbf{s}_{1:4}$ where k_i is computed as:

$$k_i = 1 + 1 \times (3 \times 5 \times 4) + 1 \times (5 \times 4) + 4 \times (4) + 2 \times (1) = 99. \tag{5.16}$$

Note that $k_i = 1, 2, \ldots, \prod_{t=1}^{i} M_t$ and $\mathbf{s}_{1:i}$ has a total of $\mathcal{M}_i = \prod_{t=1}^{i} M_t$ instances. Since s_i is independently uniformly distributed over $\mathcal{B}_i$ for $i = 1, \ldots, N$,

$$\Pr(\mathbf{s}_{1:i} = \mathbf{s}_{1:i}^{(k_i)}) = \frac{1}{\mathcal{M}_i}. \tag{5.17}$$

Derivation of $P_{i,l}$ According to Bayes's theorem, we have:

$$\begin{aligned} P_{i,l} &= \Pr(s_i = b_i^{(1)}) \Pr(c_i \leq b_i^{(1)} + d_i \,|\, s_i = b_i^{(1)}, \mathbf{s}_{i+1:N}^{sd} = \mathbf{s}_{i+1:N}) \\ &= \Pr(s_i = b_i^{(1)}) \sum_{k_{i-1}=1}^{\mathcal{M}_{i-1}} \Pr\left(\mathbf{s}_{1:i-1} = \mathbf{s}_{1:i-1}^{(k_{i-1})}\right) \\ &\quad \Pr\left(c_i \leq b_i^{(1)} + d_i \,|\, s_i = b_i^{(1)}, \mathbf{s}_{i+1:N}^{sd} = \mathbf{s}_{i+1:N}, \mathbf{s}_{1:i-1} = \mathbf{s}_{1:i-1}^{(k_{i-1})}\right) \end{aligned} \tag{5.18}$$

We plug (5.17) into (5.18) and obtain:

$$\begin{aligned} P_{i,l} = \frac{1}{M_i} \sum_{k_{i-1}=1}^{\mathcal{M}_{i-1}} \frac{1}{\mathcal{M}_{i-1}} \Pr\Big(&c_i \leq b_i^{(1)} + d_i \,|\, s_i = b_i^{(1)}, \\ &\mathbf{s}_{i+1:N}^{sd} = \mathbf{s}_{i+1:N}, \mathbf{s}_{1:i-1} = \mathbf{s}_{1:i-1}^{(k_{i-1})}\Big) \end{aligned} \tag{5.19a}$$

$$\begin{aligned} = \frac{1}{\mathcal{M}_i} \sum_{k_{i-1}=1}^{\mathcal{M}_{i-1}} \Pr\Big(&c_i \leq b_i^{(1)} + d_i \,|\, s_i \\ &= b_i^{(1)}, \mathbf{s}_{i+1:N}^{sd} = \mathbf{s}_{i+1:N}, \mathbf{s}_{1:i-1} = \mathbf{s}_{1:i-1}^{(k_{i-1})}\Big) \end{aligned} \tag{5.19b}$$

Now we find a formula for the probability in (5.19b). Note that when $s_i = b_i^{(1)}$ and $\mathbf{s}_{1:i-1} = \mathbf{s}_{1:i-1}^{(k_{i-1})}$, the inequality $c_i \leq b_i^{(1)} + d_i$ is equivalent to

$$\frac{1}{\sigma}\Big(\|\mathbf{w}_i\|_2(c_i - s_i) - \sum_{j=1}^{i-1} \frac{\mathbf{w}_i^H \mathbf{w}_j}{\|\mathbf{w}_i\|_2} s_j^{(k_{i-1})}\Big) \leq \frac{1}{\sigma}\Big(\|\mathbf{w}_i\|_2 d_i - \sum_{j=1}^{i-1} \frac{\mathbf{w}_i^H \mathbf{w}_j}{\|\mathbf{w}_i\|_2} s_j^{(k_{i-1})}\Big).$$

Then, by (5.8) and (5.12) we have:

$$\begin{aligned} &\Pr\left(c_i \leq b_i^{(1)} + d_i \,|\, s_i = b_i^{(1)}, \mathbf{s}_{i+1:N}^{sd} = \mathbf{s}_{i+1:N}, \mathbf{s}_{1:i-1} = \mathbf{s}_{1:i-1}^{(k_{i-1})}\right) \\ &= \frac{1}{2}\left(1 + \operatorname{erf}\left(\frac{1}{\sigma}\Big(\|\mathbf{w}_i\|_2 d_i - \sum_{j=1}^{i-1} \frac{\mathbf{w}_i^H \mathbf{w}_j}{\|\mathbf{w}_i\|_2} s_j^{(k_{i-1})}\Big)\right)\right). \end{aligned} \tag{5.20}$$

Therefore, from (5.19b) and (5.20), we obtain:

$$P_{i,l} = \frac{1}{2\mathcal{M}_i} \sum_{k_{i-1}=1}^{\mathcal{M}_{i-1}} \left\{1 + \operatorname{erf}\left(\frac{1}{\sigma}\Big(\|\mathbf{w}_i\|_2 d_i - \sum_{j=1}^{i-1} \frac{\mathbf{w}_i^H \mathbf{w}_j}{\|\mathbf{w}_i\|_2} s_j^{(k_{i-1})}\Big)\right)\right\}. \tag{5.21}$$

Derivation of $P_{i,m}$ and $P_{i,u}$ Similarly to the derivation of (5.21), we have:

$$\begin{aligned} P_{i,m} = \frac{M_i - 2}{\mathcal{M}_i} \sum_{k_{i-1}=1}^{\mathcal{M}_{i-1}} \Bigg\{ &\operatorname{erf}\left(\frac{1}{\sigma}\Big(\|\mathbf{w}_i\|_2 d_i - \sum_{j=1}^{i-1} \frac{\mathbf{w}_i^H \mathbf{w}_j}{\|\mathbf{w}_i\|_2} s_j^{(k_{i-1})}\Big)\right) \\ &- \operatorname{erf}\left(\frac{1}{\sigma}\Big(-\|\mathbf{w}_i\|_2 d_i - \sum_{j=1}^{i-1} \frac{\mathbf{w}_i^H \mathbf{w}_j}{\|\mathbf{w}_i\|_2} s_j^{(k_{i-1})}\Big)\right)\Bigg\}. \end{aligned} \tag{5.22}$$

$$P_{i,u} = \frac{1}{2\mathcal{M}_i} \sum_{k_{i-1}=1}^{\mathcal{M}_{i-1}} \left\{1 - \operatorname{erf}\left(\frac{1}{\sigma}\Big(-\|\mathbf{w}_i\|_2 d_i - \sum_{j=1}^{i-1} \frac{\mathbf{w}_i^H \mathbf{w}_j}{\|\mathbf{w}_i\|_2} s_j^{(k_{i-1})}\Big)\right)\right\}. \tag{5.23}$$

Eventually, we plug (5.21), (5.22), and (5.23) into (5.10) and then into (5.9). The success probability $\Pr(\mathbf{s}^{sd} = \mathbf{s})$ is thus given as:

$$\begin{aligned}\Pr(\mathbf{s}^{sd} = \mathbf{s}) &= \prod_{i=1}^{N} \{P_{i,l} + P_{i,m} + P_{i,u}\} \\ &= \prod_{i=1}^{N} \Bigg\{ \frac{1}{M_i} + \frac{M_i - 1}{2\mathcal{M}_i} \sum_{k_{i-1}=1}^{\mathcal{M}_{i-1}} \\ &\quad \Bigg[\operatorname{erf}\Bigg(\frac{1}{\sigma} \Bigg(\|\mathbf{w}_i\|_2 d_i - \sum_{j=1}^{i-1} \frac{\mathbf{w}_i^H \mathbf{w}_j}{\|\mathbf{w}_i\|_2} s_j^{(k_{i-1})} \Bigg) \Bigg) \\ &\quad + \operatorname{erf}\Bigg(\frac{1}{\sigma} \Bigg(\|\mathbf{w}_i\|_2 d_i + \sum_{j=1}^{i-1} \frac{\mathbf{w}_i^H \mathbf{w}_j}{\|\mathbf{w}_i\|_2} s_j^{(k_{i-1})} \Bigg) \Bigg) \Bigg] \Bigg\}\end{aligned} \tag{5.24}$$

5.2.2 Problem Formulation

We formulate an optimization problem based on (5.24) subject to the transmitting power constraint P_T of user terminals to maximize the success probability of SIC detection at the relay side, i.e.:

$$\max_{P_1, \cdots, P_N} \Pr(\mathbf{s}^{sd} = \mathbf{s}) \tag{5.25a}$$

$$\text{s.t.} : 0 \leq P_j \leq P_T, \text{ for j=1,..., N.} \tag{5.25b}$$

However, the function in (5.24) is not necessarily concave with respect to P_j, and the corresponding proof is difficult to obtain due to the complication of its form. We will use a numerical computing method to solve such a problem in (5.25).

5.2.3 PSO Solution

The PSO algorithm starts with random initializations of a swarm of individuals, called particles, within the problem feasible region [109]. Then each particle iteratively approaches better and better approximations to the optimal solution with moving directions

and step length that are coordinated by the entire swarm's motion. A detailed process is given in Algorithm 5.

Velocity and position At iteration $t \in \mathbb{N}$, each particle in a swarm of size S is characterized by its position vector $\mathbf{X}_m^t = [P_{m1}^t, \ldots, P_{mK}^t]^T \in \mathbb{R}_+^K$ and a velocity vector $\mathbf{V}_m^t = [v_{m1}^t, \ldots, v_{mK}^t]^T$, where $m \in \{1, \ldots, S\}$ is the particle index, P_{mj}^t is the particle m's current solution to power P_j, and v_{mj}^t is the jth velocity component, $j \in \{1, \ldots, K\}$. Each particle adjusts its trajectory towards its own previous best position, called $\mathcal{O}_{best}$, and towards a global best position attained by any member within the swarm, called $\mathcal{G}_{best}$. $\mathcal{O}_{best}$ and $\mathcal{G}_{best}$ are determined by evaluating the cost function $f(\mathbf{X}_m^t) \equiv \Pr(\mathbf{s}^{sd} = \mathbf{s})$ in (5.25a) during the particle's motion.

Penalized cost function In order to confine the particles' motion within the feasible region, we incorporate a penalty function to the cost function f, i.e.:

$$F(\mathbf{X}_m^t) = f(\mathbf{X}_m^t) - \Omega \max\{0, P_{m1}^t - P_T, \ldots, P_{mN}^t - P_T, -\mathbf{X}_m^t\}, \tag{5.26}$$

where Ω is a penalty factor with a large positive value. Once a particle motion violates the constraints, $F(\mathbf{X}_m^t)$ deteriorates dramatically to a small value. The result of this motion will thus be discarded.

Motion updates Velocity $\mathbf{V}_m^{t+1}$ directs the particle to the next new position. Its component on dimension j is given as:

$$v_{mj}^{t+1} = \omega^t v_{mj}^t + c_1 r_1^t (\mathcal{O}_{best,mj} - P_{mj}^t) + c_2 r_2^t (\mathcal{G}_{best,mj} - P_{mj}^t), \tag{5.27}$$

where ω^t is an inertia weight, c_1 and c_2 are the constant cognitive and social parameters respectively, and r_1^t and r_2^t are the randomly generated numbers. The new position on

dimension j is accordingly given as:

$$P_{mj}^{t+1} = P_{mj}^{t} + v_{mj}^{t+1}, \tag{5.28}$$

Convergence and termination The algorithm eventually comes to a stop when the motion of swarm stalls. This occurs when the largest change in the objective value for the swarm, i.e.: $\max\{\Delta_m = |F(\mathbf{X}_m^t) - F(\mathcal{F}_m^{t-1})|, m = 1, \ldots, S\}$, is less than a certain small value ϵ. In addition, based on our experience, the algorithm can always solve problem (5.25) within a certain number of iterations for a specific swarm size. Thus, we set a maximum number of iterations T_{max} as an additional stopping criterion for the algorithm. The eventual $\mathcal{G}_{best}$ is thus considered as the solution to the power allocation problem in (5.25).

Algorithm 5 PSO algorithm to solve problem (5.25)

1: **Step 1:** Input swarm size S; number of max iterations T_{max}; penalized cost function $F(\cdot)$; stopping criteria ϵ.
2: **Step 2:** Initialize parameters c_1, c_2, r_1^0, r_2^0.
3: **Step 3:**: For each particle $m = 1$ to S, initialize random particle positions $\mathbf{X}_m^0$ in the feasible region and velocity $\mathbf{V}_m^0 = \mathbf{0}$. Set particle best known position $\mathcal{O}_{best,m} = X_m^0$ and valuate each particle's cost $F(\mathbf{X}_m^0)$.
4: **Step 4:** Initialize swarm's best known position $\mathcal{G}_{best}$, where $F(\mathcal{G}_{best}) = \max\{F(\mathbf{X}_m^0)|m = 1, \ldots, S\}$.
5: **Step 5:** Initialize t=0.
6: **Step 6:** $t = t + 1$.
7: **Step 7:** Update the velocity of particles according to (5.27) and the position of particles according to (5.28).
8: **Step 8:** Evaluate $F(\mathbf{X}_m^t)$ for $m = 1, \ldots, S$ and determine $\mathcal{O}_{best,m}$, where $F(\mathcal{O}_{best,m}) = \max\{F(\mathbf{X}_m^i)|i = 1, \ldots, t\}$.
9: **Step 9:** Update $\mathcal{G}_{best}$, where $F(\mathcal{G}_{best}) = \max\{F(\mathcal{O}_{best,m})|m = 1, \ldots, S\}$.
10: **Step 10:** Randomize parameter r_1^t and r_2^t.
11: **Step 11:** If $t \leq T_{max}$ or $\max\{\Delta_m = |F(X_m^t) - F(X_m^{t-1})|, m = 1, \ldots, S\} > \epsilon$, return to **Step 6**. Otherwise, stop the iteration and output $\mathcal{G}_{best}$.

5.3 Simulation Results

In this section, numerical results are provided to demonstrate the performance of the proposed success-probability-based power allocation scheme for SIC detection. We assume

the MWRC PNC consists of $N = 4$ user terminals, and the relay has $K = 3$ antennas with transmitting power constraint $P_T = 1$. We assume the various radio links to be Rayleigh fading, i.e., the entries of the channel matrix $\tilde{\mathbf{H}}$ are modeled as independent complex circular Gaussian random variables with zero mean and unit variance. The noise variance at receiving antennas is adjusted accordingly to obtain the desired SNR level.

We first validate the derivation of (5.24) by comparing the theoretical analysis with the numerical results from Monte Carlo experiments in Fig. 5.2. In order to have a straightforward comparison and eliminate any potential distraction from optimization process, we simply allocate equal power to the transmitting user terminals with 3 groups of different PAM modulations, i.e., 2-PAM $\mathbf{s} \in \{-1, +1\}$, 4-PAM $\mathbf{s} \in \{-3, -1, +1, +3\}$, and 6-PAM $\mathbf{s} \in \{1, 2, 3, 4, 5, 6\}$. Based on the results of all three groups of comparison, we can observe that the numerical results are in accordance with their respective theoretical values.

We then demonstrate the effect of the power allocation strategy on the rate of correctly generated network code chains. In this experiment, we compare the proposed success-probability-based strategy with a conventional sum-rate-based strategy that maximizes user signals' minimal SINR. The equal power allocation strategy is also provided as a reference. The sequential coding strategy as in [104] is adopted at the relay for the code chain generation. We transmit $10,000$ signals with 4-PAM signaling from each user and compare the generated code chains to their expected results at the relay. The rate of correct code chain (CC) generation at relay thus can be used to evaluate the efficacy of relay detection, which is defined as:

$$\text{rate of correct CC generation} = \frac{\text{number of correctly generated CC}}{\text{total number of generated CC}} \tag{5.29}$$

In Fig. 5.3, we present the comparison among the proposed strategy (indicated by 'SP'), the conventional strategy (indicated by 'SINR'), and the equal power allocation strategy (indicated by 'Eq'). From the result, we can see that the proposed method effectively improves the rate of correct CC generation with an advantage of around $5dB$ over the

conventional sum-rate based method. Hence, the result demonstrates the effectiveness of the proposed in improving the relay's ability to extract network codes from the superimposed signals.

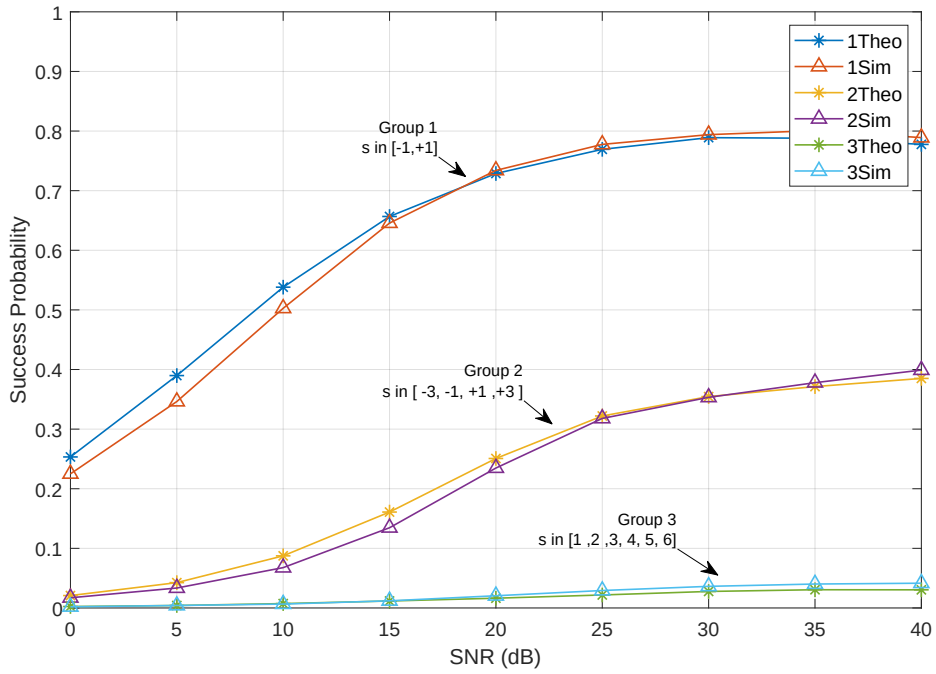

Fig. 5.2: Comparison of success probability vs SNR between theoretical analysis and simulation results.

5.4 Chapter Summary

In this chapter, we proposed a novel power allocation scheme for PNC in uplink MWRC. The power allocation was formulated as a constrained optimization problem under the user terminal transmit power constraint, with the aim of maximizing the success probability of the SIC detection at the relay. Optimization of such a metric maximizes the probability of correctly detecting all user signals, which is crucial for network code generation at the relay. Specifically, we first developed a generalized closed-form expression for the success probability of the SIC detection of the PAM signals. We then formulated a constraint optimization of this probability subject to the user terminal power constraints.

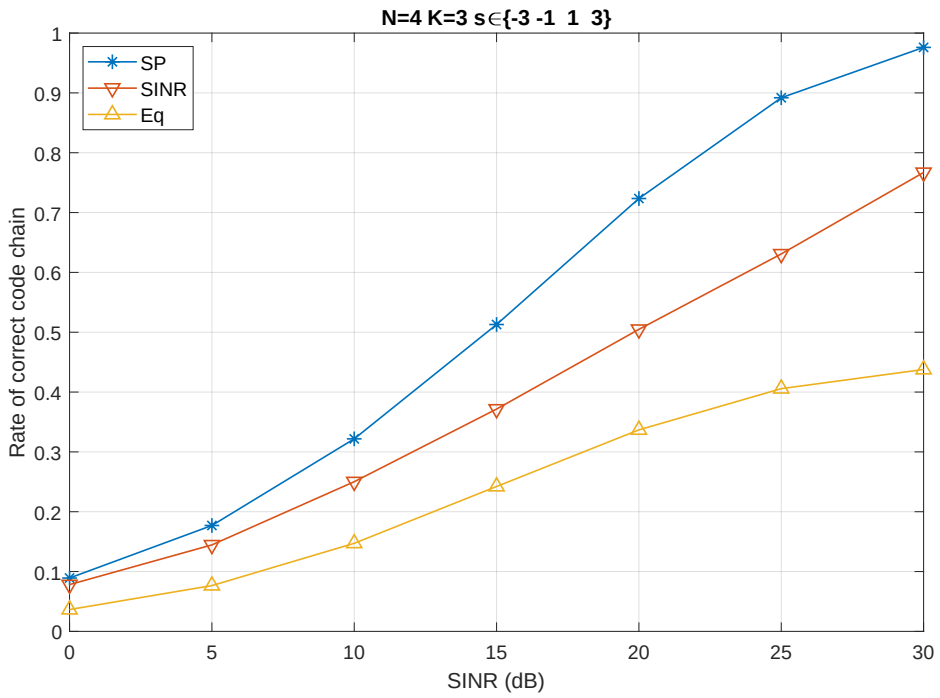

Fig. 5.3: Comparison of the rate of correct code chain generation between the effect of power allocation strategy.

We conceived an evolutionary PSO algorithm to solve the problem whose cost function is complex and not necessarily concave. The numerical results validated the probability derivation and also demonstrated the effectiveness of the proposed power allocation scheme in improving the relay's ability to extract network codes from the superimposed signals.

CHAPTER 6

Conclusion

In this chapter, we summarize the thesis and provide a plan for potential future work.

6.1 Summary

This thesis focuses on the application of PNC in MWRC, where multiple users share information through a single relay station. In the previous chapters, we have presented in detail the main works, i.e., the development of new uplink and downlink schemes for PNC in MWRC regarding signal detection and power allocation. Here, we present the summary of all contributions.

Chapter 3 proposed a novel scheme for PNC in MWRC, aiming to address these challenges from a different perspective, i.e., sequential MUD. The benefits of doing so are twofold: 1) we still treat the MWRC as a natural encoder within the wireless medium, which is consistent with the inherent idea of PNC; 2) the use of MUD offers a powerful framework for extracting the network codes with relatively low complexity. To be specific, we considered an uplink MWRC scenario where N users, each equipped with a single antenna, simultaneously transmit signals to a relay equipped with K antennas, emphasizing the case $K < N$. In contrast to existing approaches that seek to directly obtain the network codes from the superimposed user signals at the relay, we formulated

this problem as an under-determined linear system in terms of the user symbols (from which the network codes can be easily obtained). To solve this problem with low decoding complexity, the proposed method combines SIC with Babai estimation [119] for regularized ILS. Specifically, SIC decoding was first employed to estimate a selected subset of stronger user signals and remove their interfering effects. Babai estimation was then applied to provide a solution to an ILS problem with reduced dimension, allowing the extraction of the remaining weaker user signals. We developed a power allocation scheme to enhance both the SIC and ILS detection steps and discuss the optimal user pairing strategy based on the average decoding error probability. Through simulations, it was shown that the proposed method could lead to notable performance improvement in the extraction of network codes from superimposed user signals in MWRC.

In Chapter 4, we proposed a novel power allocation scheme for PNC in downlink MWRC. The power allocation is formulated as a constrained optimization problem, where the aim is to maximize the success probability under a total power constraint when using Babai estimation for signal detection. Optimizing over this metric allows us to maximize the probability of successfully decoding a chain of network codes. To meet diverse requirements for transmission quality in applications, we considered different aggregate measures of success probability over the participating user terminals, namely: the arithmetic mean, the geometric mean, and the maximin. We first used an evolutionary particle swarm optimization (PSO) algorithm to solve the problem for the arithmetic mean, which is non-concave. We then formulate an alternative concave problem for this measure and find the solution via iterative methods. We obtained the solutions of the other two problems for the geometric mean and maximin, which are shown to be concave, via efficient iterative search methods. The proposed power allocation schemes for downlink PNC in MWRC were evaluated using computer simulations over Rayleigh fading channels. The results demonstrated the effectiveness of the proposed schemes in improving the success probability in the reception of a chain of network codes.

In Chapter 5, we proposed a novel power allocation scheme for PNC in uplink MWRC. The power allocation was formulated as a constrained optimization problem under the user terminal transmit power constraint, with the aim of maximizing the success probability of the SIC detection at the relay. Optimization of such a metric maximizes the probability of correctly detecting all user signals, which is crucial for network code generation at the relay. Specifically, we first developed a generalized closed-form expression for the success probability of the SIC detection of the PAM signals. We then formulated a constraint optimization of this probability subject to the user terminal power constraints. We conceived an evolutionary PSO algorithm to solve the problem whose cost function is complex and not necessarily concave. The numerical results validated the probability derivation and also demonstrated the effectiveness of the proposed power allocation scheme in improving the relay's ability to extract network codes from the superimposed signals.

6.2 Potential future works

In this section, we present and discuss some potential work related to this thesis.

In Chapter 3, we propose an optimal pairing strategy for relay stations and study its impact on the performance of network coding in MWRC. We formulate the problem as a discrete optimization problem in which the solution is searched for by brute-force over all spanning trees of a simple undirected connected graph with N vertices. Although feasible, the approach is not cost effective and often becomes time consuming, especially when the system size is huge. Therefore, a potential future work could emphasize improving the efficiency of solving this optimization problem.

In Chapter 4, we assume that the relay has successfully received all user signals in the MA phase, which implies a success probability of 100% for uplink transmission. However, in reality, errors in the uplink will inevitably propagate in the downlink phase, which will also affect the success probability of the transmission and network code re-

covery at the user terminals. Therefore, possible future work could emphasize combining the work in Chapters 4 and 5 to jointly consider the uplink and downlink phases in the design of power allocation based on the success probability.

References

[1] S. Bi, R. Zhang, Z. Ding, and S. Cui, "Wireless communications in the era of big data," *IEEE Commun. Mag.*, vol. 53, no. 10, pp. 190–199, 2015.

[2] S. Zhang, S. C. Liew, and P. P. Lam, "Hot topic: Physical-layer network coding," in *Proc. Int. Conf. on Mobile Comput. and Netw.*, Los Angeles, USA, Sept. 2006, pp. 358–365.

[3] S.-C. Liew, S. Zhang, and L. Lu, "Physical-layer network coding: Tutorial, survey, and beyond," *Phys. Commun.*, vol. 6, pp. 4–42, 2011.

[4] F. Jamil, A. Javaid, T. Umer, and M. H. Rehmani, "A comprehensive survey of network coding in vehicular ad-hoc networks," *Wireless Netw.*, pp. 1–20, 2016.

[5] L. F. Xie, I. W. H. Ho, S. C. Liew, L. Lu, and F. C. M. Lau, "The feasibility of mobile physical-layer network coding with BPSK modulation," *IEEE Trans. on Veh. Tech.*, vol. 66, no. 5, pp. 3976–3990, May 2017.

[6] T. Peng, Y. Wang, A. G. Burr, and M. R. Shikh-Bahaei, "Physical layer network coding in network MIMO: A new design for 5G and beyond," *IEEE Trans. on Commun.*, vol. 67, no. 3, pp. 2024–2035, Mar. 2019.

[7] Y. Wu, P. A. Chou, and S. Y. Kung, "Information exchange in wireless networks with network coding and physical layer broadcast," in *Proc. Conf. on Inform. Sci. and Syst.*, Baltimore, USA, Aug. 2005.

[8] S. Y. R. Li, R. W. Yeung, and N. Cai, "Linear network coding," *IEEE Trans. on Inf. Theory*, vol. 49, no. 2, pp. 371–381, Feb. 2003.

[9] S. Deb, M. Effros, T. Ho, D. R. Karger, R. Koetter, D. S. Lun, M. Medard, and N. Ratnakar, "Network coding for wireless applications: A brief tutorial," in *Proc. Int. Workshop on Wireless Ad-hoc Netw.*, London, UK, 2005.

[10] E. Dahlman, G. Mildh, S. Parkvall, J. Peisa, J. Sachs, and Y. Selén, "5G radio access," *Ericsson Review*, vol. 6, pp. 2–7, 2014.

[11] Ericsson, Huawei, and Qualcomm, "The road to 5G: Drivers, applications, requirements and technical development," Global Mobile Suppliers Association, Tech. Rep., 2015.

[12] J. Gozalves, "Fifth-generation technologies trials," *IEEE Veh. Technol. Mag.*, vol. 11, no. 2, pp. 5–13, June 2016.

[13] I. Parvez, A. Rahmati, I. Guvenc, A. I. Sarwat, and H. Dai, "A survey on low latency towards 5G: RAN, core network and caching solutions," *IEEE Commun. Surv. Tut.*, vol. 20, no. 4, pp. 3098–3130, 2018.

[14] R. Y. Chang, S. J. Lin, and W. H. Chung, "Symbol and bit mapping optimization for physical-layer network coding with pulse amplitude modulation," *IEEE Trans. on Wireless Commun.*, vol. 12, no. 8, pp. 3956–3967, Aug. 2013.

[15] M. Noori and M. Ardakani, "On symbol mapping for binary physical-layer network coding with PSK modulation," *IEEE Trans. on Wireless Commun.*, vol. 11, no. 1, pp. 21–26, Jan. 2012.

[16] T.-T. Chan and T.-M. Lok, "Interference alignment with physical-layer network coding in MIMO relay channels," in *Proc. IEEE Int. Conf. on Commun.*, Kuala Lumpur, Malaysia, May 2016, pp. 1–6.

[17] L. Lu and S. C. Liew, "Asynchronous physical-layer network coding," *IEEE Trans. on Wireless Commun.*, vol. 11, no. 2, pp. 819–831, Feb. 2012.

[18] Q. Yang and S. C. Liew, "Asynchronous convolutional-coded physical-layer network coding," *IEEE Trans. on Wireless Commun.*, vol. 14, no. 3, pp. 1380–1395, Mar. 2015.

[19] Y. Huang, S. Wang, Q. Song, and L. Guo, "Synchronous physical-layer network coding: A feasibility study," *IEEE Trans. on Wireless Commun.*, vol. 12, no. 8, pp. 4048–4057, Aug. 2013.

[20] X. Dang, Z. Huang, Q. Li, and X. Yu, "Estimation of symbol timing in physical-layer network coding with arrival time differences," *IEEE Commun. Lett.*, vol. PP, no. 99, pp. 1–1, 2016.

[21] T. Wang and S. C. Liew, "An EM approach for joint channel estimation and channel decoding in systems employing physical-layer network coding," in *Proc. IEEE Int. Conf. on Acoustics, Speech and Signal Process.*, Vancouver, Canada, May 2013, pp. 5104–5108.

[22] X. Hu, Z. Chen, and F. Yin, "Channel and delay estimation for asynchronous physical layer network coding," *AEU - Int. J. of Electron. and Commun.*, vol. 87, pp. 101 – 106, 2018.

[23] P. Chen, L. Shi, S. C. Liew, Y. Fang, and K. Cai, "Channel decoding for nonbinary physical-layer network coding in two-way relay systems," *IEEE Trans. on Veh. Technol.*, vol. 68, no. 1, pp. 628–640, Jan. 2019.

[24] D. Gunduz, A. Yener, A. Goldsmith, and H. V. Poor, "The multiway relay channel," *IEEE Trans. on Info. Theory*, vol. 59, no. 1, pp. 51–63, 2012.

[25] Z. A. Almaalie, X. Tang, Z. Ghassemlooy, I. E. Lee, and A. A. S. Al-Rubaie, "Iterative multiuser detection with physical layer network coding for multi-pair communications," in *Proc. IEEE Int. Sym. on Commn. Syst., Netw. and Digital Signal Proc.*, Prague, Czech, Nov. 2016, pp. 9396–9406.

[26] Z. Zhao, Z. Ding, M. Peng, W. Wang, and K. K. Leung, "A special case of multi-way relay channel: When beamforming is not applicable," *IEE Trans. on Wireless Commn.*, vol. 10, no. 7, pp. 2046–2051, July 2011.

[27] Bras and F. A. Silva., "Interference suppression using MIMO and physical layer network coding," in *Proc. IEEE Workshop on Signal Process. System.*, Belfast, Ireland, 2014, pp. 1–6.

[28] J. He and S. C. Liew, "Building blocks of physical-layer network coding," *IEEE Trans. on Wireless Commun.*, vol. 14, no. 5, pp. 2711–2728, May 2015.

[29] R. Y. Chang, S. J. Lin, and W. H. Chung, "Transmission protocol design for binary physical network coded multi-way relay networks," in *Proc. IEEE Veh. Technol. Conf.*, Seoul, Korea, May 2014, pp. 1–5.

[30] M. Hekrdla and J. Sykora, "Constellations maximizing minimal distance for physical-layer network coding multi-way relaying," in *Proc. IEEE Veh. Technol. Conf.*, Glasgow, Scotland, May 2015, pp. 1–6.

[31] V. Stankovic and M. Haardt, "Generalized design of multi-user MIMO precoding matrices," *IEEE Trans. on Wireless Commun.*, vol. 7, no. 3, pp. 953–961, March 2008.

[32] Z. Shen, R. Chen, J. G. Andrews, R. W. Heath, and B. L. Evans, "Low complexity user selection algorithms for multiuser MIMO systems with block diagonalization," *IEEE Trans. on Signal Proc.*, vol. 54, no. 9, pp. 3658–3663, Sept 2006.

[33] S. Shim, J. S. Kwak, R. W. Heath, and J. G. Andrews, "Block diagonalization for multi-user MIMO with other-cell interference," *IEEE Trans. on Wireless Commun.*, vol. 7, no. 7, pp. 2671–2681, July 2008.

[34] M. Sadek, A. Tarighat, and A. H. Sayed, "A leakage-based precoding scheme for downlink multi-user MIMO channels," *IEEE Trans. on Wireless Commun.*, vol. 6, no. 5, pp. 1711–1721, May 2007.

[35] K. Singh, M.-L. Ku, and M. F. Flanagan, "Energy-efficient precoder design for downlink multi-user MISO networks with finite blocklength codes," *IEEE Trans. on Green Commun. and Netw.*, vol. 5, no. 1, pp. 160–173, 2021.

[36] J. A. Oviedo and H. R. Sadjadpour, "Fundamentals of power allocation strategies for downlink multi-user NOMA with target rates," *IEEE Trans. on Wireless Commun.*, vol. 19, no. 3, pp. 1906–1917, 2020.

[37] J. Wen and X.-W. Chang, "Success probability of the Babai estimators for box-constrained integer linear models," *IEEE Trans. on Info. Theory*, vol. 63, no. 1, pp. 631–648, Jan. 2017.

[38] X.-W. Chang and V. J. Prevost, "Success probability of a suboptimal solution to the sparse MAP detection," in *Proc. IEEE Int. Symp. on Info. Theory*, Vail, CO, US, 2018, pp. 66–70.

[39] M. O. Damen, H. El Gamal, and G. Caire, "On maximum-likelihood detection and the search for the closest lattice point," *IEEE Trans. on Info. Theory*, vol. 49, no. 10, pp. 2389–2402, 2003.

[40] J. Andrews and T. Meng, "Optimum power control for successive interference cancellation with imperfect channel estimation," *IEEE Trans. on Wireless Commun.*, vol. 2, no. 2, pp. 375–383, 2003.

[41] P. N. Son and T. T. Duy, "A new approach for two-way relaying networks: improving performance by successive interference cancellation, digital network coding and opportunistic relay selection," *Wireless Netw.*, vol. 26, pp. 1315–1329, 2020.

[42] S. Khosroazad, S. Naderi, and A. Abedi, "Using physical layer network coding to improve NOMA system throughput with energy harvesting users," in *Proc. IEEE Global Commun. Conf.*, Waikoloa, HI, US, 2019, pp. 1–6.

[43] I. Abu Mahady, E. Bedeer, S. Ikki, and H. Yanikomeroglu, "Sum-rate maximization of NOMA systems under imperfect successive interference cancellation," *IEEE Commun. Lett.*, vol. 23, no. 3, pp. 474–477, 2019.

[44] A. Kilzi, J. Farah, C. Abdel Nour, and C. Douillard, "Mutual successive interference cancellation strategies in noma for enhancing the spectral efficiency of comp systems," *IEEE Trans. on Commun.*, vol. 68, no. 2, pp. 1213–1226, 2020.

[45] S. Kusaladharma, W.-P. Zhu, W. Ajib, and G. A. A. Baduge, "Achievable rate characterization of NOMA-aided cell-free massive MIMO with imperfect successive interference cancellation," *IEEE Trans. on Commun.*, vol. 69, no. 5, pp. 3054–3066, 2021.

[46] S. G. Hong and S. Bahk, "Performance analysis and fairness maximization in NOMA systems with improper Gaussian signaling under imperfect successive interference cancellation," *IEEE Access*, vol. 8, pp. 50 439–50 451, 2020.

[47] J. Wen, K. Wu, C. Tellambura, and P. Fan, "Closed-form word error rate analysis for successive interference cancellation decoders," *IEEE Trans. on Wireless Commun.*, vol. 17, no. 12, pp. 8256–8267, 2018.

[48] L. E. Frenzel, *Principles of Electronic Communication Systems*. McGraw-Hill, 2016.

[49] M. Agiwal, H. Kwon, S. Park, and H. Jin, "A survey on 4G-5G dual connectivity: Road to 5G implementation," *IEEE Access*, vol. 9, pp. 16 193–16 210, 2021.

[50] F. Takahata, Y. Hirata, A. Ogawa, and K. Inagaki, "Development of a TDM/FDM transmultiplexer," *IEEE Trans. on Commun.*, vol. 26, no. 5, pp. 726–733, 1978.

[51] Federal Communications Commission, "Auction of flexible-use service licenses in the 3.7-3.98 GHz band closes; winning bidders announced for auction 107," Washington, DC, US, Feb. 2021.

[52] S. Zhang, S.-C. Liew, and P. P. Lam, "On the synchronization of physical-layer network coding," in *Proc. IEEE Info. Theory Workshop*, Chengdu, China, 2006, pp. 404–408.

[53] L. Lu and S. C. Liew, "Asynchronous physical-layer network coding," *IEEE Trans. on Wireless Commun.*, vol. 11, no. 2, pp. 819–831, 2012.

[54] S. Chang and B. Kelley, "An efficient time synchronization scheme for broadband two-way relaying networks based on physical-layer network coding," *IEEE Commu. Lett.*, vol. 16, no. 9, pp. 1416–1419, 2012.

[55] S. Zhang and S.-C. Liew, "Channel coding and decoding in a relay system operated with physical-layer network coding," *IEEE J. on Sel. Areas in Commun.*, vol. 27, no. 5, pp. 788–796, 2009.

[56] Z. Abu Almaalie, Z. Ghassemlooy, A. A. S. Al-Rubaie, I. E. Lee, and H. Le-Minh, "Forward error correction with physical layer network coding in two-way relay free space optical links," in *Proc. Comp. Sci. and Elect. Eng.*, Colchester, UK, 2016, pp. 1–5.

[57] L. Yang, T. Yang, J. Yuan, and J. An, "Achieving the near-capacity of two-way relay channels with modulation-coded physical-layer network coding," *IEEE Trans. on Wireless Commun.*, vol. 14, no. 9, pp. 5225–5239, 2015.

[58] Y. Tan, S. C. Liew, and T. Huang, "Mobile lattice-coded physical-layer network coding with practical channel alignment," *IEEE Trans. on Mobile Comp.*, vol. 17, no. 8, pp. 1908–1923, 2018.

[59] K. Yasami, A. Razi, and A. Abedi, "Analysis of channel estimation error in physical layer network coding," *IEEE Commun. Lett.*, vol. 15, no. 10, pp. 1029–1031, 2011.

[60] T. Wang and S. C. Liew, "Joint channel estimation and channel decoding in physical-layer network coding systems: An EM-BP factor graph framework," *IEEE Trans. on Wireless Commun.*, vol. 13, no. 4, pp. 2229–2245, 2014.

[61] W. Haiming, H. Wei, C. Jixin, S. Bo, and P. Xiaoming, "IEEE 802.11aj (45ghz): A new very high throughput millimeter-wave WLAN system," *China Commun.*, vol. 11, no. 6, pp. 51–62, 2014.

[62] T. S. Rappaport, S. Sun, R. Mayzus, H. Zhao, Y. Azar, K. Wang, G. N. Wong, J. K. Schulz, M. Samimi, and F. Gutierrez, "Millimeter wave mobile communications for 5G cellular: It will work!" *IEEE Access*, vol. 1, pp. 335–349, 2013.

[63] W. Hong, K.-H. Baek, and S. Ko, "Millimeter-wave 5G antennas for smartphones: Overview and experimental demonstration," *IEEE Trans. on Antennas and Propagation*, vol. 65, no. 12, pp. 6250–6261, 2017.

[64] S. Maleki, S. Chatzinotas, J. Krause, K. Liolis, and B. Ottersten, "Cognitive zone for broadband satellite communications in 17.3–17.7 GHz band," *IEEE Wireless Commun. Lett.*, vol. 4, no. 3, pp. 305–308, 2015.

[65] G. Corazza and R. De Gaudenzi, "Analysis of coded noncoherent transmission in DS-CDMA mobile satellite communications," *IEEE Trans. on Commun.*, vol. 46, no. 11, pp. 1525–1535, 1998.

[66] Y. Zeng, R. Zhang, and T. J. Lim, "Wireless communications with unmanned aerial vehicles: opportunities and challenges," *IEEE Commun. Mag.*, vol. 54, no. 5, pp. 36–42, 2016.

[67] L. Gupta, R. Jain, and G. Vaszkun, "Survey of important issues in uav communication networks," *IEEE Commun. Surv. Tut.*, vol. 18, no. 2, pp. 1123–1152, 2016.

[68] L. Ruan, J. Wang, J. Chen, Y. Xu, Y. Yang, H. Jiang, Y. Zhang, and Y. Xu, "Energy-efficient multi-UAV coverage deployment in UAV networks: A game-theoretic framework," *China Commu.*, vol. 15, no. 10, pp. 194–209, 2018.

[69] N. C. Beaulieu and J. Hu, "A noise reduction amplify-and-forward relay protocol for distributed spatial diversity," *IEEE Comm. Lett.*, vol. 10, no. 11, pp. 787–789, 2006.

[70] G. Kramer, M. Gastpar, and P. Gupta, "Cooperative strategies and capacity theorems for relay networks," *IEEE Trans. on Info. Theory*, vol. 51, no. 9, pp. 3037–3063, 2005.

[71] A. Wyner and J. Ziv, "The rate-distortion function for source coding with side information at the decoder," *IEEE Trans. on Info. Theory*, vol. 22, no. 1, pp. 1–10, 1976.

[72] I. Ullah, F. Ud Din, J. N. Chattha, and M. Uppal, "Compress-and-forward relaying: Prototyping and experimental evaluation using sdrs," in *Proc. IEEE 84th Veh. Tech. Conf.*, Montreal, QC, Canada, 2016, pp. 1–5.

[73] A. A. I. Ibrahim, A. C. Marcum, D. J. Love, and J. V. Krogmeier, "Channel estimation for multi-way quantized distributed wireless relaying," in *Proc. MILCOM*, Baltimore, MD, USA, 2017, pp. 342–347.

[74] G. Amarasuriya and H. V. Poor, "Impact of channel aging in multi-way relay networks with massive MIMO," in *Proc. IEEE Int. Conf. on Commun.*, London, UK, 2015, pp. 1951–1957.

[75] S. N. Islam, S. Durrani, and P. Sadeghi, "SER analysis of multi-way relay networks with M-QAM modulation in the presence of imperfect channel estimation," *J. of Commun. and Netw.*, vol. 18, no. 5, pp. 677–687, 2016.

[76] C. D. Ho, H. Q. Ngo, M. Matthaiou, and L. D. Nguyen, "Power allocation for multi-way massive MIMO relaying," *IEEE Trans on Commun.*, vol. 66, no. 10, pp. 4457–4472, 2018.

[77] S. Silva, G. A. A. Baduge, M. Ardakani, and C. Tellambura, "NOMA-aided multi-way massive MIMO relaying," *IEEE Trans on Commun.*, vol. 68, no. 7, pp. 4050–4062, 2020.

[78] Z. Zhou, K. K. Teav, and B. Vucetic, "Beamforming optimization and power allocation for MIMO asymmetric multi-way relay channels," *IEEE Commu. Lett.*, vol. 16, no. 6, pp. 820–823, 2012.

[79] T. Ding, X. Yuan, and S. C. Liew, "Algorithmic beamforming design for MIMO multiway relay channel with clustered full data exchange," *IEEE Trans. on Veh. Tech.*, vol. 67, no. 10, pp. 10 081–10 086, 2018.

[80] W. Li and M. Dong, "Joint relay beamforming and receiver processing for multi-way multi-antenna relay networks," *IEEE Trans. on Commun.*, vol. 66, no. 2, pp. 576–588, 2018.

[81] A. U. T. Amah and A. Klein, "Non-regenerative multi-way relaying with linear beamforming," in *Proc. IEEE 20th Int. Symp. on Personal, Indoor and Mobile Radio Commun.*, Tokyo, Japan, 2009, pp. 1843–1847.

[82] F. L. Duarte and R. C. de Lamare, "Cloud-driven multi-way multiple-antenna relay systems: Joint detection, best-user-link selection and analysis," *IEEE Trans. on Commun.*, vol. 68, no. 6, pp. 3342–3354, 2020.

[83] T. P. Do, Y. H. Kim, S. R. Lee, and M.-A. Jung, "Joint relay selection and power allocation for pairwise multi-way relay networks," in *Proc. Int. Conf. on Conn. Veh. and Exp.*, Vienna, Austria, 2014, pp. 338–342.

[84] F. L. Duarte and R. C. de Lamare, "Buffer-aided max-link relay selection for multi-way cooperative multi-antenna systems," *IEEE Commun. Lett.*, vol. 23, no. 8, pp. 1423–1426, 2019.

[85] M. Tang, J. Chen, and Y. Zhang, "Performance analysis for physical-layer network coding with hierarchical modulation," in *Proc. IEEE Int. Conf. on Commun. Softw. and Netw.*, Beijing, China, June 2016, pp. 33–37.

[86] M. Noori and M. Ardakani, "Optimal user pairing for asymmetric multi-way relay channels with pairwise relaying," *IEEE Commun. Lett.*, vol. 16, no. 11, pp. 1852–1855, Nov. 2012.

[87] X.-W. Chang and Q. Han, "Solving box-constrained integer least squares problems," *IEEE Trans. on Wireless Commun.*, vol. 7, no. 1, pp. 277–287, Jan 2008.

[88] P. Wolniansky, G. Foschini, G. Golden, and R. Valenzuela, "V-BLAST: An architecture for realizing very high data rates over the rich-scattering wireless channel," in *Proc. URSI Int Symp. on Signals, Syst., and Electronics*, Pisa, Italy, Sept. 1998, pp. 295–300.

[89] S. Zhang, C. Nie, L. Lu, S. Zhang, and G. Qian, "MIMO physical layer network coding based on V-BLAST detection," in *Proc. IEEE Int. Conf. on Wireless Commun. and Signal Process.*, Huangshan, China, Oct. 2012, pp. 1–5.

[90] L. Babai, "On lovász' lattice reduction and the nearest lattice point problem," in *STACS 85*, K. Mehlhorn, Ed. Berlin, Heidelberg: Springer Berlin Heidelberg, 1984, pp. 13–20.

[91] X.-W. Chang and X. Yang, "An efficient regularization approach for underdetermined MIMO system decoding," in *Proc. of the 2007 int. Conf. on Wireless Commun. and Mobile Comput.*, Honolulu, Hawaii, US, 2007, pp. 349–353.

[92] X.-W. Chang, X. Yang, T. Le-Ngoc, and P. Wang, "Partial regularisation approach for detection problems in underdetermined linear systems," *IET Commun.*, vol. 3, no. 1, pp. 17–24, 2009.

[93] J. Wen, K. Wu, C. Tellambura, and P. Fan, "Closed-form word error rate analysis for successive interference cancellation decoders," *IEEE Trans. on Wireless Commun.*, vol. 17, no. 12, pp. 8256–8267, Dec. 2018.

[94] J. Zhu, J. Wang, Y. Huang, S. He, X. You, and L. Yang, "On optimal power allocation for downlink non-orthogonal multiple access systems," *IEEE J Sel. Area Comm.*, vol. 35, no. 12, pp. 2744–2757, Dec. 2017.

[95] K. Deb, *Multi-objective Optimization*. Boston, MA: Springer US, 2014, pp. 403–449.

[96] S. N. Islam, P. Sadeghi, and S. Durrani, "Error performance analysis of decode-and-forward and amplify-and-forward multi-way relay networks with binary phase shift keying modulation," *IET Commun.*, vol. 7, no. 15, pp. 1605–1616, Oct 2013.

[97] M. Chakraborty, S. Chowdhury, J. Chakraborty, R. Mehera, and R. K. Pal, "Algorithms for generating all possible spanning trees of a simple undirected connected graph: an extensive review," *Complex Intell. Syst.*, Aug. 2018.

[98] L. Clarke, "On Cayley's formula for counting trees," *J. of London Math. Soc.*, vol. 1, no. 4, pp. 471–474, 1958.

[99] J. G. Andrews and T. H. Y. Meng, "Performance of multicarrier CDMA with successive interference cancellation in a multipath fading channel," *IEEE Trans. on Comm.*, vol. 52, no. 5, pp. 811–822, May 2004.

[100] X. Chang, J. Wen, and X. Xie, "Effects of the LLL reduction on the success probability of the babai point and on the complexity of sphere decoding," *IEEE Trans. on Inform. Theory*, vol. 59, no. 8, pp. 4915–4926, Aug 2013.

[101] S. N. Islam, S. Durrani, and P. Sadeghi, "A novel user pairing scheme for functional decode-and-forward multi-way relay network," *Phy. Commun.*, vol. 17, pp. 128 – 148, 2015.

[102] D. Han, S. Li, and Z. Chen, "Hybrid energy ratio allocation algorithm in a multi-base-station collaboration system," *IEEE Access*, vol. 7, pp. 147 001–147 009, 2019.

[103] J. Chen, G. Mao, C. Li, W. Liang, and D. Zhang, "Capacity of cooperative vehicular networks with infrastructure support: Multiuser case," *IEEE Trans. on Veh. Tech.*, vol. 67, no. 2, pp. 1546–1560, 2018.

[104] H. Li, X.-W. Chang, Y. Cai, and B. Champagne, "Efficient detection scheme for physical-layer network coding in multiway relay channels," *IEEE Access*, vol. 7, pp. 167 639–167 652, 2019.

[105] A. C. Marcum, J. V. Krogmeier, D. J. Love, and A. Sprintson, "Analysis and implementation of asynchronous physical layer network coding," *IEEE Trans. on Wireless Commun.*, vol. 14, no. 12, pp. 6595–6607, 2015.

[106] T. Wang, S. C. Liew, and S. S. Ullah, "Optimal rate-diverse wireless network coding over parallel subchannels," *IEEE Trans. on Commun.*, vol. 68, no. 8, pp. 4891–4904, 2020.

[107] S. Boyd, S. P. Boyd, and L. Vandenberghe, *Convex Optimization*. Cambridge university press, 2004.

[108] I. P. Androulakis, C. D. Maranas, and C. A. Floudas, "A global optimization method for general constrained nonconvex problems," *J. of Global Opt.*, vol. 7, no. 4, pp. 337–363, 1995.

[109] J. Kennedy and R. Eberhart, "Particle swarm optimization," in *Proc.IEEE Int. Conf. on Neural Netw.*, vol. 4, Perth, WA, Australia, 1995, pp. 1942–1948.

[110] Q. Zhao and C. Li, "Two-stage multi-swarm particle swarm optimizer for unconstrained and constrained global optimization," *IEEE Access*, vol. 8, pp. 124 905–124 927, 2020.

[111] D. Pliatsios and P. Sarigiannidis, "Power allocation in downlink non-orthogonal multiple access iot-enabled systems: A particle swarm optimization approach," in *Proc. Int. Conf. on Distributed Comput. in Sensor Syst.*, Santorini, Greece, 2019, pp. 416–422.

[112] F. Abdessamia, Y. Tai, W. Z. Zhang, and M. Shafiq, "An improved particle swarm optimization for energy-efficiency virtual machine placement," in *Proc. Int. Conf. on Cloud Comput. Research and Innovation*, Singapore, 2017, pp. 7–13.

[113] T. T. Hoang, M.-Y. Cho, M. N. Alam, and Q. T. Vu, "A novel differential particle swarm optimization for parameter selection of support vector machines for monitoring metal-oxide surge arrester conditions," *Swarm and Evol. Comput.*, vol. 38, pp. 120 – 126, 2018.

[114] J. Raitoharju, K. Samiee, S. Kiranyaz, and M. Gabbouj, "Particle swarm clustering fitness evaluation with computational centroids," *Swarm and Evol. Comput.*, vol. 34, pp. 103 – 118, 2017.

[115] A. Peimankar, S. J. Weddell, T. Jalal, and A. C. Lapthorn, "Evolutionary multi-objective fault diagnosis of power transformers," *Swarm and Evol. Comput.*, vol. 36, pp. 62 – 75, 2017.

[116] B. S. G. de Almeida and V. C. Leite, *Particle Swarm Optimization: A Powerful Technique for Solving Engineering Problems*, J. D. Ser, E. Villar, and E. Osaba, Eds. IntechOpen, 2019.

[117] M. Kohler, M. Vellasco, and R. Tanscheit, "PSO+: A new particle swarm optimization algorithm for constrained problems," *Applied Soft Comput.*, vol. 85, p. 105865, 2019.

[118] H. Alzer, "On the Cauchy-Schwarz inequality," *J. of Math. Analysis and App.*, vol. 234, no. 1, pp. 6 – 14, 1999.

[119] M. Grötschel, L. Lovász, and A. Schrijver, *Geometric Algorithms and Combinatorial Optimization*, ser. Algorithms and Combinatorics. Springer, 1988, vol. 2.